الجمهورية الجزائرية الديمقراطية الشعبية

République Algérienne Démocratique et Populaire

وزارة التعليـــم العالـــي و البحث العلمـــي

Ministère de l'Enseignement Supérieur et de la Recherche Scientifique

المدرسة الوطنية المتعددة التقنيات

Ecole Nationale Polytechnique

Département d'automatique

Laboratoire commande des processus

Nonlinear Predictive Control

Application to a Solar Thermal Process

By Mr. Yassine HIMOUR

A thesis submitted in partial fulfilment of the requirements of the degree of Doctor of Science In Control Engineering, Option of Control Engineering.

Presented and defended publicly on (09/12/2025)

Board of the jury:

President	Mr. NEZLI Lazhari	Professor, ENP, Algiers.
Promoter	Mr. TADJINE Mohamed,	Professor, ENP, Algiers.
Co-promoter	Mr. BOUCHERIT Mohamed-Seghir,	Professor, ENP, Algiers.
Examiner	Mr. BOUDANA Djamel,	Professor, ENP, Algiers.
Examiner	Mr. GROUNI Said,	Professor, Univ. Tamanrasset.
Examiner	Mr. ALLAOUI Tayeb,	Professor Univ Tiaret.
Examiner	Mr. BENMANSOUR Khelifa,	Professor, ESDAT.

ENP, 2025

Laboratoire commande des processus, Ecole Nationale Polytechnique (ENP)

10, Avenue des Frères Oudek, Hassen Badi, BP 182, 16200 El Harrach, Alger, Algérie

http://www.enp.edu.dz

الجمهورية الجزائرية الديمقراطية الشعبية

République Algérienne Démocratique et Populaire

وزارة التعليـــم العالـــــي و البحث العلمـــــي

Ministère de l'Enseignement Supérieur et de la Recherche Scientifique

المدرسة الوطنية المتعددة التقنيات

Ecole Nationale Polytechnique

Département d'automatique

Laboratoire commande des processus

Nonlinear Predictive Control

Application to a Solar Thermal Process

By Mr. Yassine HIMOUR

A thesis submitted in partial fulfilment of the requirements of the degree of Doctor of Science In Control Engineering, Option of Control Engineering.

Presented and defended publicly on (09/12/2025)

Board of the jury :

President	Mr. NEZLI Lazhari	Professor, ENP, Algiers.
Promoter	Mr. TADJINE Mohamed,	Professor, ENP, Algiers.
Co-promoter	Mr. BOUCHERIT Mohamed-Seghir,	Professor, ENP, Algiers.
Examiner	Mr. BOUDANA Djamel,	Professor, ENP, Algiers.
Examiner	Mr. GROUNI Said,	Professor, Univ. Tamanrasset.
Examiner	Mr. ALLAOUI Tayeb,	Professor Univ Tiaret.
Examiner	Mr. BENMANSOUR Khelifa,	Professor, ESDAT.

ENP 2025

Laboratoire commande des processus, Ecole Nationale Polytechnique (ENP)

10, Avenue des Frères Oudek, Hassen Badi, BP 182, 16200 El Harrach, Alger, Algérie

http://www.enp.edu.dz

الجمهورية الجزائرية الديمقراطية الشعبية

République Algérienne Démocratique et Populaire

وزارة التعليـــم العالـــــي و البحث العلمـــــي

Ministère de l'Enseignement Supérieur et de la Recherche Scientifique

المدرسة الوطنية المتعددة التقنيات

Ecole Nationale Polytechnique

Département d'automatique

Laboratoire commande des processus

Commande Prédictive Non-linéaire

Application à un Processus Solaire Thermique

Par Mr. Yassine HIMOUR

Thèse de Doctorat Es-Science en Automatique

Option Automatique

Soutenu publiquement le (09/12/2025)

Composition du jury:

Président	Mr. NEZLI Lazhari	Professeur, ENP, Algiers.
Promoteur	Mr. TADJINE Mohamed,	Professeur, ENP, Algiers.
Co-promoteur	Mr. BOUCHERIT Mohamed-Seghir,	Professeur, ENP, Algiers.
Examinateur	Mr. BOUDANA Djamel,	Professeur, ENP, Algiers.
Examinateur	Mr. GROUNI Said,	Professeur, Univ. Tamanrasset.
Examinateur	Mr. ALLAOUI Tayeb,	Professeur Univ Tiaret.
Examinateur	Mr. BENMANSOUR Khelifa,	Professeur, ESDAT.

ENP 2025

Laboratoire commande des processus, Ecole Nationale Polytechnique (ENP)

10, Avenue des Frères Oudek, Hassen Badi, BP 182, 16200 El Harrach, Alger, Algérie

http://www.enp.edu.dz

ملخص

تتميز درجة الحرارة عند مخرج حقول جمع الطاقة الحرارية الشمسية بأنها أنظمة غير خطية إلى حد كبير، كما أن مصدرها الرئيسي للطاقة لا يقبل التوجيه، مما يجعل من عملية التحكم في حرارة المخرج مهمة صعبة للغاية. لا تستطيع وحدات التحكم الخطية التعامل مع الانحرافات غير المرغوب فيها لدرجة حرارة المخرج على مدى كل نطاق الجانب الديناميكي لهذا النوع من الأنظمة. علاوة على ذلك، فإن التحكم التنبئي غير الخطي الذي يعتمد على التحسين الرياضي غير الخطي في الوقت الحقيقي يعاني من معضلة طول التنفيذ و بعض مشكلات الحساب العددي. في هذه المذكرة، تم تصميم وتطبيق بعض طرق التحكم العصبوني التنبئي غير الخطي، وأيضا تحكم تنبئي عصبوني مجدول ذو مكاسب غير منتهية للتحكم في درجة الحرارة في حقل شمسي ذي الحوض المكافئ الموزع. تمت مقارنة أداء كل من خاصيتي التتبع و إلغاء تاثير الاضطراب لوحدة التحكم المقترحة بتلك الخاصة باستراتيجيات التحكم التنبئي غير الخطي. حيث تم إثبات تفوق استراتيجية التحكم المقترحة بشكل جيد من خلال بعض المؤشرات في نتائج المحاكاة. تختتم الأطروحة بتوصيات واقتراحات للأعمال المستقبلية.

الكلمات المفتاحية: التحكم التنبئي غير الخطي، مكاسب مجدولة غير منتهية، الشبكات العصبونية، المركزات الشمسية الإسطوانية المقعرة.

Résumé

Les processus solaire thermique sont des systèmes hautement non linéaires, et qui ont une source d'énergie non maniable. Cela fait de leur commande une tâche trop difficile. Les contrôleurs linéaires ne sont pas capables à maitriser la température de sortie des ces processus dans tous leurs modes de fonctionnement. De plus, la commande prédictive non linéaire, qui se base sur la résolution d'un problème d'optimisation non linéaire et en ligne, peut démontrer des problèmes de temps d'exécution et de calcul. Dans cette thèse, quelques stratégies de commande prédictive non linéaire et un contrôleur prédictive neuronal à gains préprogrammés infinis sont conçus et appliqués à un champs solaire distribué à base de concentrateurs cylindro-parabolique. La comparaison des résultats en termes de poursuite et rejet des perturbations dévoile une supériorité du contrôleur proposé selon certains indices de performance. La thèse conclut avec des recommandations et perspectives.

Mots-clés : Commande prédictive non linéaire, gains préprogrammés infinis, réseaux de neurones, concentrateurs solaires cylindro-paraboliques.

Abstract

Solar thermal plants have high nonlinearities and non-manipulated energy source which make their control task a very challenging work. Linear controllers can't cope with undesirable deviations of the outlet temperature over all the operation range of the dynamics of this type of plants. Moreover, nonlinear predictive control relying on online nonlinear optimisation have the drawback of time consuming and numerical calculus issues. In this work, neural nonlinear predictive control and an infinite gain scheduling neural predictive control are designed and applied to control the temperature in a distributed parabolic trough solar collector field. The performance of both tracking and disturbance rejection of the proposed controller is compared to those the nonlinear predictive control strategies. The superiority of the proposed control strategy is well demonstrated through some indices in simulation results. The thesis concludes with recommendations and perspectives for future works.

Keywords: Nonlinear predictive control, Infinite gain scheduling, Neural networks, Parabolic solar trough.

Table of contents

List of tables

List of figures

Nomenclature

Abbreviation

ANN Artificial neural networks

ARX Autoregressive with exogenous inputs

BFGS Predictive control using the BFGS optimization method

CARIMA Controlled autoregressive integrated moving average

CLF Control Lyapunov Functions

CPC Compound parabolic concentrator

CSE Control system effort

CSP Concentrating solar power

DMC dynamic matrix control

DSCF Distributed solar collector field

ET Mean execution time for one iteration

FFNN Feedforward neural network

GPC Generalized predictive control

GMV Generalized minimum variance

HFC Heliostat field collector

HTF Heat transfer fluid

IAC Integral of the absolute control

IAE Integrated absolute error

IDCOM Identification and command algorithm

ISE Integrated squared error

ISG Infinite scheduling gain predictive control

IP Interior point

IPIM Constrained predictive control using an ideal prediction model

IPOPT Interior Point Optimizer

KKT Karush-Kuhn-Tucker

LFR Linear Fresnel reflector

LM Predictive control using the Levenberg-Marquardt optimization method

MHOC Horizon optimal control

MLP Multilayer perceptron

MPHC Model predictive heuristic control

MPC Model predictive control

MUSCOD Multiple Shooting Code for Optimization

NARX Nonlinear autoregressive with exogenous inputs

NLP Nonlinear problem

NMPC Nonlinear model predictive control

NOE Nonlinear output error

NSSE Normalized sum of squared errors

OS First overshoot

PDR: Parabolic dish reflector

PID Proportional-Integral-Derivative

PTC Parabolic trough collectors

PV Photovoltaic

QDMC Quadratic dynamic matrix control

QP Quadratic programming

ReLU Rectified linear unit

RHC Receding horizon control

SSE Sum of squared errors

ST Settling time

RT Rise time

Symbols

A Coefficient matrix of the linear constraints

A_f cross-sectional area of the absorber tube

$A(q^{-1})$ CARIMA or ARX outputs polynomial

b Constant term vector of the linear constraints

$B(q^{-1})$ CARIMA or ARX inputs polynomial

c Reduction rate of the barrier parameter

C Matrix mapping the linear relationship between the states and the outputs

$C(q^{-1})$ CARIMA noise polynomial

c_f Fluid specific heat capacity

c_i Constraint in the interior point method

d Filtering parameter

d_u Delay time according to the manipulated input

d_R Delay time according to the solar irradiance

d_T Delay time according to the inlet HTF temperature

d_v Delay time according to measured disturbances

$diag(\cdot)$ is the diagonal matrix.

$D(q^{-1})$ Measured disturbance polynomial

$e(t,\theta)$ Prediction error during ANN supervised learning

$\tilde{e}(t,\theta)$ Approximated prediction error during ANN supervised learning

$E(q^{-1})$ Diophantine polynomial

$F(\cdot)$ Global function of a neural network or a state space model

$F(q^{-1})$ Diophantine polynomial

$f(\cdot)$ The activation function used for all the hidden neurons

G Matrix of step response coefficients according to u(t)

G Concentrator aperture

$G(\theta)$ Gradient of the cost function in ANN learning

$G_{apprx}(\theta_k)$ Approximation of the gradient of the cost function in ANN learning

$g(\cdot)$ The activation function used for all the output neurons.

H Matrix of step response coefficients according to v(t)

$H^{-1}(\theta_k)$ Inverse of the Hessian matrix of the cost function in ANN learning

$H_{apprx}(\theta_k)$ Approximation of the Hessian matrix of the cost function in ANN the learning

I Identity matrix

J Cost function of the optimization problem

j_{apprx} Approximation of the cost function

k Time sample

$Ln(\cdot)$ Logarithmic function

l Space variable

L Total length of the absorber tube

N_1 Prediction start time

N_2 Prediction horizon

N_h Number of neurons in the hidden layer

N_u Control horizon

N_x The number of inputs of the FFNN

N_y The number of neurons in the output layer

n_R Order of past T_in inputs in NARX model

n_T Order of past R(t) inputs in NARX model

n_u Order of past manipulated inputs in NARX model

n_y Order of past outputs in NARX model

$P_k(q^{-1})$ Model polynomials symbol in the filtering expression

q^{-1} Time backward shift operator

$r(k)$ Reference at time k

R Vector of reference over the prediction horizon

$R(t)$ Solar irradiance

$tanh$ Hyperbolic tangent function

T Sampling period

$T_{in}(t)$ HTF inlet temperature

$T_{out}(t)$ HTF outlet temperature

V Hidden layer to output layer weight's matrix

$v(t)$ Measured disturbance

V_0 Hidden layer to output layer biases vector

W Input layer to hidden layer weights' matrix

W_0 Inputs layer to hidden layer biases' vector

$W_{:,i}$ i^{th} column of matrix W

$x(k)$ Vector of state space variables

$\hat{Y}$ Vector of predictions

$z(t)$ Vector of inputs of the ARX neural network

$u(k)$ Control signal

U Vector of control signal over the control horizon.

$\bar{u}(t)$ Fluid volumetric flow

λ (1) Penalty factor on the control increments in the MPC cost function

(2) Lagrange multiplier

θ Weights vector containing W and V

Δ differencing operator

δ_k Difference between two successive values of the decision variables

γ_k Difference between two successive values of the gradient

∇ The gradient

∇^2 Hessian matrix

ϕ Free response in the GPC predictor

Φ (1) Free response in GPC predictor with measured disturbances

(2) Augmented cost function in the interior point method

μ The barrier parameter in the interior point method

ε Desired precision in an optimization algorithm

$\xi(t)$ Zero mean white noise

$\zeta(\tau)$ Linearization offset

ρ_f fluid mass density

η optical efficiency

σ_k ratio in the LM supervised learning algorithm

Acknowledgment

الحمد لله.

I would like to thank my supervisors, Professor Mohammed Tadjine and Professor Mohamed-Seghir Boucherit, for everything they did to make this work successful.

I would like also to thank the jury members for accepting to examine, review, discuss and participate in enhancing this work.

My thanks go to my wife for being supportive and patient during the long hours I have been concentrating on reading articles and books, implementing programs, and writing this thesis.

Special thanks to Professor Dwight Kimberly and his wife Patti, Professor John Natzke, Mr. Joseph Snyder and his wife Jane, and Professor Sean Conley from the Institute for Collaborative Learning.

Thanks to Sara Ruiz-Moreno in the research group headed by Pr. E.F Camacho, from university of Sevilla, Spain, for providing simulation data of the ACUREX plant. Surly they will be of use in my future researches. Thanks also to Dr. Charaf Abdelkarim MOSBAH for providing his PhD thesis, some articles and recommendations.

Thanks to my father, my brother Badis and my friend Dr. Ridha Djeghader for encouraging me to take a shot for a second time.

I wouldn’t forget to thank all professors I had contact and discussion with from George Fox University, Oregon State University, and Portland State University.

Chapter I. Introduction

I.1. Overview of solar energy

Abundant, non-polluting, renewable, and sustainable—these are the main advantages that make solar energy the most promising energy source in the future. Indeed, the sun provides the earth permanently, with energy reaching 150,000 terawatts. If only 1% of this quantity could be converted into electrical energy, and with an efficiency of only 10%, this would give around 105 terawatts, i.e., 4 times the predictions of global consumption in 2050 (Goswami, 2007).

The use of solar energy experienced a strong boost during the second half of the 1970s, just after the first major oil crisis. At that time, economic problems were the most significant factor in this increase, and therefore interest in this type of process decreased as oil prices went down (Camacho, Berenguel and Rubio, 1997). Today, however, the main problem is that the proven reserves of oil and gas, at current consumption rates, would be sufficient to meet the world's demand for no more than 41 and 67 years, respectively (Goswami, 2007). Furthermore, there is widespread global worry that the shift to a carbon-neutral state must be accomplished by 2050 to restrict the increase in global temperatures to 1.5°C (Goswami, 2022).

In such a situation, governments around the world tend to encourage the exploitation of solar energy through tax cuts in order to address the cost of exploiting this type of energy, which today remains relatively expensive compared to traditional sources. However, if the cost is a major obstacle to the exploitation and usage of this energy, there are other difficulties to consider in the production and/or storage process, either for photovoltaic technology or thermal technology.

I.2. Motivation

Due to its numerous advantages for the environment as well as its benefits for the economy, solar energy usage has been gaining more and more attraction in recent decades. Generating electricity power without emitting harmful pollutant into the atmosphere is a very significant advantage solar energy can offer to humanity and earth. Solar energy can be harnessed with two methods: photovoltaic (PV) method, and thermal method. While PV technology is more known and utilized, solar thermal energy has proven to be more efficient. As reported by Goswami (Goswami, 2022), While the commercial efficiency of solar photovoltaic panels can slightly surpass 20%, that of solar thermal systems ranges from 40% to 60%. This is thanks to the storage capacity of the thermal energy— it can be stored easily and inexpensively in comparison with

storing the electrical energy itself. This enables to produce a high-quality electrical energy, convenient to be connected to the distribution grids. Hence allowing to provide a reliable source of energy for both residential and commercial use.

Besides electrical power generation, solar thermal energy is being used and is promising to have good use in a wide range of applications such as agriculture, industrial chemistry, stream generation, heating and domestic cold (Jebasingh and Herbert, 2016; Kalogirou, 2023). In fact, solar thermal energy is considered the simplest and the least expensive method for seawater desalinating, which is very encouraging for countries with limited fresh water resources (Sathyamurthy *et al.*, 2017).

Among the different available solar thermal technologies, the concentrating solar power (CSP) technologies are the most used in the industry. And the parabolic trough collectors (PTC) are the most popular among the CSPs. They account for about 73% of operational and under-construction projects (Baharoon *et al.*, 2015). A solar PTC consists of an absorber or receiver tube, in which a heat transfer fluid (HTF) flows. The absorber tube is wrapped in a glass envelope, between which a vacuum pressure is maintained in order to create a greenhouse effect. The goal of this mechanism is to hinder absorbed heat loss. The absorber is placed in the focal line of the trough mirrors. All the stuff is posed on a rigid structure equipped with a solar radiation tracking system.

On the other hand, model predictive control (MPC) was demonstrated to be a solid candidate to control the outlet temperature in PTC plants (Camacho, F. R. Rubio, *et al.*, 2007; Cirre *et al.*, 2007; Camacho and Gallego, 2015; Pipino *et al.*, 2020; Ramón D. Frejo and F. Camacho, 2020)**.** It is frequently used because it can handle challenging issues other techniques struggle with. As its concepts are intuitive and its tuning is relatively straightforward, it has the advantage of appealing to staff with limited control knowledge. Additionally, MPC is versatile and capable of controlling a wide range of processes, from those with simple dynamics to more complex ones, including those with long delay times, nonminimum phase, or unstable characteristics (Camacho and Bordons, 2007). It naturally includes feedforward action that deals with measurable disturbances. MPC includes no explicit derivative, no explicit integrator and no lag error on polynomial set points — no effect of measurement noise and no anti-windup is necessary. In the multivariable case, MPC can be effectively applied, and it inherently compensates for dead times. Furthermore, MPC is straightforward to implement, and its design enables handling constraints by including them systematically in the design phase. It is appreciated in particular in controlling

processes where future references are known or predictable. It's a flexible methodology open to potential future extensions.

In conclusion, solar thermal energy is a promising source of energy that has proven to be reliable in generating electrical power. It also, has a wide range of applications in different industrial fields. Improving the efficiency of PTC fields, will grow the use of this technology, providing a sustainable source of energy for future generations. One way to improve the efficiency of PTC fields is reliable control of the outlet temperature of the HTF. In this context, MPC has demonstrated a great ability to handle hurdles and challenges in maintaining the outlet temperature in desired values.

I.3. Challenges and problem formulation

The intermittent nature of solar energy is one of its main challenges. Solar collectors are capable of capturing solar energy during the day. Nevertheless, the amount of energy available for harvesting decreases dramatically as the sunset approaches and totally vanishes at night. This is due to the fact that solar collectors need direct sunlight to function optimally. Also, the quantity of solar radiation that is captured can be significantly affected by meteorological factors. The quantity of sunrays that reach the solar collectors is diminished during overcast or rainy days. Similarly, the amount of energy that can be captured during the winter can also be limited by shorter days and a lower solar angle.

Furthermore, from a control point of view, the controlled variables are corrected by adjusting some manipulated variables. These latter influence the outputs according to some dynamics. Most of the time, the manipulated variables are the source of energy itself. Unfortunately, that's not the case in distributed solar collector fields (DSCF), where solar energy is not manageable (Camacho *et al.*, 2010). The solar irradiation is subject to daily solar cycle as well as to passing clouds, which could affect in a fast way the solar field outlet temperature. Moreover, the temperature of the HTF at the inlet of the absorber tube and the reflectivity of the concentrators contribute significantly to the behavior of the outlet temperature of the field, but they are also not manipulated variables. Then, all that remains to control the outlet temperature of the HTF is to act on its flow rate, considering the three mentioned quantities as disturbances. Other known disturbances may also affect the behavior of the HTF temperature, among them the ambient temperature and the wind speed, which can deflect the concentrators from their desired position. Not only do these inconveniences make

the control of the outlet temperature in a DSCF a very challenging task, but a commercial PTC plant could be composed of a great number of loops and occupy a large surface that can reach more than 100 hectares (Camacho, Berenguel and Gallego, 2014). Moreover, its dynamic characteristics show changes over time, such as the dominant time constant and the time delay (Cirre *et al.*, 2007) (Normey-Rico and Camacho, 2008). It also exhibits strong nonlinearities, resonance modes (Meaburn and Hughes, 1993), and non-minimal phase characteristics in some of its operation modes (Brus and Zambrano, 2010).

Consequently, the classical Proportional-Integral-Derivative (PID) controllers are not the most suitable to be used in controlling the temperature in DSCFs (Lemos, Neves-Silva and Igreja, 2014). Particularly, they are unable to handle the whole operating range of this type of process. Many more advanced control techniques have been developed and applied in this context. As mentioned previously, MPC was shown to be a strong contender for controlling this kind of plant; nevertheless, there are incentives to develop nonlinear model predictive control (NMPC) strategies because of the distributed solar collector field's strong nonlinear behavior. However, some difficulties arise when using NMPC, amongst which theoretical analysis of properties such as stability(Camacho and Gallego, 2015). Furthermore, for robustness reasons, additional ad hoc solutions are often required. These solutions add another layer of complexity to the control law and must effectively address these computational issues (Nørgaard *et al.*, 2000):

- Does the optimization algorithm converge to the desired accuracy?
- Is the convergence of the algorithm guaranteed in the appropriate lapse of time?
- Are there any numerical problems?
- Has the solution obtained been verified as the globally optimal solution, considering different starting points for the algorithm?

In summary, the exploitation of solar energy in its thermal form presents significant control challenges, in particular the control of the outlet temperature of the distributed solar collector fields. Traditional PID controllers can’t cope with the complexity of DSCFs. Nonlinear model-based predictive control offers more reliable and robust alternative, able to handle the systems delays, nonlinearities, and other operational difficulties. However, implementing NMPC also introduces complexities such as theoretical analysis and computational problems. Finding a solution to these complexities is primordial for an efficient use of the thermal solar energy in large-scale applications.

I.4. Aims and objectives

The main objective of this thesis is to design a predictive control strategy to overcome the aforementioned challenges and difficulties in controlling the output temperature in the solar parabolic trough collectors. The proposed design has to cope with the high nonlinearities of the dynamics of the outlet temperature in PTC fields. It must be free of numerical problems and calculus burdens related to the NMPC optimization stage, without losing its performance. Furthermore, the measured disturbances, namely the input temperature and the solar irradiance, have to be treated in an appropriate way to reduce their effects on the outlet of the PTC field. The results of the proposed design are to be compared with some other NMPC techniques. Throughout the journey to accomplish those aims, some objectives are to be achieved in the meantime:

- Elaborate a simulation model that imitates the behavior of the temperature in a PTC field. This model will be the benchmark process to be controlled in this work.
- Identify a nonlinear neural network model based on the data given by the simulation model. This new model will be used as a control model for the process.
- Implement nonlinear model predictive control to command the outlet temperature in the DSCF. The proposed control laws have to cope with the above-mentioned challenges. Particularly, exploit the available measurements of disturbances in an effective way, handle the nonlinear characteristics, and consider the material constraints on the plant variables.
- Propose a contribution to improve the NMPC control strategy to address its shortcomings in terms of time calculus, numerical problems, model mismatches, etc.

I.5. Thesis scope

This work concerns controlling the temperature in solar thermal energy plants using neural model predictive control, more specifically, it deals with the control of the outlet temperature of the heat transfer fluid in a distributed solar collector field based on parabolic trough concentrators. Artificial neural networks are used to model the behavior of the process. However, because of the leak for real data of such plants, the data used for the simulation is given by a first principal model, and the forecasts for the solar irradiation are proposed as artificial values. To reduce using artificial data, a reduced complexity simulation model of the process, a trade-off between complexity and precision is used.

In order to maintain clarity and relevance, certain aspects fall outside the scope of this research. Specifically, this thesis will not cover the design aspects of the PTCs nor the control or the modelling of the power generation block. The forecasting of irradiance data and predicting of the temperature in the input of the distributed solar collector field are not treated as well. The simulation model parameters of the studied real plant are not identified in this work but obtained from the literature. And following the engineers' pragmatic methodology that led to the extension of industrial application of MPC, stability and robustness analysis are pushed back to future works. Despite these limitations, this thesis intends to achieve the above-mentioned aim by thoroughly examining the application of non-linear predictive control to a PTC based solar field. By narrowing the focus, this work aims to provide in-depth insights and practical contributions to improve the NMPC application to the solar field and surpass the challenges and difficulties previously cited in this chapter.

I.6. Thesis layout

The rest of this thesis is organized as follows. The second chapter gives a solid state-of-the-art about predictive control and its application to control the outlet temperature in the solar parabolic trough fields. It begins by explaining the principle of the MPC and then it gives a brief historical overview about it. The chapter continues with a comprehensive explanation about PTC fields, and a state-of-the-art of the outlet temperature control, including MPC control strategies in this context. This enables to conclude by identifying the research gaps and defining the orientation of the thesis contribution based on those gaps.

In chapter three, based on the orientations of the previous chapter, the foundational and analytical basis of the neural control strategies are developed for the PTC field. Firstly, the chapter develops a trade-off model between complexity and precision; afterwards, the neural identification procedure is explained, and the resulting neural model usage in unconstrained and constrained NMPC control schemes is developed.

Chapter four tackles the practical implementation in simulation of the developed identification task and the control strategies. The ACUREX plant, a benchmark for solar thermal research, is described, after which the identification and predictive control schemes are applied, and their performance is assessed through some indices. The chapter includes detailed discussion and insights of the results.

The thesis finishes with a conclusion that summarizes the key findings, emphasizing the contributions to the field of solar thermal energy control. Future directions are proposed, focusing on the applicability of the developed methodologies to large commercial fields.

Chapter II. State-of-the-art in Predictive Control for Solar PTC fields

II.1. Introduction

This chapter is meant to be a basis for the decision making on the strategy to tackle the task of controlling the outlet temperature in PTC fields. It provides a sufficient vison on the state-of-the-art of predictive control and its application to the outlet temperature control in the parabolic trough collector fields.

In a first stage, the principal and the basic elements of predictive control are explained. Then, the need to explore its capabilities is satisfied through a review of historical development, where many of its advances and variants took place in responding to industrial application requirements and challenges. Thus, setting a stage for deeper investigation and reflection on its utilisation in controlling the outlet temperature of PTCs.

The chapter also gives on overview of parabolic trough collectors, their operating principles and some of their applications. It's also important to highlight the importance and objectives of the outlet temperature control, in particular for the optimization of the energy production. A state-of-the-art about this task is investigated and different control techniques and strategies from the literature are mentioned with the focus on model predictive control. That helps in understanding this control loop challenges and focusing on the convenient control techniques. The advantages of using neural networks in system identification and control is also explored, in particular with MPC.

The chapter finishes with an outline of gaps in the existing research, underlining undressed challenges, and the need for further investigations into nonlinear predictive control within the context of controlling the outlet temperature in PTC fields. This aims at determining a solid decision on the research trajectory that will be adopted in the subsequent chapters.

II.2. Basics of predictive control

This section explains the principle and the components of model predictive control. The functioning logic behind MPC, and the elements to concretize this logic are detailed. The objective is to give a deep insight to MPC to enable reflect on its capacities, hence exploit it in a good manner for resolving the problem of the outlet temperature in PTC fields.

II.2.1 The intuitive principle of MPC

Predictive control is intuitive and natural, it is used in our daily activities. For example, when driving a car, one looks ahead on a certain horizon, then takes into consideration what he sees in making decisions about the action he takes in that moment. If, for example, there's a bend at a certain distance, then decreasing the speed is a suitable action at this moment to prepare to go safely, after some time, through that bend. A more detailed example is when playing chess. A player thinks about many steps ahead, then plays only one step. In his next turn, this player will not take the second step he has already reasoned about, but he will repeat the same work by thinking about some steps ahead, taking into consideration the move his opponent has already made and those he will make (by predicting his future moves), and then he will play only the first step. Notice that the more he knows about his opponent's strategy (model), the more he has the chance to win. The methodology adopted here goes through three stages: predict, plan, and act which are exactly the same stages in predictive control.

Similarly, on the basis of the obtained measurements at instant k, the predictive controller uses explicitly a model to predict the future dynamic behavior of the system over a prediction horizon N_2, and determines over a control horizon N_u the command that optimizes a cost function expressing the open loop performances. If there were no disturbances and no difference in behavior between the prediction model and the real system, and if the optimization problem could be solved for the infinite horizon, then we could apply the function of the input found at $k = 0$ for all times $k > 0$. However, this is not possible due to disturbances and model-system disparity, and thus only the first command is applied to the plant. The entire procedure i.e., prediction and optimization, is repeated to find new more convenient command in light of the next measurements at time $k + 1$ and the new predictions. This is done by moving forward the prediction and the control horizons.

II.2.2 The main elements of MPC

All predictive control techniques have common elements and different options can be chosen for each of these elements, thus giving a variety of predictive control algorithms. The MPC main elements are:

II.2.2.1. The prediction models

Some predictive control schemes use detailed fundamental models, but these may be difficult to obtain or unavailable. Often a substantial portion of the implementation cost of advanced controls may be the cost of modelling, hence the use of empirical models becomes very attractive. Once constructed, these models require less computation than fundamental models. According to Ungar et al (Ungar *et al.*, 1996) it is recommended to use neural networks in predictive control where the actions of the control have considerable constraints, or for processes that are unstable or those that show an inverse response.

II.2.2.2. The cost functions

Several types of cost functions are used to obtain a predictive control law, the main objective is (Biao and Ramesh, 2008):

- Future outputs must follow a determined reference signal on a desired trajectory,
- The required control effort must be considered in the cost function.

A general expression for such a cost function is:

$$J = \sum_{i=N_1}^{N_2} \ell(\hat{x}(k+i|k), u(k+i)) \qquad \text{II-1}$$

Where $\hat{x}(k+i|k)$ is the prediction of the state variables at time $k+i$ from time k and $u(k+i)$ is the command.

In the simplest and most commonly used case, the function $\ell(\cdot)$ is defined by the standard quadratic form which gives the following cost function:

$$J = \frac{1}{2}\sum_{i=N_1}^{N_2} (r(k+i) - \hat{y}(k+i|k))^2 + \frac{1}{2}\sum_{i=1}^{N_u} \lambda \left(\Delta u(k+i-1)\right)^2 \qquad \text{II-2}$$

Where, $r(k+i)$ the reference signal, $\hat{y}(k+i|k)$ the predictions at time $k+i$ calculated at time k, $\Delta u(k)$ is the control increments, λ the penalty factor of the control increments.

II.2.2.3. Prediction and control horizons

The first prediction horizon N_1, is usually taken equal to the delay of the controlled system, if the system does not show any delay, the control horizon is taken equal to 1. The idea is that the optimized commands on the horizon N_u will drain the predictions in the window between N_1 and N_2 to follow the reference signal. The command increments between N_u and N_2 are taken equal to 0.

II.2.2.4. Reference trajectory

The reference trajectory is a sequence of desired outputs of the process in the future. In fact, there exist an error between the actual output and the desired ones due to performance limitations of the control systems, such as hard constraints on the actuators, process time delay, behavior mismatch between the model and the process, etc. Considering these limitations, the objective functions use a reference trajectory that may not necessarily coincide with the true reference. But is a smooth approximation of the current values of the outputs to the known reference (Biao and Ramesh, 2008).

II.2.2.5. Constraints

One of the primary reasons for the success of predictive control in general is its ability to explicitly handle the constraints. Constraints are physical limits of the systems, or imposed economic and safety limits. Therefore, in practical predictive control systems, constraints on the values of the control signal, the increments of the control signals and the outputs, are usually considered:

$$u_{min} \leq u(k) \leq u_{max} \quad ,\forall k \qquad \text{II-3}$$

$$y_{min} \leq \hat{y}(k+i|k) \leq y_{max} \quad ,\forall k \qquad \text{II-4}$$

$$\Delta u_{min} \leq u(k) - u(k-1) \leq \Delta u_{max} \quad ,\forall k \qquad \text{II-5}$$

Where $u_{\min}$ and u_{max} are the control constraints, $y_{\min}$ and y_{max} are the output constraints and $\Delta u_{\min}$ and Δu_{max} are the control increments limits.

According to equation II-4 the constraints are not considered on the real outputs of the system, but on the predicted outputs, and this is due to unpredictable disturbances. This underlines the important of precise prediction models in predictive control.

II.3. A brief overview of historical development and evolution of MPC

Model predictive control, receding horizon control (RHC) or moving horizon optimal control (MHOC), is an advanced control approach that has roots dating back to the works of Bellman (Bellman, 1967) on optimality in the late of the 50s. It is nontrivial in this context to remind that predictive control is an optimal control since it solves an optimal control problem each sampling time. Later on, in 1960, Kalman (Kalman, 1960) observed that *optimality does not imply stability* and introduced then the Control Lyapunov Functions (CLF) concept to analyse stability of closed loop systems. The receding horizon principle, which is an important concept in MPC, was proposed by Propoi in 1963 (Propoi, 1963), and it was just until 1967 that Lee and Markus (Lee and Markus, 1967) proposed to only apply the first part of the optimal control sequence and repeat such a scenario each sampling time.

First applications of MPC in industry came in the end of the 70s with the works of Richalet and co-authors (Richalet *et al.*, 1977, 1978), who presented the IDCOM algorithm (identification and command); and the works of engineers from Shell, Cutler and Ramaker (Cutler and Ramaker, 1979), who developed the DMC (dynamic matrix control). The two works use an impulse or step response model and are based on heuristic methods, also known as model predictive heuristic control (MPHC) which had a big impact in chemical process industries because of its simplicity and being intuitive. Yet, these algorithms had not handled constraints[1] until Garcia and Morshedi (Garcia and Morshedi, 1986) first introduced the concept of quadratic programming (QP) to solve constrained problems of linear systems under quadratic cost function; the resulting algorithm was known as quadratic dynamic matrix control (QDMC) which is an improved version of Shell's DMC.

[1] The works of Richalet did not claim to obtain optimal controls. Instead, the future controls where determined iteratively until they met the constraints.

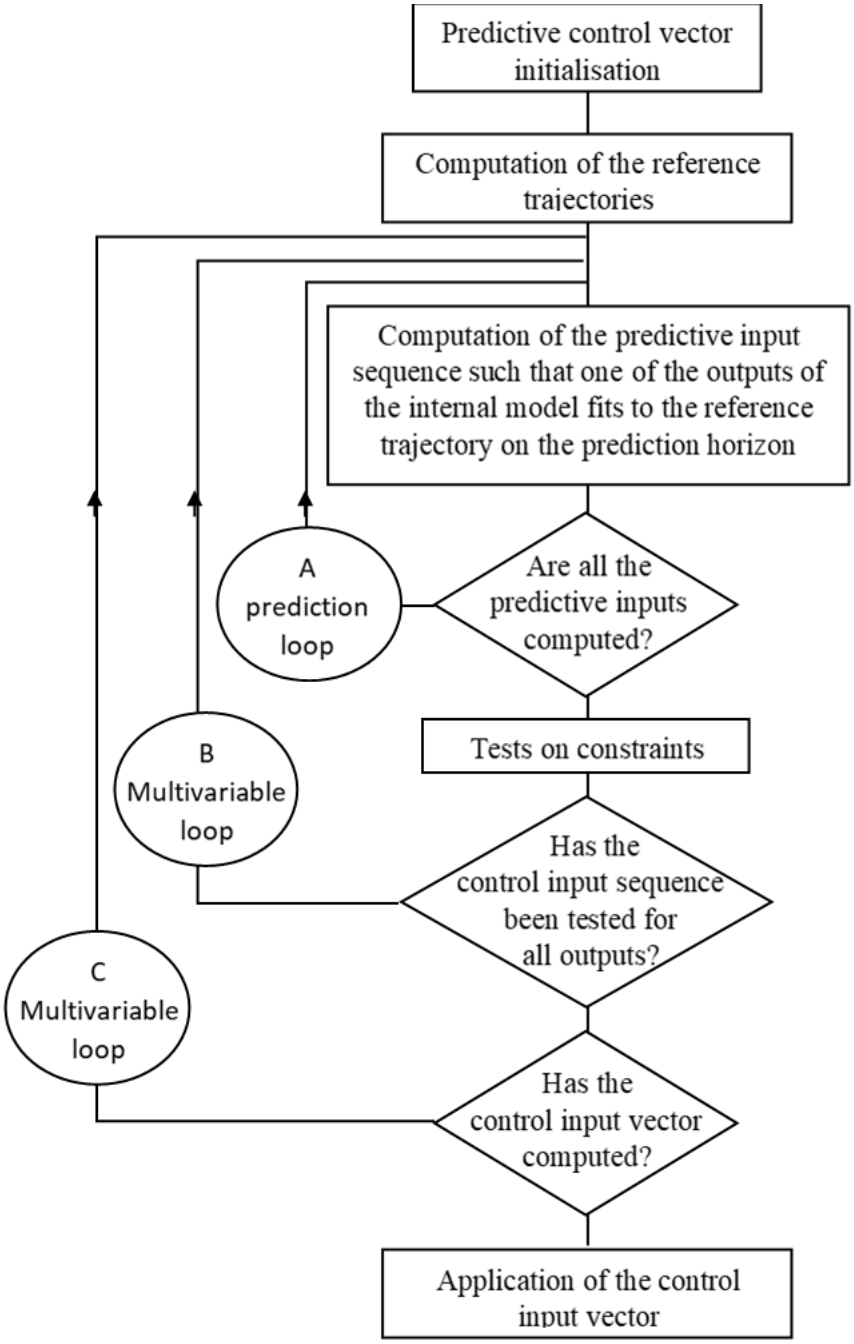

Figure II-1Flow-chart of the model predictive heuristic control (Richalet *et al.*, 1978)

In 1987, David Clarke and co-authors (D. W. Clarke, Mohtadi and Tuffs, 1987; D.W. Clarke, Mohtadi and Tuffs, 1987) introduced the generalized predictive control method (GPC), then hard constraints on input and output variables were included in (Clarke and Scattolini, 1991; Demircioglu and Clarke, 1992). GPC used ideas from generalized minimum variance (GMV) by Clarke and Gauthrop (Clarke and Gawthrop, 1979), and besides the MPC features it had the following main elements:

1. a controlled autoregressive integrated moving average (CARIMA) model,
2. recursion of the Diophantine equation,
3. weighting of control increments, which are set equal to zero beyond a horizon N_2.

The GPC has been attracting more and more interest of the wider community and have been having a big impact on the development of the field. It became one of the most referenced works in its domain(Goodwin, Carrasco and Seron, 2012)(Camacho and Bordons, 2007).

During the 1990s, the model predictive control had been gaining more and more interests in industrial domains, in particular in chemical and petrochemical industries, where the ability of MPC to manage multivariable processes and constraints have led to increasingly performant efficiency and safety. Qin and Badgwell (Qin and Badgwell, 2003) illustrated the foundation applications of the MPC, they depicted MPC practical implementations in different domains. Their review pointed out how MPC could improve control systems strategies; it inspired more researchers and engineers about how MPC could make a transition from conventional PID controllers to more advanced predictive control methodologies. Further, case study works confirmed the effectiveness of MPC in industry, making a foundation for future advancement in the domain (Wilkinson, Morris and Tham, 1994).

Nonetheless, the linear MPC approaches were not very suitable for the fast-developing industrial requirements in terms of performance. The need for handling strong nonlinearities of processes was obvious, and quickly NMPC emerged to cater to this gap. The NMPC includes the resolution of nonconvex nonlinear optimization problems at each sampling time, which result in enhanced flexibility and performance when dealing with complex dynamics. Consequently, several constrained non-convex optimization solutions, including Multiple Shooting Code for Optimization (MUSCOD) (Leineweber, 1996) and Interior Point Optimizer (IPOPT) (Wächter and Biegler, 2006)were created.

At the beginning, and despite the success of the NMPC in the industrial world, the stability of most applications in open-loop and the pragmatic reasoning of engineers, explain why the theoretical aspect of stability in NMPC was not tackled. Then, in 1988, Keerthi and Gilbert (Keerthi and Gilbert 1988) demonstrated the asymptotic stability of the NMPC for discrete time systems using Lyapunov methods. Mayne and Michalska (Mayne and Michalska, 1990) gave a proof for the continuous time case. The contributions of Allgöwer and Zheng (Allgöwer and Zheng, 2000) about modelling, computation aspects, and theoretical and practical issues in NMPC were of the most

pionner in the field among others. Many other studies underlined challenges and potential solutions relating to NMPC, especially those concerning the stability (Mayne *et al.*, 2000).

With the increasing demand for fast control decisions, researchers such as Bemporad and co-authors (Bemporad *et al.*, 2000) focused on explicit MPC. It's a variant of MPC that get rid of online optimization burden by computing the control law off-line. The operating regions in which the optimal control moves are determined so that the online calculus is scaled down to a simple function evaluation. Such function is in most cases piecewise affine and the task requires only basic arithmetic operations (Bemporad, 2021). And as control systems struggle with uncertainties resulting from model inaccuracies and disturbances, advances in robust MPC have become paramount. One of the pioneer works in robust MPC is the work of Kothare and co-authors (Kothare, Balakrishnan and Morari, 1996).

Recently, the development of Stochastic MPC presented a novel approach by incorporating probabilistic constraints and probabilistic objectives, improving resilience against unpredictable scenarios. The notable work of Kouvaritakis and co-authors (Kouvaritakis and Cannon, 2016), applies the tube framework to model predictive control problems including hard or probabilistic constraints to deal with multiplicative and stochastic model uncertainties. It also offers a comprehensive treatment of both robust and stochastic MPC, integrating probabilistic elements into the control formulation.

Application of machine learning and data driven techniques has been regaining the field of model predictive control in recent years (Simpson *et al.*, 2024) (Masero *et al.*, 2023), machine learning models such as neural networks, deep learning and reinforcement learning are used to approximate systems dynamics, enabling controllers to adapt in real time to environmental changes or systems uncertainties. Many approaches, among which temporal difference learning for MPC, use the good abilities of the reinforcement learning in decision-making combined with MPC to give more efficient adaptation in applications (Chitnis *et al.*, 2024).

To conclude this review, one can say that model predictive control has been improving since its beginning, taking advantage of new findings in related fields such as optimization, adaptive and robust control, computational techniques and machine learning… etc. Today, MPC is used in a wide range of industrial applications (Schwenzer *et al.*, 2021), a fact that demonstrates its effectiveness in managing complex systems.

II.4. Parabolic Trough Collector Fields

In solar concentrating collectors, solar radiation is optically reflected or refracted by means of mirrors or lenses, to be afterwards converted into heat by an absorber focal zone. There exist five types of solar energy concentrators(Kalogirou, 2023):

1. Parabolic trough collector (PTC);
2. Linear Fresnel reflector (LFR);
3. Parabolic dish reflector (PDR);
4. Heliostat field collector (HFC);
5. Compound parabolic concentrators (CPC).

As it is mentioned in section I.2, the parabolic trough technology is the most used solar thermal technology in industry, it is also considered as the most mature and advanced one.

II.4.1 PTCs basic design and components

A parabolic trough collector consists of a reflector with high reflectivity, e.g., a mirror, stainless steel sheet or anodized aluminium, in the shape of a through with a parabolic cross-section. A receiver tube is placed in the focal line of the reflector, and it is enveloped in an antireflective glass cover to create a sort of greenhouse effect in order to hinder the absorbed heat loss to the air by convection. Depending on the reflecting area of the collector and the receiving area of the absorber tube, the concentration ratio can reach 30 to 80 (Gharat *et al.*, 2021). To increase absorption, the receiver tube's outer surface is coated with nickel or chromium. As the temperature of the absorber tube increases, it is conferred via convection to the heat transfer fluid. The HTF flows appropriately in the receiver tube to transport the harnessed heat to the usage tank. The concentrators and the absorber tube are posed on a rigid metallic structure endowed with a sun track system. A parabolic trough collector is modulated to a limited number of concentrators for a length that can reach 100m (Goswami, 2022), see Figure II-2. Concatenating parabolic trough collectors in an appropriate scheme gives a PTC-based distributed solar collector field. It's worth to remind that the outlet temperature of a PTC-based DSCF can reach 400°C, depending upon the reflector type, the receiver tube materials and the HTF thermal characteristics. Gharat et al (Gharat *et al.*, 2021) give a comprehensive chronicle development of the PTCs design and components.

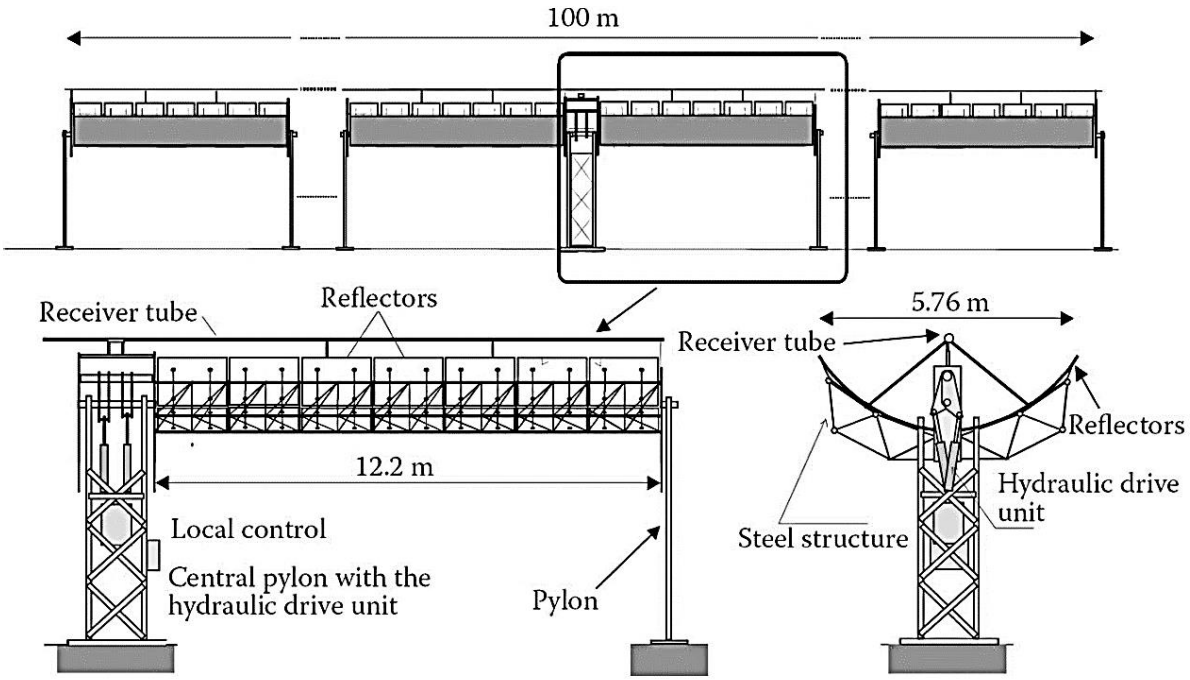

Figure II-2 Sketches of the commercial LS3 Parabolic Trough Collector (Goswami, 2022)

II.4.2 Economic aspects

One important factor of the PTC fields in resisting to economic difficulties is that it's a renewable promising technology for generating electricity and for other industrial uses. It's expected to be a main technique for generating electricity in a soon future.

II.4.2.1. Competitivity and cost efficiency

PTC technology has considerable experience in the field of solar thermal energy, and a big reputation in markets. Moreover, it is most facile to fabricate, and the highly cost effective in comparison with other solar thermal technologies (Kalogirou, 2023). It was demonstrated that it is possible to optimize the design of PTCs such as the collector structure, the tracking system, and the reflector, to reach a capital cost of 75$ to 100$/m^2 of aperture (Gharat *et al.*, 2021). The best of this cost range allows to supply dispatchable electricity, i.e. electrical power when needed, at 0.091 to 0.0103$/kWh , which is more less than that of the electricity generated with natural gas (natural gas driven engines produce electricity at $0.134/kWh) (Biswas *et al.*, 2020).

II.4.2.2. Industrial applications

The harnessed solar energy in a PTC field is very appropriate to be used in thermal electricity power generation plants with steam turbine or other heat engine(Gharat *et al.*, 2021), as well as in many other different industrial processes demanding heat. Tagle-Salazar et al (Tagle-Salazar, Nigam and Rivera-Solorio, 2020) divide industrial applications of PTCs to three main groups Figure II-3 : 1- Electrical 2- Thermal 3- Physical or chemical. While underlying the wide range of applications of PTCs in industry, and as its not of the scope of this work to expound it, the reader is invited to refer to the mentioned reference for more details on the three groups of applications, as well as to (Goswami, 2022) and (Kalogirou, 2023) for comprehensive and deeper details about solar thermal power applications. Meanwhile, 0 gives a list of processes with temperature range where PTC-based DSCFs are used or demonstrated to be appropriate to be used.

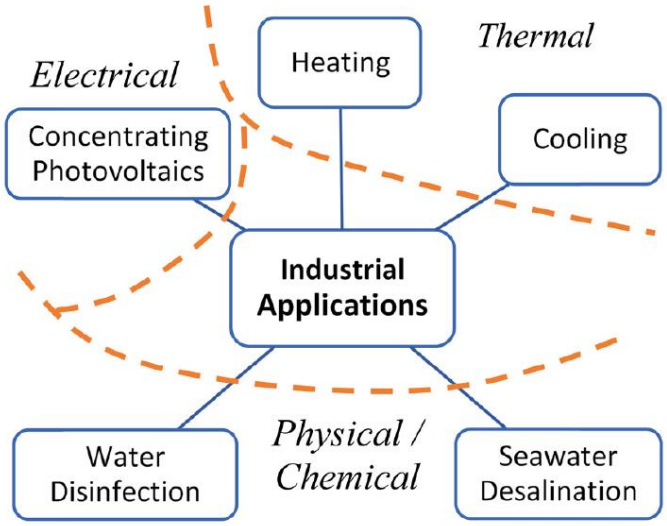

Figure II-3 Classification of industrial applications of PTCs (Tagle-Salazar, Nigam and Rivera-Solorio, 2020).

II.4.3 Control objectives of the outlet temperature in PTC Fields

The main control loop in PTC distributed solar fields aims at driving the temperature of the HTF, leaving the field, to a desired value by acting on the HTF flow rate. The desired value must achieve a maximum solar energy harness. However, reaching the maximum solar energy harvesting must be done along some conditions, constraints and objectives:

II.4.3.1. Maximizing thermal collect efficiency

Maximizing the harvested solar energy does not mean increasing the outlet temperature to highest values. It's possible to harness the same heat quantity in different temperature values. Operating at optimal HTF temperature, can enhance heat absorption, and reduce losses such as radiative and convective ones (Navas, Ollero and Rubio, 2017).

II.4.3.2. Alignment with specification design and preventing system overheating

Maintaining the outlet temperature at appropriate and design range based on materials, coatings, and system constraints, prevents degradation of the HTF, damage in piping, and increase components longevity and the collector performance.

II.4.3.3. Enhancing power generation efficiency

The downstream power generation block, has its own optimum operating conditions, e.g., temperature and pressure, which must be verified. A stabilized temperature on these operating conditions increases the efficiency of the power conversion, hence yields in maximizing electricity generation. It is reported (Camacho, Berenguel and Gallego, 2014) that high temperature improves efficiency in general Rankine vapor cycles.

II.4.3.4. Enabling adaptive energy management and integrating energy storage

A precise control of the outlet temperature allows energy management in PTC based DSCFs. For example, when the solar irradiation fluctuates due to weather changes, controlling temperature ensures consistent energy supply and grid stability. Moreover, precise temperature enhances storage efficiency and extends operational hours.

II.5. State-of-the-art of outlet temperature control in PTC fields

To cater to the objectives cited in the previous section II.4.3, and to surpass difficulties and challenges related to controlling PTC-based DSCFs mentioned in section I.3, many works appeared and many strategies have been proposed and explored. Many overviews also are available in specific and in general contexts (Camacho, F. R. Rubio, *et al.*, 2007; Camacho, F.R. Rubio, *et al.*, 2007; Cirre *et al.*, 2007; Camacho, Berenguel and Gallego, 2014; Lemos, Neves-Silva and Igreja, 2014; Camacho *et al.*, 2024). The methods described in the literature include: proportional-integral-

derivative control and feedforward control (Camacho, Berenguel and Rubio, 1997), cascade control (Rato *et al.*, 1997), adaptive control including gain-scheduling control (GS), Lyapunov functions control and self-tuning control (Camacho, Rubio and Hughes, 1992; Meaburn and Hughes, 1994; Johansen, Hunt and Petersen, 2000; Lemos, Neves-Silva and Igreja, 2014), model predictive control (Camacho, F. R. Rubio, *et al.*, 2007; Camacho and Gallego, 2015; Pipino *et al.*, 2020; Ramón D. Frejo and F. Camacho, 2020), internal model control (Farkas and Vajk, 2002), nonlinear control (Cirre *et al.*, 2007), robust control (Limon *et al.*, 2008), fuzzy logic control (Manjunath and Raman, 2011; Elmetennani and Laleg-Kirati, 2014), and neural network control (Arahal, Berenguel and Camacho, 1998).

II.5.1 Dealing with measured disturbances

The solar irradiance and the inlet HTF temperature are not manipulated variables in the control loop of the outlet temperature in PTC fields. However, they have a main influence on the controlled variable. Thus, they are considered as measured disturbances for which it incumbent to the controller to mitigate their effects on the output. To do so, feedforward controllers are used combined with other control laws. The overall control signal is the sum of the two controllers signals (Camacho, Rubio and Hughes, 1992; Rubio, Berenguel and Camacho, 1995; Cirre *et al.*, 2007; Li, Li and He, 2020). Another method to consider measured disturbances is cascade control, in this strategy two control loops are implemented, an inner loop (slave loop) whose the role is compensating for disturbances, and an outer loop for controlling the output (Rato *et al.*, 1997; Silva *et al.*, 1997). In (Henriques *et al.*, 2002) and (Cardoso, Henriques and Dourado, 1999), the authors took advantage of the information of measured disturbances to elaborate a neural pseudo-inverse model and a fuzzy switch supervisor, respectively, to switch between local PID controllers.

Model predictive control is one of the methods that can directly handle the measured disturbances. MPC's optimization process can take into account the measured disturbances in elaborating the control signals without considering them decision variables. Application of MPC in controlling PTC's outlet temperature will be treated in section II.5.3.

II.5.2 Dealing with the high nonlinearities of the PTC temperature process

As illustrated in (Barão, Lemos and Silva, 2002) and (Camacho, Berenguel and Rubio, 1997), a classical PID controller can't handle all the dynamic modes of the temperature outlet in a

solar PTC field, this is because of high nonlinearity demonstrated by this process. Consequently, unacceptable behavior can show up when relaying on simple PID controllers. For example, oscillations could appear when there is a set-point change, Figure II-4. Understanding PTCs nonlinearities and taking them into account when designing controllers for the outlet temperature can lead to improved performance and stability.

II.5.2.1. Feedback linearization control

In this context, the authors in (Barão, Lemos and Silva, 2002) resorted to an adaptive nonlinear controller based on feedback linearization combined with Lyapunov based adaptation. They performed a nonlinear transformation of the accessible variables of the process, such that the transformed system behaves as an integrator, to which they were able to apply a linear control technique. Other works based on feedback linearization control strategies can be found in the literature as well (Camacho, F.R. Rubio, *et al.*, 2007). Cirre et al (Cirre *et al.*, 2005) used a simple feedback linearization control method with lumped parameter model of the PTC plant, and in a second work (Cirre *et al.*, 2007) with same method, they tried to overcome the drawbacks of the feedforward controllers by considering the inlet-outlet temperature transport delay.

II.5.2.2. Neural networks

Neural networks are also among techniques used to perform nonlinear control for temperature outlet in PTC plants, they were used as controllers, models of the plant, or decision-making systems to optimize or to schedule between other controllers' types. Arahal et al in the two works (Arahal, Berenguel and Camacho, 1997, 1998) used a multilayer perceptron to predict the free response and a linear model to predict the forced response of the system, in order to implement an MPC control law that cope with the system nonlinearities and disturbances. In (Henriques *et al.*, 2002) the authors trained a neural network for scheduling between a set of a priori tuned PID controllers. The neural network is a pseudo inverse-model of the plant in steady state, it has as inputs the solar radiation, the inlet temperature, and the outlet temperature. Henrique et al, (Henriques, Gil and Dourado, 2002) exploited the effectiveness and the stability of the output regulation theory to combine it with a recurrent neural network to result in a straightforward method for solving nonlinear control problem. More recently, Ruiz-Moreno et al (Ruiz-Moreno, Frejo and Camacho, 2021) proposed a neural network that replicates a predictive controller based on nonlinear optimization, thus reducing calculation time and avoiding numerical problems. Based

on the same idea, authors in (Masero *et al.*, 2023) used neural networks to approximate the solutions for optimization problems in a coalitional MPC control law.

II.5.2.3. Fuzzy logic

As in the case of neural networks, fuzzy logic systems were used as direct controllers, as model of the controlled plant or as decision making systems to schedule between other type controllers. The pioneer work (Rubio, Berenguel and Camacho, 1995) used a special subclass of fuzzy inference systems, the triangular partition and triangular partition with evenly spaced midpoints systems, to generate suitable control signals for all the dynamic operating range of a PTC field. Based on this work, two years later, Berenguel et al (Luk *et al.*, 1997) used a fuzzy inference logic to modify the parameters of a PID controller. Recently, Bayas et al (Bayas, Škrjanc and Sáez, 2018) presented a control strategy using Takagi-Sugeno fuzzy models combined with parametric uncertainty robust control approach to deal with nonlinearities of a process and the disturbances that act on it. Many of the works based on fuzzy logic took use of this artificial intelligence technique by combining it with MPC, some of these works will be mentioned in section II.5.3.

II.5.2.4. Adaptive control

Thanks to its inherent responsive quality to nonlinearities, it can be said that adaptive control is a kind of nonlinear control (Camacho *et al.*, 2012). The need for adaptive control in PTC fields comes from the highly time-varying behavior of their dynamics and solar radiation changes. It has been inspiring researchers and engineers in the field of PTCs since the beginning. In (Rubio, Camacho and Carmona, 1986) an adaptive control algorithm, that encompasses a recursive least square identifier with a variable forgetting factor and a PI regulator, was implemented. The regulator uses a supervision level to improve the control. Camacho et al (Camacho, Rubio and Hughes, 1992) used a pole placement self-tuning controller to cope with the problem of high nonlinearities of a PTC plant, and combined it with a series feedforward compensator to deal with measured disturbances, i.e. solar radiation and the HTF inlet temperature changes. A comparison of their results, see Figure II-5, and the results of a constant gain classical PID in Figure II-4, shows the improvements introduced by the adaptive controller in cancelling the oscillations of the temperature when in high values i.e., low level of HTF flow.

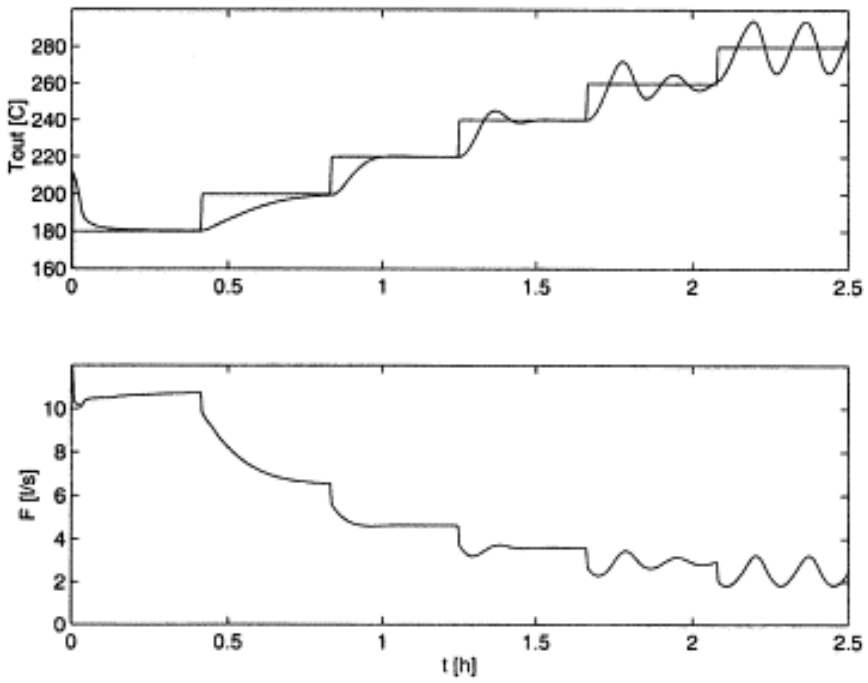

Figure II-4 Constant gain PID control results, the output temperature and the control signal in a PTC (simulation results from (Barão, Lemos and Silva, 2002)).

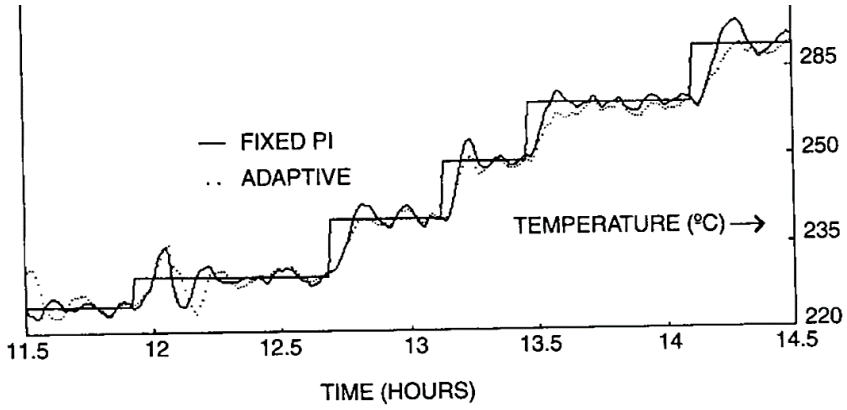

Figure II-5 Self-tuning and series compensator control results for the output temperature of a PTC field (Results from (Camacho, Rubio and Hughes, 1992))

Silva et al. (Silva, Lemos and Rato, 2003) developed a controller relying on a variable sampling time, their approach results in a linearized model of the plant and allows to deal with high sudden changes in the reference signal. In (Lemos, 2006), a trade-off is demonstrated to exist between data-driven and model driven adaptive control in controlling a PTC field. By incorporating more information about plant dynamics, it was shown that the control algorithms yield an increased

performance. Other adaptive control schemes blended with model predictive control are mentioned in the next section.

II.5.3 Model based predictive control in PTCs fields

Model predictive control is the most used technique in controlling the output temperature of PTC fields. This is thanks to its different advantages (see section I.2), and the possibility to be blended with other techniques. In (Meaburn and Hughes, 1996), the authors underlined that using whether adaptive or fixed parameter PI controllers, had been shown to be unsuitable for controlling the output temperature in PTC fields. The reason is that at low frequency the PTC fields possess resonance dynamics that could restrict the bandwidth of such controllers. In their work, it is used an MPC technique that is based on a transfer function representation of the resonance dynamics, tuned using obtained experimental data.

Most of MPC strategies applied to control the temperature in thermal solar power plants are robust, adaptive and nonlinear schemes, including a feedforward term(Camacho, F.R. Rubio, *et al.*, 2007). Mainly, the adaptive predictive control took a large interest of researchers and practitioners in this domain (Camacho, F. R. Rubio, *et al.*, 2007; Lemos, Neves-Silva and Igreja, 2014; Camacho and Gallego, 2015). In (Camacho, Berenguel and Bordons, 1994), a linear adaptive generalized predictive controller was tested in a solar trough field. It was implemented using a method which avoids the heavy computation requirement of this type of controller. More recently, and in the aim of reducing the calculus burden in nonlinear predictive control of the temperature,(Pipino *et al.*, 2020) proposed a formulation of an adaptive MPC application developed within a linear parameter varying formalism.

The work of (Flores *et al.*, 2005), gives a design of two fuzzy predictive controllers and the comparison of their results with a classical MPC. Fuzzy objectives and constraints are used in a fuzzy optimization framework considering multi-objective problems. Ponce et al. (Ponce, Sáez and Núñez, 2014) used a fuzzy Takagi-Sugeno model of the plant to implement a predictive controller in series with a feedforward controller.

A robust adaptive MPC is implemented in (Camacho and Berenguel, 1997). An MPC controller combined with a robust identification mechanism is used to deal with the process dynamics having bounded uncertainties. Different sliding mode predictive controllers are applied

to a PTC field in (Pérez de la Parte *et al.*, 2008), the controllers are based on a first-order model plus a dead time. Limon et al. (Limon *et al.*, 2008) developed a robust model predictive controller based on a linear model with additive bounded uncertainties on the states. The controller is designed for tracking peace-wise constant references. More recently, and always in the context of robust predictive control, the authors in (Pataro *et al.*, 2024) proposed a stochastic nonlinear MPC based on a constraint-chance formulation. This idea coincides well with the nature of the system disturbances, such as solar irradiance, which are mainly a stochastic signal.

Recently, many works using MPC tackling different aspects and difficulties in controlling the temperature in PTC fields have appeared. For example, to maximize the harvested solar power in a PTC field, the work (Ramón D. Frejo and F. Camacho, 2020) proposes a centralized model predictive control. In this work, a comparison is achieved between different MPC approaches: local, distributed and centralized; and also, between different objectives: power maximization, temperature maximization, temperature minimization and no-valves situation. In the same context Masero et al. (Masero *et al.*, 2021; Masero, Maestre and Camacho, 2022) developed a market and a light clustering model predictive control. In (Velarde *et al.*, 2023) it is developed an MPC control strategy for energy scheduling in a parabolic trough collector field, the objective is to sell energy to the grid in the right times in spite of disturbance, namely the intermittence of the irradiance. The work of Song et al (Song *et al.*, 2023) aims at dealing with large-scale commercial trough solar power plants, where the problem of uneven distribution of hydraulic parameters and radiation intensity rises. In (Gallego et al., 2022) it is proposed a nonlinear MPC to control the thermal balance between the CSP loops, thus avoiding overheating problems and energy loss. The issue of the calculus burden in nonlinear model predictive control (NMPC) schemes for large scale solar concentration fields has been recently treated in (Ruiz-Moreno, Frejo and Camacho, 2021) by training a deep neural network to replace an NMPC controller, and by coalitional model predictive techniques in (Masero *et al.*, 2023; Sánchez-Amores *et al.*, 2023).

II.5.4 Gaps in the existing researches and orientation of this work

Usually, NMPC uses analytical first principal models to predict the behaviour of the real process on a given horizon. That requires an online repeated solution of nonlinear optimization problem with a set of nonlinear differential equations, which is time consuming i.e., it’s difficult to ensure the convergence to a solution in a required time, and may lead to numerical problems i.e., the optimal solution is not guaranteed. Furthermore, the theoretical analysis of properties, e.g., the stability, become more difficult. The difficulties related to the optimization process in the NMPC,

can be avoided by the use of artificial neural networks (ANN) (Saki and Fatehi, 2020; Alhajeri *et al.*, 2022). According to (Ungar *et al.*, 1996) it is advisable to use neural networks in nonlinear predictive control for unstable nonlinear dynamic systems or those with inverse actions. In (Hornik, Stinchcombe and White, 1989), the authors demonstrated that with as few as one hidden layer, neural networks are capable of approximating any measurable function to any desired degree of accuracy. In (Saki and Fatehi, 2020), the authors presented a method for neural system identification, in order to be used in nonlinear model predictive control of highly nonlinear dynamic processes, covering both frequent and infrequent operating points, where the simplicity of the ANN to reduce the online optimization burden in the NMPC is considered. In (Masero *et al.*, 2023) it is reported that using neural network in a coalitional MPC strategy provides a reduction in computing time of up to 99.74% compared to the coalitional model predictive controller used as the baseline.

Adaptive MPC control of PTC fields needs extra supervisory mechanisms to side-step some of adaptation problems such as persistent excitations, system/adaptation time scales, etc. In this context, gain scheduling MPC controllers have shown better performance (Cirre *et al.*, 2007). To the best of the knowledge of this work author, neural infinite scheduled gain predictive control has not been applied to solar thermal plants so far. Scheduling gain generalized predictive control was applied to the ACUREX field, at the Platforma Solar de Almeria, in (Camacho, Berenguel and Rubio, 1994), and more recently to the new TCP-100 plant in the same facility, and a Fresnel collector field in (Gallego, Yebra and Camacho, 2018; Gallego, Merello, *et al.*, 2019) respectively. In the three works, the measured disturbances were treated separately of the gain scheduling method by a feedforward controller. This methodology prevents the model based predictive controller from taking advantage of the precious information on the two most significant disturbances i.e., the HTF inlet temperature and the solar irradiance. An interesting strategy was proposed in (Johansen, Hunt and Petersen, 2000) where a pole placement gain scheduling controller is proposed. In this strategy, the dynamics of the plant are divided into 6 operating regimes, a local controller is designed for every local ARX model. The weighting functions used in the interpolation of the gain and the time constant of the overall model are designed to give smooth transition between the operating regimes. It's believed by the authors that the performance of the proposed gain-scheduled controller could be improved by fine tuning the local models and the controllers. However, the number of the considered operating regime was not chosen on a solid basis that ensures the linear models cover all the dynamics of the system, in particular, the anti-resonance modes. In (Alsharkawi and Rossiter, 2017) the authors applied a gain scheduling dual

mode predictive control to the ACUREX field taking into account the measured disturbances by identifying linear models for every disturbance in four operating modes. Unfortunately, this strategy reduces the performance of the overall prediction of the plant output.

In conclusion, NMPC has emerged as powerful technique in controlling the outlet temperature in PTC fields. However, it is confronted to serious challenges like repeated nonlinear optimization in real time under first principles models. This can cause delays, convergence issues, numerical instability. Many works resorted to adaptive linear predictive control to alienate these problems. Again, some problems rise in this case, for example the persistent excitations. In front of such hurdles, gain-scheduling predictive control has done better. On another aspect, artificial neural networks have emerged as a performant tool for complex systems identification such as PTC fields. Meanwhile, blending gain-scheduling MPC with ANN for controlling outlet temperature in PTC fields remains unexplored. Existing strategies using gain-scheduling MPC have shown potential but, in the case of PTC fields, suffer from insufficient consideration of measured disturbances, and unmodeled dynamics when considering operating regimes because of high nonlinearities and resonance in this type of systems. Therefore, developing a gain-scheduling MPC strategy based on a well-trained neural networks model that explicitly exploit available information on the main disturbances, presents a promising research direction in this context.

II.6. Conclusion

This chapter has provided a review of predictive control development and its applications to control the outlet temperature in parabolic trough collector fields. Historical development has been explored to highlight how MPC has adapted to meet the different industrial applications needs and challenges. Besides the foundational principles of MPC, the contribution of related fields in the development of MPC has been depicted— advanced applications incorporating adaptive control, robust control, machine learning and optimization techniques. Parabolic trough collector fields basics were explored as well.

The importance of the outlet temperature control in optimizing energy efficiency, ensuring operational stability, and enabling adaptive energy management was underlined. The chapter explored different control strategies, complexities of PTC systems due to high nonlinearities and changing environmental conditions. The explored state-of-the-art demonstrates that while the classical control techniques offer foundational stability, modern ones provide enhanced

performance and can deal with larger-scale systems. The identified gaps in research include consideration of high nonlinearities of the outlet temperature in PTC fields, the need for fast implementation of NMPC without calculus and numerical problems, and a systematic integration of measured disturbances in the control laws.

The findings of this chapter establish a solid basis for the next chapter by focusing on tailored predictive control strategies for solar PTC fields. Addressing the mentioned gaps promises for further enhancement in controlling the outlet temperature in PTC fields, and consequently in the efficiency and cost-effectiveness of solar thermal PTCs.

Chapter III. Neural Nonlinear Modelling and Control Strategy Development

III.1. Introduction

This chapter details the theoretical foundations for the development of the control strategies based on model predictive control that will be applied to a solar PTC field.

The first part of this chapter focuses on the modelling of the outlet temperature in PTC fields in general, taking into account the distributed nature of this type of processes, and considering the influence of the solar irradiance, HTF inlet temperature, and its flow rate. Following the orientations proposed in the last chapter, this chapter delves into the identification of dynamic nonlinear systems by neural networks, leveraging their capacity of learning and parallel computing in improving the performance of the proposed control strategies. Consequently, the identification procedure using neural networks is detailed.

The second part of this chapter concerns using neural networks in implementing NMPC control strategies to address high nonlinearities and measured disturbances of the PTC plants. Three main schemes are developed, two are for the sake of comparison: constrained neural NMPC and unconstrained neural NMPC. The third is inspired from the findings of the previous chapter: a neural infinite gain scheduling GPC.

III.2. Modelling the outlet temperature in PTC solar fields

In a PTC field, the HTF temperature evolves over time but also along the absorber pipe. This is because the HTF harnesses the thermal solar energy while it flows. Thus, one can realize that it is a distributed parameter process which should be expressed by partial differential equations (PDE). It is also obvious that the HTF flow rate influence inversely its outlet temperature. That gives the opportunity to control the outlet temperature by manipulating the flow rate. This is must be without neglecting the big effect of other variables on this output e.g., the solar irradiance, the HTF inlet temperature, and the collector's concentration efficiency. Etc. All these latter variables are non or considered as non-manipulated variables. Consequently, some of them are considered as measured disturbances, namely, the solar irradiance and the HTF inlet temperature(Camacho *et al.*, 2012).

According to the expected use of the model, many models have been developed for the parabolic trough concentrator fields (Camacho, F. R. Rubio, *et al.*, 2007). In (Camacho, Berenguel and

Rubio, 1997) a distributed model and a concentrated parameter model are detailed and implemented. Other works proposed different modifications and designs to fit to their proposed control techniques (Pipino *et al.*, 2020), and the plant size (Gallego, MacÍas, *et al.*, 2019). The following hypothesis are adopted here for modelling the PTC fields (Camacho, Berenguel and Rubio, 1997):

1. In every element Δl, see Figure III-1, it is considered that:
   - The properties of the heat transfer fluid are considered functions of the actual temperature value.
   - The flow is considered uniform, i.e., equals to its average value.
   - The HTF flow and the irradiance are always the same (an incompressible fluid is considered).
2. Tube wall temperature variations are not taken into account.
3. Losses caused by the conduction of axial heat on both sides of the wall and from the fluid are negligible. The wall is thin and have high heat resistance, and HTF conductivity is poor.

III.2.1 A trade-off precision-complexity model

In the following, the methodology of modelling the outlet temperature of the PTC field is based on the three works in (Carmona, 1985; Lemos et al., 2014; Stuetzle et al., 2004). Some simplifications or extensions are made, namely, neglecting the heat losses and assuming incompressibility of the HTF. Meanwhile, to preserve the property of the high non-linearity of the process, the hypothesis of considering the properties of the oil as functions of the temperature is kept valid. The resulting model is a model with a complexity between that of the aforementioned two models. As mentioned in the thesis scope, the objective is to reduce the need for artificial data because of the leak for real ones.

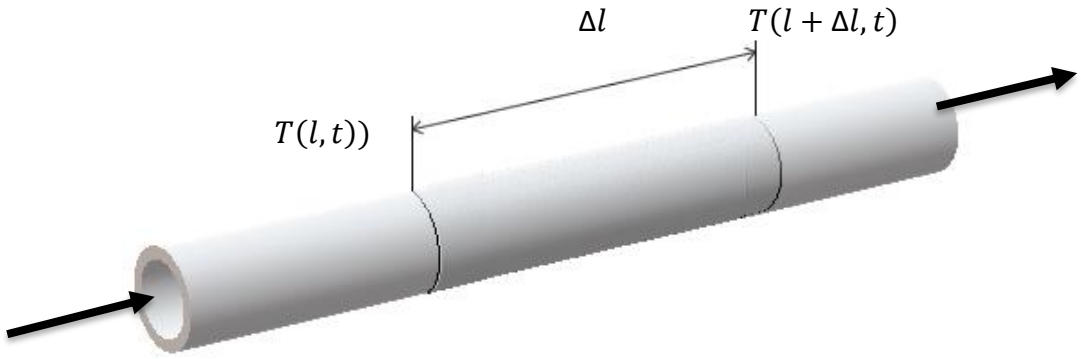

Figure III-1Considered element of the absorber tube.

To find the relation between the influencing physical quantities on the behavior of the outlet temperature in the PTC field, let consider the elementary length in Figure III-1. The enthalpy accumulated in a Δl length element volume of the absorber tube, between two instants time t and $t + \Delta t$ is given by the thermodynamics law:

$$E = \rho_f \, c_f \, A_f \, \Delta l \, [T(l, t + \Delta t) - T(l, t)] \qquad \text{III-1}$$

Where:

l : the space variable (m).

A_f: cross-sectional area of the absorber tube (m^2).

ρ_f : fluid mass density (Kg/m^3).

c_f : fluid specific heat capacity (J /Kg °C).

$T(l, t)$: fluid temperature (°C).

This enthalpy is the sum of two enthalpies (Lemos, Neves-Silva and Igreja, 2014). The first is the difference between the enthalpy entering and the enthalpy leaving the considered element due to fluid flow in Δt time, mathematically:

$$E_1 = \rho_f c_f \, \bar{u}(t) \Delta t \, (T(l, t) - T(l + \Delta l, t)) \qquad \text{III-2}$$

Where $\bar{u}(t)$ is the fluid volumetric flow rate (m^3 /s).

The second one is due to the harvested solar energy between the two points l and Δl in Δt time:

$$E_2 = \eta \, G \, R(t) \, \Delta l \, \Delta t \qquad \text{III-3}$$

Where

$R(t)$: solar irradiance (W/m^2),

η : optical efficiency (Unit-less),

G : concentrator aperture (m).

From the four last equations it follows:

$$\rho_f \, c_f \, A_f \, \Delta l \, [T(l, t + \Delta t) - T(l, t)] = \rho_f c_f \, \bar{u}(t) \Delta t \, (T(l, t) - T(l + \Delta l, t)) + \eta \, G \; R(t) \, \Delta l \, \Delta t \qquad \text{III-4}$$

Dividing by $\Delta t \times \Delta l$, while noting the velocity of the fluid by:

$$u(t) = \frac{\bar{u}(t)}{A_f} \qquad \text{III-5}$$

And defining:

$$\alpha \triangleq \frac{\eta G}{\rho_f c_f A_f} \qquad \text{III-6}$$

It results:

$$\frac{T(l,t+\Delta t)-T(l,t)}{\Delta t} = -u(t)\,\frac{T(l,t)-T(l-\Delta l,t)}{\Delta l} + \alpha R(t) \qquad \text{III-7}$$

The continuous time evolution of the temperature is considered as Δt tends to zero. Then equation III-7 becomes:

$$\frac{\partial T(l,t)}{\partial t} = -u(t)\frac{T(l,t)-T(l-\Delta l,t)}{\Delta l} + \alpha R(t) \qquad \text{III-8}$$

To cover the entire length of the absorber tube, n equations are used:

$$\frac{\partial T(i\,\Delta l,t)}{\partial t} = -\frac{u(t)\left(T(i\,\Delta l,t)-T\big((i-1)\Delta l,t\big)\right)}{\Delta l} + \alpha_i R(t) \qquad \text{III-9}$$

$$i = 1,\ldots n, \text{ and } \; n\times\Delta l = L$$

L is the total length of the absorber tube (m).

The term α in equation III-9 is sub-indexed to express the dependency of the density and heat capacity of the fluid to the actual temperature values.

Define now, $T(i\,\Delta l,t) \stackrel{\text{def}}{=} x_i(t), that$ gives $x_0(t) = T(0,t)$). And noting $\alpha_i = \alpha(x_i)$. Then, the set of differential equations given by equation III-9 can be written in the following form:

$$\begin{aligned}
\dot{x_1}(t) &= -\frac{u(t)}{\Delta l}\left(x_1(t)-x_0(t)\right) + \alpha(x_1(t))R(t)\\
\dot{x}_2(t) &= -\frac{u(t)}{\Delta l}\left(x_2(\mathrm{t})-x_1(t)\right) + \alpha(x_2(t))R(t)\\
\dot{x}_3(t) &= -\frac{u(t)}{\Delta l}\left(x_3(\mathrm{t})-x_2(t)\right) + \alpha(x_3(t))R(t)\\
&\vdots \quad \vdots \qquad \vdots \qquad \vdots\\
\dot{x_n}(t) &= -\frac{u(t)}{\Delta l}\left(x_n(\mathrm{t})-x_{n-1}(t)\right) + \alpha(x_n(t))R(t)
\end{aligned} \qquad \text{III-10}$$

The system of nonlinear differential equations III-10 is implemented in a Simulink® model where every equation is implemented by a copy of the same subsystem block. Note that in Figure III-2 where 10 volume elements are used, the numbered blocks are all the same.

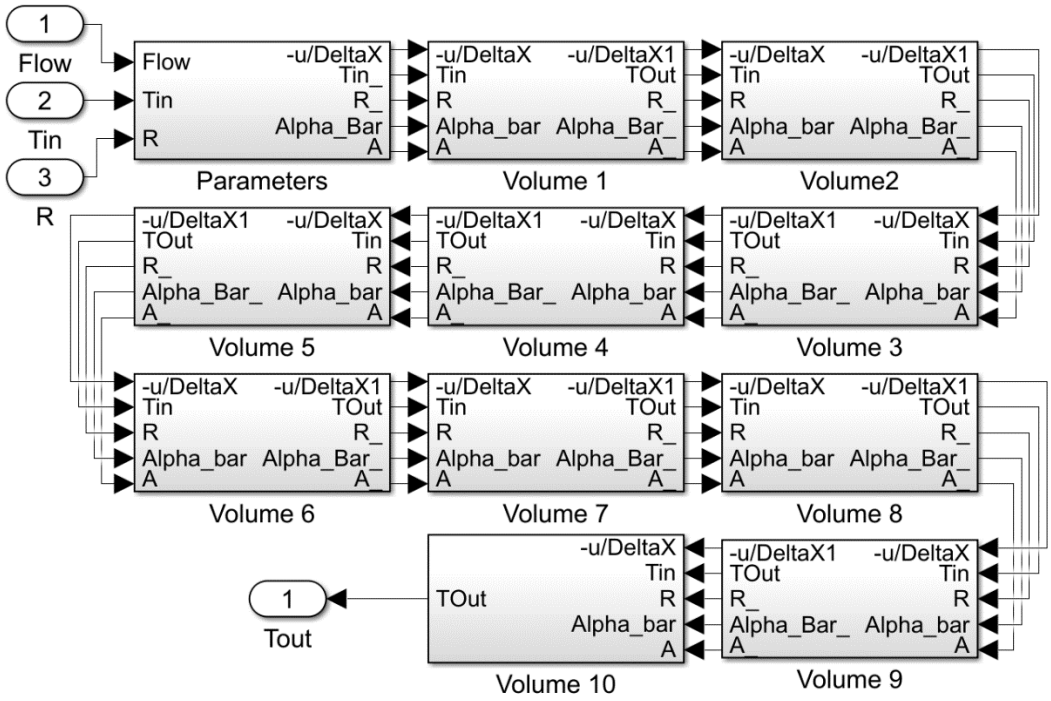

Figure III-2. Simulink® model of a parabolic trough solar field with 10 element volumes

The modification of the space sampling step size is made by deleting or adding (copy and paste) volume blocks from/to the set of the in series linked blocks. A parameter block is used to make easy the modification of the parameters in case where the user is about to model a parabolic trough solar plant other than the one used in this work.

III.3. Neural identification of nonlinear dynamic systems

Neural networks have been an attractive tool for modelling nonlinear dynamic systems. Their ability to learn based on input-output data and generalization to unseen data, have been conferring them a large place of interest in academic and professional fields. Besides the advantages mentioned in section II.5.4, neural networks have the ability to model high nonlinearities, deal with uncertainties, and assume unknown dynamics.

In this section, a brief study of the identification of nonlinear dynamic systems by neural networks is given. Firstly, principals of feedforward neural networks are explained. Afterwards, the Levenberg-Marquardt algorithm for neural networks training is detailed. Then, it is detailed the identification process of nonlinear dynamic systems by neural networks. It’s worth to mention that the fields of neural networks and dynamic systems identification are very large. however, the

content of this section is narrowed to focus on the needed knowledge to understand and enhance the methodology adopted in the next chapter.

III.3.1 Neural networks principals

Neural networks are computer programs for nonlinear computations. A neural network is composed of a set of interconnected processing elements inspired by the biological neurons and operate in parallel. Nodes or neurons can have any number of inputs, and only one output. Weighted connections are used to calculate the output of the neuron by multiplying its inputs by the corresponding weights and summing the results, the result of summation is added to a bias, the overall result is then passed to an activation function to give the output of the neuron. A bias is a weight corresponding to a constant input that equals to 1. Biases allow the neural networks to model more complex relationships by applying an offset to the weighted sum of inputs before passing the result through the activation function. Figure III-3 illustrates a schematic representation of a neuron, the basic processing element of a neural network.

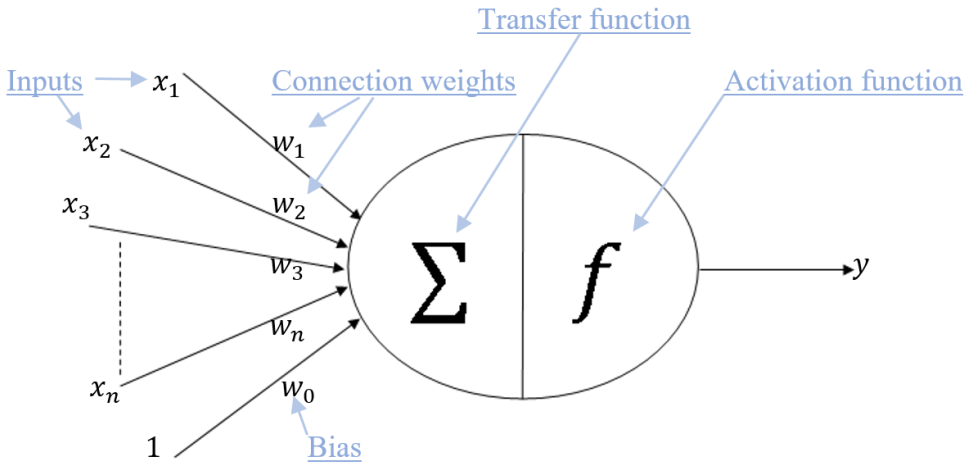

Figure III-3 Schematic representation of an artificial neuron

The output of the neuron in Figure III-3 is calculated as follows:

$$y = f\left(\sum_{i=1}^{n} w_i x_i + w_0\right) \qquad \text{III-11}$$

Connecting the outputs of some neurons to the inputs of other neurons gives an artificial neural network (ANN). The first layer in an ANN is the input layer, where an identity transfer function is used with no activation function, i.e., it only distributes the inputs to the next layer neurons. The layers between the input layer and the output layer are called the hidden layers. It's meant by the output layer the layer that the outputs are the outputs of the neural network. When there are no

connections from the neurons of a layer to the neurons of its previous layers, the ANN is called a feedforward neural network (FFNN). And when every neuron is connected to all neurons of the next layer, the network is called a fully connected feedforward neural network. An example of the structure of a fully connected feedforward ANN is depicted in Figure III-4 with one hidden layer, 4 inputs, 5 neurons in the hidden layer and 3 neurons in the output layer.

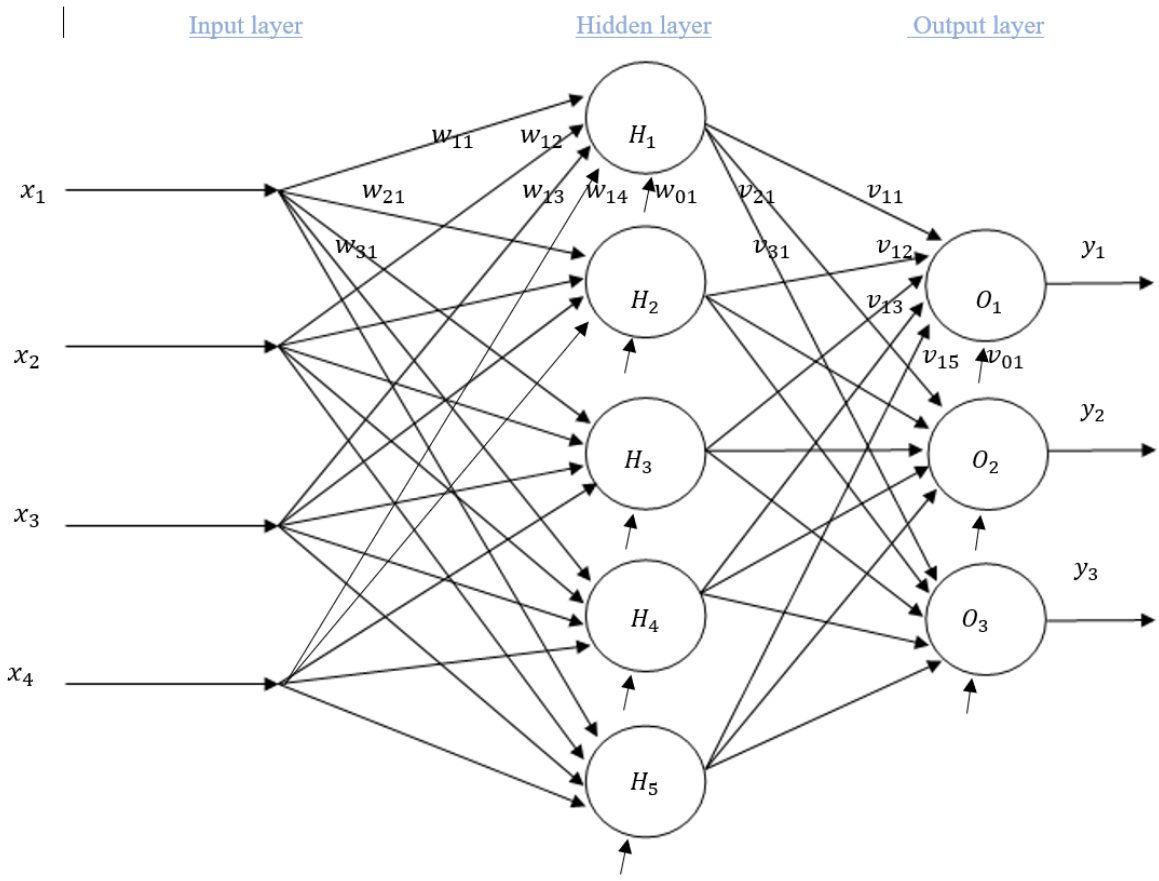

Figure III-4 Fully connected one hidden layer feedforward ANN

To calculate the output of this neural network, let h_i be the output of the i^{th} neuron of the hidden layer, and y_i the output of the i^{th} neuron in the output layer. For the sake of simplicity, let $f(\cdot)$ be the activation function used for all the hidden neurons, and $g(\cdot)$ the activation function used for all the output neurons. It's worth to remind here that generally, neurons in the same layer can have different activation functions. From equation III-11, the outputs of the hidden layer are: $h_i = f\left(\sum_{j=1}^{N_x} w_{ij}x_i + w_{0i}\right), i = 1,2,\dots N_h,$ and those of the output layer are: $y_i = g\left(\sum_{j=1}^{N_y} v_{ij}h_i + v_{0i}\right), i = 1,2,\dots,N_y,$ where N_x is the number of inputs, N_h and N_y are the

numbers of neurons in the hidden and output layers respectively. This gives the outputs of the network as follows,

$$\hat{y}_k = g\left(\sum_{i=1}^{N_h} v_{ki}\ f\left(\sum_{j=1}^{N_x} w_{ij}x_j + w_{0i}\right) + v_{0k}\right), \qquad k = 1,2,\dots,N_y \tag{III-12}$$

Or in a matrix form while considering inputs and outputs as time series data,

$$\hat{y} = F(x,\theta) = g(V\ f(W\ x\ + W_0) + V_0) \tag{III-13}$$

Where, $F(\cdot)$ is the overall function of the neural network, θ is the parameter that includes all the adjustable parameters of the network, i.e., the weights and biases $\{W, W_0, V, V_0\}$, $\hat{y}$ is the N_y dimension vector of outputs, x is the N_x dimension vector of inputs, $V(N_y \times N_h)$ is the weights matrix connecting the hidden neurons to the output layer neurons, V_0 is the biases vector of the output layer neurons of dimension N_y, $W_{N_h \times N_x}$ the matrix of weights connecting the input layer to the hidden layer neurons, and W_0 is the vector of biases of the hidden layer neurons.

III.3.2 Neural networks supervised learning

A neural network learns the behavior of dynamic systems by adjusting its weights to minimize the error between the real system outputs and its own output. This type of neural networks training where the network is fed with target data to learn a behavior is called supervised learning. The process is done using unconstrained optimization combined with the chain rule to retro-propagate the error information to the weights. The first known algorithm in this context was proposed by (Rumelhart, Hinton and Williams, 1986) where the gradient optimization method was used, and the resulting method has been called gradient backpropagation algorithm. To compensate to the drawbacks of the gradient method, e.g., convergence speed, orthogonal direction in the case of optimal step. Etc, the Levenberg-Marquardt optimization algorithm (Marquardt, 1963) was introduced to train neural networks (Hagan and Menhaj, 1994).

Levenberg-Marquardt algorithm is an approximation to the Newton's method, that was designed for least-squares estimation of nonlinear parameters (Marquardt, 1963). In the case of supervised learning of neural networks, one choice to minimize the error between the ANN outputs and the real system outputs is to minimize the following objective function:

$$j(t,\theta) = \frac{1}{2N}\sum_{t=1}^{N}[y(t) - \hat{y}(t,\theta)]^2 = \frac{1}{2N}\sum_{t=1}^{N} e^T(t,\theta)e(t,\theta) \qquad \text{III-14}$$

Where, $y(t)$ contains the plant measured outputs, $\hat{y}(t)$ the neural network outputs given by equation III-13. The minimum of this objective function using Newton's method is calculated recursively as follows,

$$\theta_{k+1} = \theta_k - H^{-1}(\theta_k)\, \mathrm{G}(\theta_k) \qquad \text{III-15}$$

With $H^{-1} = [\nabla^2 j(t,\theta_k)]^{-1}$ and $G(\theta) = \nabla j(t,\theta_k)$ are the Hessian and the gradient of the objective function III-14 respectively.

If the first order Tylor approximation of the error $E(t,\theta)$ around $\theta_k$is considered, i.e.,

$$\begin{aligned} e(t,\theta) \approx \tilde{e}(t,\theta) &= e(t,\theta_k) + [e'(t,\theta)]^T(\theta - \theta_k) \\ &= e(t,\theta_k) + [J(t,\theta_k)]^T(\theta - \theta_k) \end{aligned} \qquad \text{III-16}$$

With $J(t,\theta_k)$ is the Jacobian matrix,

$$J(t,\theta_k) = \frac{\partial \hat{y}(t,\theta)}{\partial \theta}\Big|_{\theta=\theta_k} \qquad \text{III-17}$$

The objective function becomes,

$$j_{apprx}(t,\theta) = \frac{1}{2N}\sum_{t=1}^{N} \tilde{e}^T(t,\theta)\tilde{e}(t,\theta) \qquad \text{III-18}$$

In this case the gradient is the same as for $j(t,\theta)$,

$$G_{apprx}(\theta_k) = G(\theta_k) = \sum_{t=1}^{N} J(t,\theta_k)\left(y(t) - \hat{y}(t,\theta_k)\right) \qquad \text{III-19}$$

But the Hessian differs,

$$H_{apprx}(\theta_k) = \frac{1}{N}\sum_{t=1}^{N} J^T(t,\theta_k)\, J(t,\theta_k) \qquad \text{III-20}$$

$H_{apprx}(\theta_k)$ is called Gauss-Newton Hessian, and using it in calculating θ_{k+1} gives the Gauss-Newton method for updating the neural network weights,

$$\theta_{k+1} = \theta_k - H_{apprx}^{-1}(\theta_k)\, \mathrm{G}(\theta_k) \qquad \text{III-21}$$

In practice, the Gauss-Newton step $\theta_{k+1} - \theta_k = \Delta\theta_k$ is calculated without the inversion of H_{apprx} but by solving,

$$H_{apprx}(\theta_k)\Delta\theta_k = -G(\theta_k) \qquad \text{III-22}$$

The optimum solution θ^* given here came from an approximation of the objective function by first order Tylor series (see equation III-16). It's expected to be optimal only around the neighborhood of the actual iterate θ_k. Consequently, it is proposed to search for the minimum of $J_{apprx}(t,\theta)$ in a ball neighborhood around the current iterate, of a radius ρ_k that expresses a "trust region". This can be expressed by the following constrained optimization problem,

$$\theta_{k+1} = \arg\min_{\theta} J_{apprx}(t,\theta) \text{ subject to } |\theta - \theta_k| \leq \rho_k \qquad \text{III-23}$$

An update expression for θ based on this problem formulation is given in (Marquardt, 1963), which is the core of the Levenberg-Marquardt algorithm,

$$\theta_{k+1} = \theta_k + \Delta\theta_k \qquad \text{III-24}$$

$$\big(H_{apprx}(\theta_k) - \lambda_k I\big)\Delta\theta_k = -G(\theta_k) \qquad \text{III-25}$$

Where, I is an identity matrix with same dimensions as $H_{apprx}(\theta_k)$.

In fact, there is close correspondence between reducing λ_k and increasing the trust region, and vice versa. It's also clear that increasing or decreasing λ_k is a process of switching the behavior of this algorithm between the Gauss-Newton method and the gradient method (steepest descent method). This gave the opportunity to many researchers to propose different methods for adjusting this parameter. In this work, the method explained in (Nørgaard *et al.*, 2000) is adopted.

Table III-1 Levenberg-Marquardt algorithm for neural networks training

1.	Select initial values for θ_0 and λ_0.
2.	Calculate the $\Delta\theta_k$ by using equation III-25.
3.	Calculate the ratio: $\sigma_k = \frac{j(t,\theta_k) - j(t,\theta_k+\Delta\theta_k)}{j(t,\theta_k) - J_{apprx}(t,\theta_k+\Delta\theta_k)}$.
4.	If $\sigma_k > 0.75$ then $\lambda_k = \frac{\lambda_k}{2}$, else if σ_k<0.25 then $\lambda_k = 2\lambda_k$.
5.	If $j(t,\theta_k) > j(t,\theta_k + \Delta\theta_k)$, then accept $\theta_{k+1} = \theta_k + \Delta\theta_k$ and let $\lambda_{k+1} = \lambda_k$.
6.	If the stopping criterion is not satisfied go to step 2.

To exhaust all the details that allow to implement this algorithm, the calculation details of the Jacobian matrix $J(t, \theta_k)$ in equation III-17 are reported in Appendix B.

III.3.3 The identification procedure

System identification is the process of inferring a mathematical representation of the behavior of dynamic systems, using a set of input-output measurements. If the identification process is based only on the measurements data, assuming no or only diminutive information on the real system, then the process is called black-box identification. When a certain knowledge about the real system is used to improve the empirical modelling, gray-box identification is used. This section deals with black-box identification of nonlinear dynamic systems using feedforward neural networks, more precisely, a multilayer perceptron neural network. For more different types of neural networks used in identification of dynamic systems in the framework of MPC, the reader can refer to the tutorial review in (Ren *et al.*, 2022). The objective of this section is to develop a generic identification procedure to be followed in the next chapter, in order to elaborate a neural model of the PTC field.

In this work, the identified neural model of the PTC field will be used in an MPC control scheme. MPC is a model-based control technique, where the controller uses predictions given by the model and the actual data given by sensors, to calculate the convenient control signals that minimize the error between the desired reference and the output of the plant. Hence, the performance of the MPC controller relies on that of the model. Consequently, robust and precise models are very needed in this type of control laws. The first step in neural network black-box identification is to collect input-output data from the real system. Then the structure of the neural network is selected and the weights are trained to acquire the behavior pattern of the system in the input-output data. The resulting neural model is validated in the final step before being implemented in real world. In the following, the steps for the identification of nonlinear dynamic systems using neural networks, depicted in Figure III-5 are detailed.

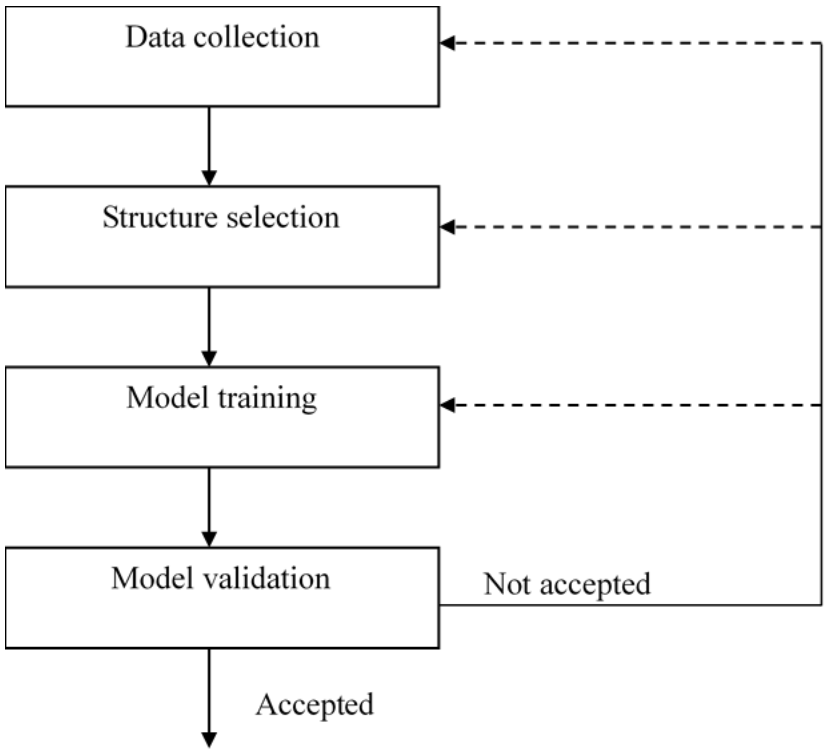

Figure III-5 Neural black-box identification flow chart

III.3.3.1. Data collection in the PTC plant

In this step an experiment on the system is done by exciting it with some inputs and observing the impact on its outputs. However, certain aspects must be considered in this context:

- The choice of the sampling period, where physical insights on the system or observation of the time constants can help in making decision on the value of this period. Capacity of computing and sensors time response must also be taken into account.
- To ensure good and performant results, the plant must be excited by persistent inputs to cover all its operating regimes. Covering all the working amplitude ranges of the system variables does also matter in developing a model that suits for all operating regimes of the plant (Arahal, Berenguel and Camacho, 1998). These two points are almost impossible due to practical constraints such as unmanipulated inputs and safety issues.
- Data pre-processing is a stage where the objective is to obtain an informative data about the system behavior without noise, outliers or effects of unmeasured signals. Data normalization to a specific range is an essential step in data pre-processing in the case of neural identification of dynamic systems. It helps speed up the training and prevent significant differences in the gradient between different input and output variables, which

can lead to drastic changes in weight values, making the training process unstable (Ren *et al.*, 2022). Z-score method, equation III-26, is a technique to perform data normalization and also it is proved to be an efficient way to eliminate outliers (Ren *et al.*, 2022).

$$z = \frac{x - \mu}{\sigma} \qquad \text{III-26}$$

Where, x is the data to be normalized, z is the normalized data, μ is the mean of the data and σ is its standard deviation.

Special situations in the case of solar PTC fields when collecting data for the identification task are to be noticed:

- Because of accumulation of dust on the mirrors, their reflectivity changes. This poses a problem when collecting direct solar radiation data for identification. For this reason, reliable experiments could be done just after cleaning the mirrors.
- Low flow values are not very common during the normal functioning of the plant, but have tremendous importance in the initial operation, where the HTF inlet temperature changes because of stratification in the storage tank and pipelines(Arahal, Berenguel and Camacho, 1998).
- In PTC fields, the experiment could be done under clear and cloudy days to ensure most regimes are covered. It's worth to notice that input-output patterns of under control plants, which is the case of PTC fields, variables are highly correlated, thus giving a poor information data.

III.3.3.2. Neural network's structure selection

As in the classic linear identification of dynamic systems, in neural networks identification, one has to select a structure of the model. By analogy to the linear case, there exists a range of nonlinear model structures, among which one should select the structure that could fit to the application dealt with. A category of such models is autoregressive models e.g., the autoregressive with exogenous inputs (ARX) model, which in the nonlinear case is called nonlinear autoregressive with exogenous inputs (NARX).

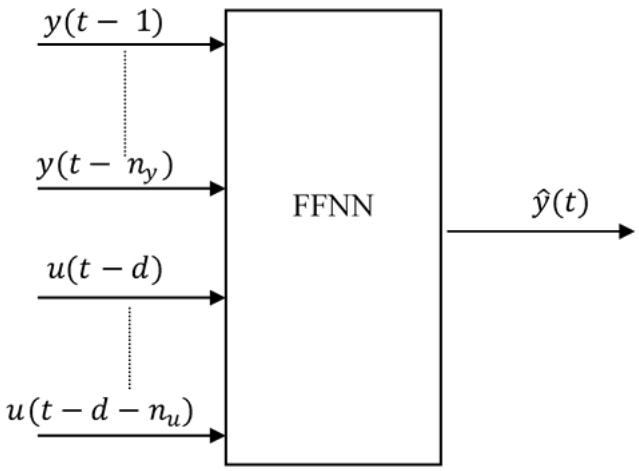

Figure III-6 Nonlinear autoregressive with exogenous inputs model (NARX) structure

In this figure (Figure III-6), n_y and n_u are the numbers of past outputs and past inputs respectively, and d is the dead time of the model. It's to notice that the past outputs are measured outputs but not values of predicted ones. In this latter case, the structure is called the nonlinear output error (NOE). It's also important to say that without the past inputs and outputs of the system fed to the inputs of the model, the FFNN can't model dynamic systems but just static functions. It was reported that in theory the use of NARX feedforward neural models rather than recurrent networks results in no computational loss even though their feedback is limited. And that they are at least equivalent to Turing machines (Siegelmann, Horne and Giles, 1997).

Besides the selection of the nonlinear model structure, and the parameters $n_y, n_u,$ and d for the case of NARX structure. Other hyperparameters of the neural networks are to be determined, namely, the number of hidden layers and neurons in every hidden layer. For the first one, and as it was mentioned earlier in section II.5.4, a neural network with one hidden layer is a universal function approximator when convenient parameters and rich data are used. Many studies about the determination of the number of neurons in hidden layers could be found in the literature(Arahal, Berenguel and Camacho, 1998). One of these methods is the trial-and-error method, where the number of neurons is chosen small enough then increased gradually until no enhancement appears on the performance of the neural network. This procedure is the key idea of many of the so-called constructive algorithms where the topology of the neural network is determined by the training algorithms. Finally, it was reported in (De Ryck, Lanthaler and Mishra, 2021) that using the hyperbolic tangent ($tanh$) activation function makes the optimisation process much easier and results in shallow networks being as expressive as deeper ReLU networks.

III.3.3.3. Model training and validation

In this step, the input-output collected data is divided into two sets, the training dataset and the validation dataset. Sometimes into three datasets (Ren *et al.*, 2022) where the validation dataset is used to adjust the neural network hyperparameters, and a third unseen dataset, the testing dataset, which is used to evaluate the performance of the neural model. The training set is given to the supervised training algorithm, such as the Levenberg-Marquardt algorithm explained in section III.3.2 in order to adjust the weights. The weights adjustment is done offline by minimizing the error between the real output of the system (given by sensors) and the model output, see Figure III-7. In fact, the error minimization is done by minimizing a more convenient objective function, say, the normalized sum of squared errors (SSE) defined in equation III-14.

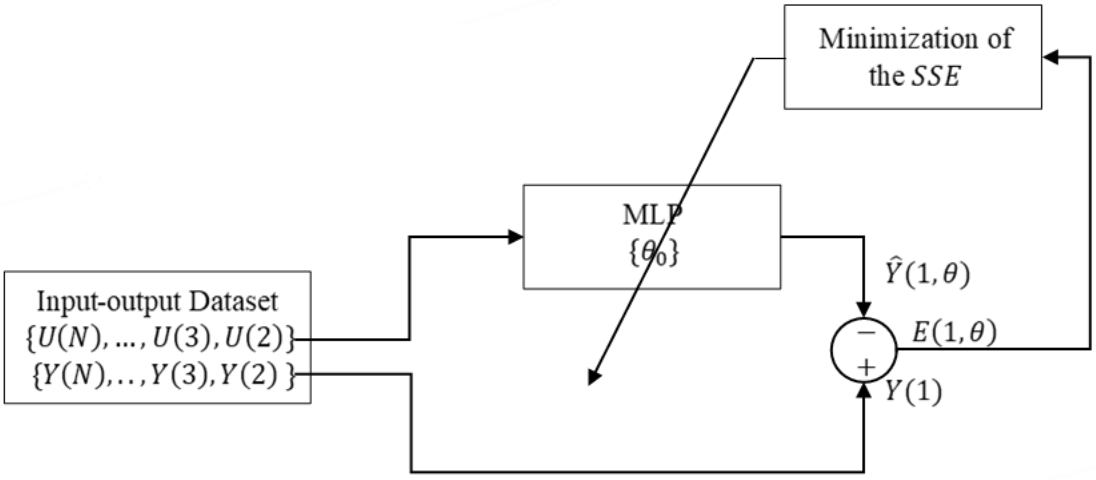

Figure III-7 Adjustment of the weights of an MLP

The provided initial weights in θ_0 could have influence on the results according to the used optimization algorithm. A common way to initialize them is to use random small values (Nørgaard *et al.*, 2000). After the weights are adjusted to a local minimum, the model needs to be tested against unseen validation dataset to check its generalization performance. The residuals, or the prediction errors of the model from the validation data should have no correlation with the used inputs, i.e., the inputs of the validation data. Any correlation is an indication that the model has not fully captured the influence of those inputs on the corresponding outputs. On the other hand, if the prediction errors are small enough, then the training is successful; else, there is either an under-training i.e., the training is not enough, or an over-training i.e., the network has stacked to the example.

III.4. Neural nonlinear predictive control

III.4.1 NMPC problem formulation

The problem of the nonlinear predictive control is to solve online an optimal control problem in a finite horizon under the dynamic constraints of the nonlinear system involving its states and control signals, and probably other limit constraints on the command, the increments of the command and limit on the outputs. These three latter ones are expressed in inequations II-3, II-4, and II-5. In general, the cost function is that mentioned in equation II-1, or more simply the equation II-2. The resulting NMPC problem is presented in equation III-27:

$$\min_{\Delta U} J = \min_{\Delta U}\left(\frac{1}{2}\sum_{i=N_1}^{N_2}\left(r(k+i)-\hat{y}(k+i|k)\right)^2+\frac{1}{2}\sum_{i=1}^{N_u}\lambda\left(\Delta u(k+i-1)\right)^2\right) \quad \text{III-27}$$

$$\begin{aligned} s.t: \quad & u_{min} \le u(k) \le u_{max} \\ & y_{min} \le \hat{y}(k+i|k) \le y_{max} \\ & \Delta u_{min} \le u(k)-u(k-1) \le \Delta u_{max} \end{aligned}$$

With,

$$\begin{aligned} \hat{y}(k+i|k) &= C\,x(k+i|k) \\ x(k+i|k) &= F(\Delta u, x(k+i-1), x(k+i-2), \dots) \\ u(k+i|k) &= u(k+i-1|k)+\Delta u(k+i|k) \end{aligned}$$

Where, $x(k)$ contains the state variables, $F(\cdot)$ is the state space nonlinear function, and C is the matrix mapping the linear relationship between the states and the outputs.

Resolving the resulting optimization problem requires the consideration of a non-convex non-linear problem (NLP) which gives rise to many computational difficulties, where it's not guaranteed to find a global solution and in the worst case a local one. The online solving method must guarantee rapid convergence and must be able to cope with extreme non-linearities.

At each sampling instant, a set of future control actions is calculated over the control horizon $N_u \le N_2$ by solving the NLP in equation III-27. As it is mentioned in paragraph II.2.2.3, for $N_u < i \le N_2$, $u(i)$ are taken equal to $u(N_u)$. Just the first element of the found control set, i.e., $u(k)$, is

applied to the real system, where k is the actual time sample (Lee and Markus, 1967). At the next time sample, new measurements are obtained and the NLP is solved again.

III.4.2 Using a neural network as an internal model in NMPC

In neural nonlinear predictive control, the neural network can be the controller itself (Ruiz-Moreno, Frejo and Camacho, 2021; Masero *et al.*, 2023), a model to predict the free response of the system (Arahal, Berenguel and Camacho, 1997, 1998), or the internal model used to predict future behaviour of the process (Syed and Khalid, 2021). In the latter method, a neural model with one step ahead prediction is used in a loop over the prediction horizon N_2, or a neural structure with N_2-step ahead predictions is used for once. In this work, and based on the explanations given in the paragraph III.3.3.2 a neural network with 1-step ahead prediction is used. Moreover, the neural network is a one hidden layer MLP with the NARX structure model, the activation function for all the hidden layer neurons is the hyperbolic tangent (tanh) and no activation function in the output layer. In this case the cost function in the NMPC optimization problem becomes,

$$\min_{\Delta U} J = \min_{\Delta U}\left(\frac{1}{2}\sum_{i=N_1}^{N_2}(r(k+i)-(V\,tanh(W\,z(k)+W_0)+V_0))^2 + \frac{1}{2}\sum_{i=1}^{N_u}\lambda\left(\Delta u(k+i-1)\right)^2\right) \qquad \text{III-28}$$

where, $z(t) = [y(k-1)\ldots y(k-n)\,u(t-\,d_u-1)\ldots u(k-d_u-m)]$.

Solving this optimization problem by iterative algorithms needs in most cases the calculation of the gradient and the Hessian of the objective function *J*.

III.4.2.1. Calculation of the gradient

$$\frac{\partial J}{\partial \Delta u(k+j)} = \frac{\partial}{\partial \Delta u(k+j)}\left(\frac{1}{2}\sum_{i=N_1}^{N_2}\left(r(k+i)-\hat{y}(\,k+i\mid k\,)\right)^2\right) + \frac{\partial}{\partial \Delta u(k+j)}\left(\frac{1}{2}\sum_{j=1}^{N_u}\lambda\left(\Delta u(k+j-1)\right)^2\right)$$

Let's consider the first term, for each $i \in [N_1, N_2]$, and $j \in [1, N_u]$:

$$\frac{\partial}{\partial \Delta u(k+j)}\left(\frac{1}{2}\left(r(k+i)-\hat{y}(k+i\mid k)\right)^2\right)=-\left(r(k+i)-\hat{y}(k+i\mid k)\right)\frac{\partial \hat{y}(k+i\mid k)}{\partial \Delta u(k+j)}$$

$$=-\left(r(k+i)-\hat{y}(k+i\mid k)\right)\cdot V\frac{\partial\left(tanh(W\,z(k)+W_0)\right)}{\partial \Delta u(k+j)}$$

$$=-\left(r(k+i)-\hat{y}(k+i\mid k)\right)$$

$$\cdot\, V\; diag(1-tanh^2(W\,z(k)+W_0))\,W\,\frac{\partial z(k)}{\partial \Delta u(k+j)}$$

Where, $diag(\cdot)$ is the diagonal matrix.

The second term is straightforward, for each $j \in [1, N_u]$:

$$\frac{\partial}{\partial \Delta u(k+j)}\frac{1}{2}\lambda\left(\Delta u(k+j-1)\right)^2=\lambda \Delta u(k+j-1)$$

The gradient of the cost function in equation III-28 is then:

$$\frac{\partial J}{\partial \Delta u(k+j)}=-\sum_{i=N_1}^{N_2}\left(r(k+i)-\hat{y}(k+i\mid k)\right)$$
$$\cdot V\; diag(1-tanh^2(W\,z(k)+W_0))\,W\frac{\partial z(k)}{\partial \Delta u(k+j)} \qquad \text{III-29}$$
$$+\lambda \Delta u(k+i-1)$$

Where, $j = 1,2,\dots,N_u$

The term $\frac{\partial z(k)}{\partial \Delta u(k+j)}$ is a vector of zeros unless for its element that corresponds to $u(k+j)$ which equals to one (see
Appendix C).

Equation III-29 can be written in compact matrix format:

$$\nabla J=-\left(R-\hat{Y}\right)^T\frac{\partial \hat{Y}}{\partial \Delta U}+\lambda\,\Delta U \qquad \text{III-30}$$

Where, R and $\hat{Y}$ are the reference and the predictions vectors over the prediction horizon N_2, $\frac{\partial \hat{Y}}{\partial \Delta U}$ is the Jacobian matrix of the predictions w.r.t control increments vector (in the case of one output, it would be the gradient of the prediction). ΔU is the control increments vector over the control horizon.

III.4.2.2. Calculation of the Hessian

The Hessian $\nabla^2 J$ contains second derivatives of J with respect to $\Delta u(k+m)$ and $\Delta u(k+n)$ with $n, m \in [1, N_u]$.

Let's consider the first term $\frac{1}{2}\frac{\partial^2 (r(k+i)-\hat{y}(k+i|k))^2}{\partial \Delta u(k+m)\partial \Delta u(k+n)}$, for each $i \in [N_1, N_2]$, and $n, m \in [1, N_u]$:

$$\frac{1}{2}\frac{\partial^2 \left(r(k+i)-\hat{y}(k+i \mid k)\right)^2}{\partial \Delta u(k+m)\partial \Delta u(k+n)} = \frac{\partial \hat{y}(k+i \mid k)}{\partial \Delta u(k+m)} \cdot \frac{\partial \hat{y}(k+i \mid k)}{\partial \Delta u(k+n)} - \left(r(k+i)-\hat{y}(k+i \mid k)\right) \cdot \frac{\partial^2 \hat{y}(k+i \mid k)}{\partial \Delta u(k+m)\partial \Delta u(k+n)}$$

where,

$$\frac{\partial \hat{y}(k+i|k)}{\partial \Delta u(k+n)} = V\ diag(1-tanh^2(W\ z(k)+W_0))\ W\ \frac{\partial z(k)}{\partial \Delta u(k+n)};$$

$$\frac{\partial^2 \hat{y}(k+i|k)}{\partial \Delta u(k+m)\partial \Delta u(k+n)} = V \cdot diag\left(-2tanh(W\ z(k)+W0) \cdot \frac{\partial (W\ z(k)+W_0)}{\partial \Delta u(k+m)} \cdot \frac{\partial (W\ z(k)+W_0)}{\partial \Delta u(k+n)}\right);$$

$\frac{\partial (W\ z(k)+W_0)}{\partial \Delta u(k+n)} = W\ \frac{\partial z(k)}{\partial \Delta u(k+n)} = W_{:,j}$, with j is the index for which $z_j(k)$ corresponds to $\Delta u(k+n)$, (see

Appendix C).

Let's now consider the second term $\frac{1}{2}\frac{\partial^2 \lambda\left(\Delta u(k+m-1)\right)^2}{\partial \Delta u(k+m)\partial \Delta u(k+n)}$, for each $n, m \in [1, N_u]$:

$$\frac{1}{2}\frac{\partial^2 \left(\lambda\left(\Delta u(k+m-1)\right)^2\right)}{\partial \Delta u(k+m)\partial \Delta u(k+n)} = \begin{cases} \lambda, if\ m = n, \\ 0, if\ m \neq n. \end{cases}$$

The Hessian of the cost function in equation III-28 is then:

$$\frac{1}{2}\frac{\partial^2\left(r(k+i)-\hat{y}(k+i\mid k)\right)^2}{\partial\Delta u(k+m)\partial\Delta u(k+n)}$$

$$=\sum_{i=N_1}^{N_2}\left[\frac{\partial\hat{y}(k+i\mid k)}{\partial\Delta u(k+m)}\cdot\frac{\partial\hat{y}(k+i\mid k)}{\partial\Delta u(k+n)}\right.$$

$$\left.-\left(r(k+i)-\hat{y}(k+i\mid k)\right)\cdot\frac{\partial^2\hat{y}(k+i\mid k)}{\partial\Delta u(k+m)\partial\Delta u(k+n)}\right]+\lambda\delta_{mn} \qquad \text{III-31}$$

Where, $n,m=1,2,\dots,N_u$. and $\delta_{mn}=\begin{cases}1, & if\ m=n,\\ 0, & if\ m\neq n.\end{cases}$

Equation III-31 can be written in compact matrix format:

$$\nabla^2 J=\left(\frac{\partial\hat{Y}}{\partial\Delta U}\right)^T\frac{\partial\hat{Y}}{\partial\Delta U}-(R-Y)^T\frac{\partial^2\hat{Y}}{\partial\Delta^2 U}+\lambda\delta_{mn}I. \qquad \text{III-32}$$

With I is the identity matrix.

III.4.3 Unconstrained neural NMPC using the BFGS algorithm

The Broyden-Fletcher-Goldfarb-Shanno (BFGS) algorithm, is a quasi-Newton iterative method for solving unconstrained nonlinear optimization problems. It was separately developed in (Broyden, 1970; Fletcher, 1970; Goldfarb, 1970; Shanno, 1970). As other quasi-Newton methods, the expression for updating the control signal increments using the BFGS is:

$$\Delta U_{k+1}=\Delta U_k+\alpha\, H_k^{-1}\nabla J_k \qquad \text{III-33}$$

Where, ΔJ the gradient of the cost function III-28, it is calculated as in equation III-30 or with more details in equation III-29. α_k is the optimal step size, calculated usually using the Armijo rule, see Appendix D for more details on how to use Armijo rule to calculate an optimal step.

The expression for updating the approximated Hessian inverse in the BFGS algorithm is given by:

$$H_{k+1}^{-1}=\left(I-\frac{\delta_k\gamma_k^T}{\delta_k^T\gamma_k}\right)H_k^{-1}\left(I-\frac{\delta\gamma_k^T}{\delta_k^T\gamma_k}\right)+\frac{\delta_k\delta_k^T}{\delta^T\gamma_k} \qquad \text{III-34}$$

Where, $\delta_k=\Delta U_{k+1}-\Delta U_k$, $\gamma_k=\nabla J_{k+1}-\nabla J_k$, and I is the identity matrix.

The BFGS algorithm for computing the control signal in neural NMPC is given in the following table.

Table III-2 The BFGS algorithm for neural NMPC

1.	Initialization: ΔU_0, $H_0^{-1} = I, \varepsilon$(precision), $k = 0$ and go to 2
2.	Find the optimal step size by Armijo rule (see Appendix D)
3.	Calculate the new iterate ΔU_{k+1} by using equation III-33
4.	Calculate $\delta_k = \Delta U_{k+1} - \Delta U_k, \gamma_k = \nabla J_{k+1} - \nabla J_k$, (use equation III-29 to calculate ∇J)
5.	Calculate H_{k+1}^{-1} from equation III-34
6.	If $\lvert \Delta U_{k+1}^*(k) - \Delta U_k^* \rvert < \varepsilon$ stop, else go to next step.
7.	$k = k + 1$, and go to step 2.

III.4.4 Constrained neural NMPC using the interior-point method

Interior Point methods (IP) or barrier methods are a class of algorithms designed to find optimal solution in constrained linear and nonlinear optimization problems by searching for the minimum in the interior of the feasible region. Interior point methods use a barrier term in an augmented objective function to prevent inequality constraints violation. The foundational works of this method are (Dikin, 1967; Karmarkar, 1984).

Let's consider the nonlinear predictive control problem presented by the nonlinear optimization problem in equation III-28, under the inequality constraints related to control signal in the problem in equation III-27. These constraints can be written in the standard form $c_j(\mathrm{u}) \leq 0$ as follows:

$$c_j(\mathrm{u}) = \begin{cases} u_{min} - u(k+i), & \text{for inputs lower bounds,} \\ u(k+i) - u_{max}, & \text{for inputs upper bounds,} \\ \Delta u_{min} - \Delta u(k+i), & \text{for increments lower bounds,} \\ \Delta u(k+i) - \Delta u_{max}, & \text{for increments upper bounds.} \end{cases}$$

The interior point method tackles the resulting constrained optimization problem by reformulating it into an unconstrained problem using the inequality constraints as a barrier function, the cost function of the resulting unconstrained problem is as following:

$$\Phi = J - \mu \sum_{j=1}^{m} \ln\left(-c_j(\mathrm{u})\right) \qquad \text{III-35}$$

Where, J is the cost function in equation III-28, μ is the barrier parameter, m is the number of inequality constraints, $\ln(\cdot)$ is the logarithmic function, and $c_j(\mathrm{u})$ are the inequality constraints.

The gradient of the cost function Φ is the sum of the gradient of J (already developed, see equation III-29) and the gradient of the barrier function. The derivative of the barrier function of every constraint w.r.t $u(k+i)$ for $i \in [1, N_u]$ is:

$$\frac{\partial\left(-\mu \ln\left(-c_j(u(k+i))\right)\right)}{\partial u(k+i)} = -\frac{\mu}{-c_j(u(k+i))}\frac{\partial c_j(u(k+i))}{\partial u(k+i)}$$

And its Hessian is the sum of the Hessian of J (already developed, see equation III-31) and the Hessian of the barrier function. The second derivative of the barrier function of every constraint w.r.t $u(k+i)$ for $i \in [1, N_u]$ is:

$$\frac{\partial^2\left(-\mu \ln\left(-c_j(u(k+i))\right)\right)}{\partial^2 u(k+i)}$$
$$= \sum_{j=1}^{m}\left(\frac{\mu}{c_j^2 u(k+i)} \cdot \frac{\partial c_j\big(u(k+i)\big)}{\partial u(k+i)} \cdot \frac{\partial c_j\big(u(k+i)\big)}{\partial u(k+i)}\right.$$
$$\left. - \frac{\mu}{c_j(u(k+i))}\frac{\partial^2 c_j(u(k+i))}{\partial^2 u(k+i)}\right)$$

In the case where there are no equality constraints, the problem of minimizing the augmented cost function Φ in equation III-35 can be solved with any unconstrained optimization method (steepest descent, BFGS…, etc.).

However, in the existence of linear or linearized equality constraints in the form of $A\,u(k+i) = b$, the resulting optimization problem can be resolved by resolving the Karush-Kuhn-Tucker (KKT) system:

$$\begin{bmatrix} \nabla^2\Phi(\Delta U, \mu) & A^T \\ A & 0 \end{bmatrix}\begin{bmatrix} \Delta U \\ \lambda \end{bmatrix} = \begin{bmatrix} -\nabla\Phi(\Delta U, \mu) \\ b \end{bmatrix} \qquad \text{III-36}$$

Where, $\nabla^2\Phi$ is the hessian of the cost function, Φ, and $\nabla\Phi$ is its gradient, λ is the Lagrangian multiplier of the equality constraints.

The interior point algorithm steps are explained the following table.

Table III-3 The interior point algorithm for neural NMPC

1.	Initialization: $\Delta U_0 \mid c_j(\Delta U_0) < 0, \mu_0 > 1, c < 1, k = 0, \varepsilon$(precision).
2.	Minimize Φ in equation III-35 by using any of the unconstrained optimization methods (In the case of the presence of equality constraints solve the KKT system in equation III-36).

3.	If $\lvert\Delta U^*_{k+1}(k) - \Delta U^*_k\rvert < \varepsilon$ stop, else go to next step.
4.	$\mu_{k+1} = c\,\mu_k$
5.	$k = k + 1$, and go to step 2.

III.5. Generalized predictive control

Generalized predictive control is an MPC control technique that was proposed by (D. W. Clarke, Mohtadi and Tuffs, 1987). It uses the concept of prediction and control horizons as well as the weights of control increments in its cost function. GPC design framework enables a larger diversity of control objectives compared to other MPC approaches. It can deal with open-loop unstable and nonminimum phase systems(Camacho and Bordons, 2007). One important characteristic of this technique is that, in the case of unconstrained control, it provides an analytical solution of the optimal control signal.

III.5.1 The GPC predictor

It has been argued in (D. W. Clarke, Mohtadi and Tuffs, 1987) that plants with non-stationary disturbances (for example plants with changes in material quality or plant relying on energy balance), admit a locally linearized model around an operating point in the form of a controlled autoregressive integrated moving average model (CARIMA):

$$A(q^{-1})y(t) = q^{-d_u}B(q^{-1})u(t-1) + \frac{C(q^{-1})\xi(t)}{\Delta} \qquad \text{III-37}$$

Where, q^{-1} is the time backward shift operator, the differencing operator: $\Delta = (1 - q^{-1})$, $y(t)$ and $u(t)$ are the output and the input of the model, d_u is the dead time according to the input $u(t)$. And $\xi(t)$ is a zero mean white noise.

The polynomials $A(q^{-1})$ and $B(q^{-1})$ are defined by:

$$A(q^{-1}) = 1 + a_1 q^{-1} + \cdots + a_n q^{-n}.$$
$$B(q^{-1}) = b_0 + b_1 q^{-1} + \cdots + b_m q^{-m}.$$

The polynomial $C(q^{-1})$is chosen equal to 1 for simplicity. The model in equation III-37 becomes then:

$$A(q^{-1})y(t) = q^{-d_u}B(q^{-1})u(t-1) + \frac{\xi(t)}{\Delta} \qquad \text{III-38}$$

A k-step ahead predictor $\hat{y}(t+k|t)$ is derived based on the model in equation III-38 by using the Diophantine equation defined as follows (D. W. Clarke, Mohtadi and Tuffs, 1987):

$$1 = \Delta\, A(q^{-1})E_k(q^{-1}) + q^{-k}F_k(q^{-1}) \qquad \text{III-39}$$

Given $A(q^{-1})$ and the prediction interval j, the polynomials $E_k(q^{-1})$ and $F_k(q^{-1})$ with degrees $(k-1)$ and n respectively, are uniquely defined:

$$F_k(q^{-1}) = f_{k,0}q^{-1} + f_{k,1}q^{-1} + \cdots + f_{k,n}q^{-n}$$
$$E_k(q^{-1}) = 1 + e_{k,1}q^{-1} + \cdots + e_{k,k-1}q^{-(k-1)}$$

Multiplying III-38 by $E_k(q^{-1})\Delta$ gives:

$$E_k(q^{-1})\Delta\, A(q^{-1})y(t) = E_k(q^{-1})\, \Delta\, q^{-d_u}B(q^{-1})u(t-1) + E_k(q^{-1})\xi(t) \qquad \text{III-40}$$

Equation III-39 can be written as:

$$E_k(q^{-1})\Delta A(q^{-1}) = 1 - q^{-k}F_k(q^{-1})$$

By substituting this latter in equation III-40 it results:

$$\left(1 - q^{-k}F_k(q^{-1})\right)y(t) = E_k(q^{-1})\Delta\, q^{-d_u}B(q^{-1})u(t-1) + E_k(q^{-1})\xi(t)$$

Now multiplying by q^{+k}:

$$y(t+k) - F_k(q^{-1})y(t) = E_k(q^{-1})B(q^{-1})\Delta u(t+k+d_u-1) + E_k(q^{-1})\xi(t+k)$$

It's to notice that as $E_k(q^{-1})$ has a degree of $(k-1)$ the noise components, when multiplied by the polynomial $E_k(q^{-1})$, are all in the future. By taking the expectation operator, $E[\xi(t)] = 0$ and the expected value of $y(t+k)$ becomes:

$$\hat{y}(t+k|t) = G_k(q^{-1})\,\Delta u(t+k-d_u-1) + F_k(q^{-1})y(t) \qquad \text{III-41}$$

Where $G_k(q^{-1}) = E_k(q^{-1})B(q^{-1})$

The Table III-4 gives an implementation of the recursion of the Diophantine explained in (D. W. Clarke, Mohtadi and Tuffs, 1987; Nørgaard *et al.*, 2000; Camacho and Bordons, 2007) for the calculation of the polynomials $E_k(q^{-1})$ and $F_k(q^{-1})$.

Table III-4 Algorithm to calculate the Diophantine polynomials

1.	$\tilde{A}(q^{-1}) = (1 - q^{-1})A(q^{-1})$
2.	$G(1) = B(q^{-1})$
3.	$E_1(q^{-1}) = 1$
4.	$F_1(q^{-1}) = q[1 - \tilde{A}(q^{-1})]$
5.	For $k = 1$ to N_2
6.	$G_{1+k}(q^{-1}) = G_k(q^{-1}) + q^{-1}B(q^{-1})f_{k,0}$
7.	$e_{k,k+1} = f_{k,0}$
8.	For $i = 0$ to n
9.	$f_{k+1,i} = f_{k,i+1} - \tilde{a}_{i+1} f_{k,0}$
10.	End
11.	End

From equation III-41, the k-step ahead predictions can be written as:

$$\begin{aligned}
\hat{y}(t+1|t) &= G_k(q^{-1})\Delta u(t+d_u) + F_k(q^{-1})y(t) \\
\hat{y}(t+2|t) &= G_k(q^{-1})\Delta u(t+1+d_u) + F_k(q^{-1})y(t) \\
&\vdots \qquad\qquad \vdots \qquad\qquad \vdots \\
\hat{y}(t+N_2|t) &= G_k(q^{-1})\,\Delta u(t+N_2-d_u-1) + F_k(q^{-1})y(t)
\end{aligned}$$

Multiplying by q^{d_u} and separating past and future terms, these predictions can be put in matrix form as follows:

$$\hat{Y} = \mathrm{G}\,\Delta U + \mathrm{F}(q^{-1})\,y(t) + \mathrm{G}'(q^{-1})\,\Delta u(t-1) \qquad \text{III-42}$$

Where, $\hat{Y} = \begin{bmatrix} \hat{y}(t+d_u+1|t) \\ \hat{y}(t+d_u+2|t) \\ \vdots \\ \hat{y}(t+d_u+N_2|t) \end{bmatrix}$, $\Delta U = \begin{bmatrix} \Delta u(t) \\ \Delta u(t+1) \\ \vdots \\ \Delta u(t+N_2-1) \end{bmatrix}$, $\mathrm{G} = \begin{bmatrix} g_0 & 0 & \dots & 0 \\ g_1 & g_0 & \dots & 0 \\ \vdots & \vdots & \vdots & \vdots \\ g_{N-1} & g_{N_2-2} & \dots & g_0 \end{bmatrix}$

$$\mathrm{G}'(q^{-1}) = \begin{bmatrix} \left(G_{d_u+1}(q^{-1}) - g_0\right)q \\ \left(G_{d_u+2}(q^{-1}) - g_0 - g_1 q^{-1}\right)q^2 \\ \vdots \\ \left(G_{d_u+N_2}(q^{-1}) - g_0 - g_1 q^{-1} - \dots - g_{N_2-1}q^{-(N_2-1)}\right)q^{N_2} \end{bmatrix}, \quad \mathrm{F}(q^{-1}) = \begin{bmatrix} F_{d_u+1}(q^{-1}) \\ F_{d_u+2}(q^{-1}) \\ \vdots \\ F_{d_u+N_2}(q^{-1}) \end{bmatrix}.$$

With N_2 is the prediction horizon.

By putting $\phi = F(q^{-1})\, y(t) + G'(q^{-1})\, \Delta u(t-1)$ the predictor becomes:

$$\hat{Y} = \mathrm{G}\, \Delta U + \phi \qquad \text{III-43}$$

Where, ϕ is the free response depending on past and present signals. It can be also calculated recursively (Camacho and Bordons, 2007).

III.5.2 The GPC control law

Once the predictor is ready, it is now time to choose the objective function to be minimized. Reconsider again the cost function in equation II-2, putting $N_2 = N_u$ and $N_1 = 1$, rewriting it in a matrix form and substituting the predictions over the horizon N_2 by their expression in equation III-43, gives:

$$J(t, \Delta U) = [R - \mathrm{G}\, \Delta U - \phi]^T [R - \mathrm{G}\, \Delta U - \phi] + \lambda\, \Delta U^T\, \Delta U \qquad \text{III-44}$$

When there's no constraints, increments of the control actions are given in an analytical expression obtained by setting the derivative of this criterion equal to zero:

$$\frac{\partial J(t, \Delta U)}{\partial \Delta U} = 2\mathrm{G}^T \mathrm{G}\, \Delta U - 2\mathrm{G}^T (R - \phi) + 2\lambda\, \Delta U = 0$$

Which gives:

$$\Delta U = [G^T G + \lambda\, I]^{-1} G^T (R - \phi) \qquad \text{III-45}$$

Just the first element of ΔU is applied and the same calculation is repeated next time new measurements are provided by sensors. If a control horizon is considered, then the elements of ΔU after the sample time N_u are equal to zero, which reduce the computations, in particular of the inverse matrix which becomes of dimension $N_u \times N_u$.

III.6. A neural gain-scheduling GPC control of the PTC field

III.6.1 The control strategy

As it was explained in section II.5.4, MPC gain-scheduling would be a good strategy when the measured disturbances are taken into account directly by the MPC controller. MPC is a natural way to consider measured disturbance because it elaborates an optimal control signal based on future predictions and estimations. In this part of the thesis, the objective is to elaborate a gain

scheduling GPC controller for the PTC field expressed by the nonlinear model in equation III-10, where it's important to remind that $x_0(t) = T(0,t)$ and $R(t)$ are measured disturbances that have important influence on the field outlet temperature. The strategy is to use an ANN model to reduce the computations and to assure a maximum performance and capture of the plant nonlinear dynamics. In every sampling time, the neural model is linearized around the actual operating point, and a linear GPC control law is applied using the linearized model. This strategy presents a lot of advantages among which reducing the computation time and avoiding the problems encountered when resolving the NLP, by providing an analytical solution. The instantaneous linearization of the neural model is a smart low calculus way to deal with high nonlinearities of the temperature process in the PTC fields. It results in more precise local linear models than considering only some operating regimes.

III.6.2 Instantaneous linearization of the neural model

Assume the function linking the input to the output of the considered process has been identified by a nonlinear autoregressive exogenous (NARX) model under the form of a one hidden layer multi-perceptron, with a hyperbolic tangent activation function in the hidden layer, and a linear activation function in the output layer. With this topology, the neural overall function in equation III-13 becomes:

$$y(t) = F\big(z(t)\big) = V\tanh(W\,z(t) + W_0) + V_0 \qquad \text{III-46}$$

Where, $z(t)$ is the input vector of the NARX neural model:

$$z(t) = [y(t-1)\ldots y(t-n)u(t-\ d_u - 1)\ldots u(t-d_u-1-m)]$$

Using the first-order Taylor series expansion to linearize the function $F([y(t-1)\ldots y(t-n)u(t-\ d_u-1)\ldots u(t-d_u-1-m)])$ around an operating point $z(\tau)$ gives:

$$y(t) = -a_1\tilde{y}(t-1) - \ldots - a_n\tilde{y}(t-n)\ + b_0\tilde{u}(t\ -\ d_u - 1) + \ldots + b_m\tilde{u}(t\ -\ d_u - 1 - m) \qquad \text{III-47}$$

Where ,

$$\tilde{y}(\,t-i\,) =\ y(t-i\,) - y(\tau - i\,)$$
$$\tilde{u}(\,t-i\,) =\ u(t-i\,) - u(\tau -\ i)$$

And

$$a_i = -\frac{\partial F\big(z(t)\big)}{\partial y(t-i)}\bigg|_{z(t)=z(\tau)}$$

$$b_i = \frac{\partial F\big(z(t)\big)}{\partial u(t-d_u-i)}\bigg|_{z(t)=z(\tau)}$$

The details of developing a general expression for the calculation of the partial derivatives of the function $F(z(t))$ with respect to any input $z_i(t)$ i.e., $\frac{\partial F(z(t))}{\partial z_i(t)}$ is given in Appendix C.

Putting the elements of the current instant τ in equation III-47 on one side gives:

$$y(t) = \big(1 - A(q^{-1})\big)y(t) + q^{-d_u}B(q^{-1})u(t-1) + \zeta(\tau)$$

Or

$$A(q^{-1})y(t) = q^{-d_u}B(q^{-1})u(t-1) + \zeta(\tau) \qquad \text{III-48}$$

The linearization offset $\zeta(\tau)$ is defined by:

$$\zeta(\tau) = y(\tau) + a_1 y(\tau-1) + \ldots + a_n y(\tau-n) - b_0 u(\tau-d_u-1) + \cdots + b_m u(\tau-d_u-1-m)$$

It's clear that the resulting model in equation III-48 is an ARX linear model, affected by a disturbance $\zeta(\tau)$ depending on the current operating point. Modelling the offset term $\zeta(\tau)$ as an integrated white noise and determining the future predictions as the minimum variance predictions makes this model identical to the CARIMA model, in equation III-38, used in the development of the GPC control law.

III.6.3 Taking the measured disturbances into account

As it was explained earlier, in the PTC fields, the solar irradiance $R(t)$ and the HTF inlet temperature $T(t,0)$ (or $T_{in}(t)$) have a big influence on the outlet temperature $T_{out}(t)$.It's needed then to consider a such situation. In this case, where the process behaviour is affected with a measured disturbances $v(t)$, they are taken into account as unmanipulated inputs. This means the measured disturbances and their future predictions are fed to the MPC controller, i.e., they are known (they are not decision variables in the optimization problem). The input vector to the neural network is then:

$$z(t) = [y(t-1) \dots y(t-n)\ u(t-d_u) \dots u(t-d_u-m)\ v(t-d_v) \dots v(t-d_v-p)]$$

With $v(t)$ is the measured disturbance and d_v is the dead time according to $v(t)$.

Thus, a term is added to the model in equation III-48:

$$y(t) = \left(1 - A(q^{-1})\right)y(t) + q^{-d_u}B(q^{-1})u(t-1) + q^{-d_v}D(q^{-1})v(t) + \zeta(\tau) \qquad \text{III-49}$$

Where,

$$D(q^{-1}) = d_0 + d_1 q^{-1} + \cdots + d_p q^{-l}$$

The elements d_i of $D(q^{-1})$ are given by:

$$d_i = \left.\frac{\partial F\left(z(t)\right)}{\partial v(t-d_v-i)}\right]_{z(t)=z(\tau)}$$

Running through the same steps taken in developing the predictor in equation III-43, the predictor for the case with measured disturbances is:

$$\hat{Y} = G\ \Delta U + H\ \Delta V(t) + \phi \qquad \text{III-50}$$

Where $H = E_k(q^{-1})D(q^{-1})$. H components are the coefficients of the system step response according to the measured and future estimated disturbance signals, respectively $v(t)$ and $\hat{v}(t)$.

Putting $H\ \Delta V(t) + \phi\ = \Phi$, the predictor in equation III-50 becomes:

$$\hat{Y} = G\ \Delta U + \Phi \qquad \text{III-51}$$

Φ is the process response due to the initial conditions and the future disturbances.

The predictor now has the same form as the predictor developed for the case without measured disturbances, equation III-43 Consequently, the generalized predictive controller for the process with measured disturbances is obtained by replacing ϕ in the analytical solution in equation III-45 by Φ. The overall scheme of the explained neural network infinite gain scheduling predictive control is depicted in Figure III-8 where the future estimated disturbances are noticed by $\hat{v}(t+N_1 \dots t+N_2)$, and the future references are noticed by $r(t \dots t+N_2)$.

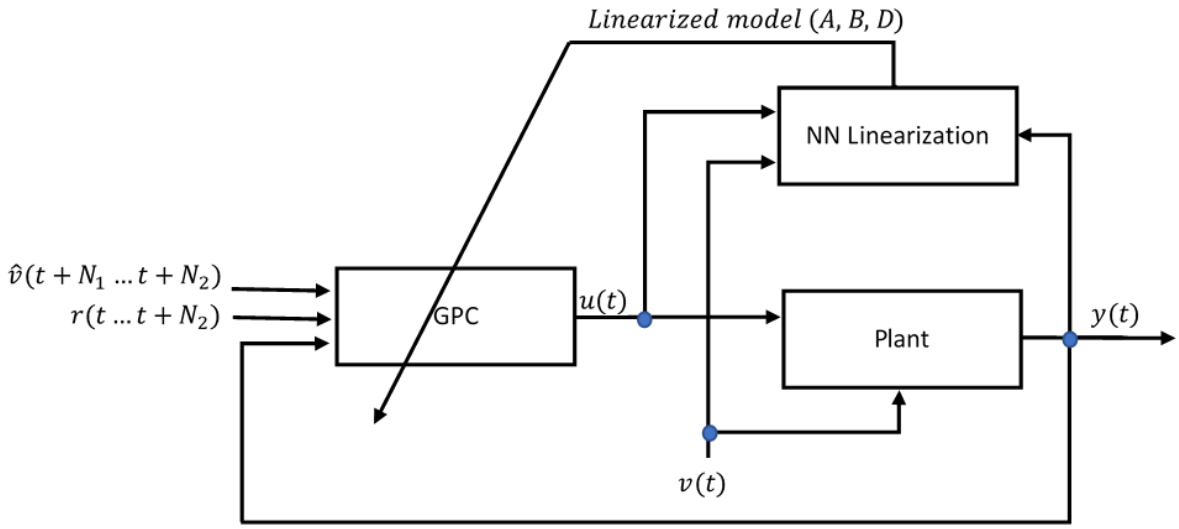

Figure III-8 Neural network infinite gain scheduling predictive control general schematic.

III.6.4 Smoothing the local models' parameters adaptation

The linearized models are supposed to be used near the operation points around which the nonlinear model is linearized every sampling time. However, in the scheduling-gain predictive control, the local linearized models are used to predict the dynamics of the nonlinear system on a prediction horizon. Consequently, using local linear models to predict the output for long horizons can lead to important modelling errors. In (Camacho, Berenguel and Rubio, 1994), this problem is treated by interpolating the controller gains between four operating points chosen on the basis of the oil flow rate. Inspired by this idea, the authors in (Gallego, Merello, *et al.*, 2019) used an interpolation of the linearized models' parameters. However, the control design developed here does not use known operating points to linearize the nonlinear model, consequently there is no known nominal variable values to be used in interpolating the controller gains or the linearized model parameters. Henceforth, it's proposed here to introduce a tuning parameter to smooth the adaptation of the polynomials of the linearized models every sampling time as follows (Himour, Tadjine and Boucherit, 2023):

$$\hat{P}_k(q^{-1}) = (1-d)P_k(q^{-1}) + d\,\hat{P}_{k-1}(q^{-1}) \qquad \text{III-52}$$

Where, $P_k(q^{-1})$ is every polynomial of the model in III-49, k is the actual sample time, and d is the introduced tuning parameter.

The proposed filter has the effect of smoothing the variation of the parameters of the successively linearized models. Increasing the parameter d slows the adaptation of the model and vice versa.

The filtering process would improve the performance of the gain-scheduled GPC controller when there are disturbances or abrupt changes in the reference. In the absence of these two factors, the filter would have no noticeable effect. In the next chapter a simulation test will be held to explore simulation results of this proposition.

III.7. Comments on stability and robustness

In all cases, elaboration of mathematical models of real-life processes includes simplifications. This is why, in practice, models are not able to ideally express the behavior of physical processes. Then model-based controllers have to assume modelling errors and uncertainties, and this is what is called robustness. Besides modelling errors and uncertainties, controllers must also cope with other type of errors, e.g., gross errors, and measurement errors, etc. Using soft computing techniques such as neural networks in modelling nonlinear and complex processes is a good choice to deal with such errors and high nonlinearities[2]. Some key works of robustness techniques applied in MPC have been mentioned in paragraph II.3. However, before talking about robustness, closed loop stability has to be ensured before application of the control strategies in real world systems.

Different proposals have been appeared to deal with the stability problem in MPC in general, one of them is the infinite prediction and control horizons (Keerthi and Gilbert, 1988), where the objective function can be considered as Lyapunov function providing nominal stability. The same authors proposed a finite horizons method by including terminal constraint on the system state. To overcome the extra calculus of this later method, (Michalska and Mayne, 1993) enlarged the terminal state constraint into a region around the terminal state, then a linear controller drives the system to the final state. This idea was extended in (Chen and Allgöwer, 1997) to a terminal cost included in the cost function. These and other formulation where summarized in (Mayne *et al.*, 2000).

All stability results account only with perfect models, which is not the case in real world systems as mentioned in the beginning of this paragraph. Robustness analysis, which is stability in the presence of modelling errors is more complex and “logically worse” (Camacho and Bordons, 2007). Stability of MPC have been one of the gaps between academia and industry, and as it is

[2] Using techniques like data reconciliation (e.g., Kalman filter), and fault tolerant control techniques are recommended for cases with high measurement errors and common gross errors.

mentioned in paragraph II.3, the stability of most applications in open-loop and the pragmatic reasoning of engineers was the factor that spurred MPC to realize it's success in the industrial world. In fact, in practice, a way to ensure good performance vis-à-vis stability and robustness of MPC is extensive simulation in different operating modes of the process and under different disturbances.

III.8. Conclusion

A solid theoretical foundation for modelling and control strategy development targeting PTC plants has been laid in this chapter. The chosen approach for modelling the plant is a trade-off between complexity and accuracy. This is to suit to the leak of real data and to avoid using a lot of artificial measurements. NMPC techniques combined with neural networks are developed to address the challenges, mentioned in the introduction chapter, confronted when controlling the outlet temperature in PTC fields. The inspired control strategy from the findings of the state-of-the-art chapter is based on the instantaneous linearization of a neural network model of the process. Thus, modelling errors caused by the linearization operation are dramatically reduced. Moreover, it is made possible to use a linear predictive control scheme free of the recursive optimization burden calculus with precise predictions of the highly nonlinear plant. Furthermore, the measured disturbances are treated intuitively in an infinite gain scheduling generalized predictive control law. A filtering process of the polynomials of the linearized models is introduced to improve their performance in predicting the temperature over the prediction horizon, hence the performance of the controller. And finally, some comments on stability and robustness were outlined.

The studies and developments made in this chapter, will be validated in the next chapter throughout simulation.

Chapter IV. Application to the ACUREX PTC field

IV.1. Introduction

This chapter deals with the application in simulation of the presented control strategies in the last chapter, to the ACUREX parabolic trough collector (PTC) solar field. The ACUREX plant is an experimental facility located in southern Spain that has been used as a benchmark system for the evaluation of solar thermal energy technologies, in particular advanced control techniques of the solar PTC fields outlet temperature. The chapter begins by describing the ACUREX plant and presenting its parameters extracted from the literature. These parameters are used in the previously developed model in equation III-10 to serve as the real plant in the simulation. The neural identification process of the ACUREX plant is detailed, and various NARX neural network configurations are tested. Then, the resulting neural model is used as an internal model in the proposed nonlinear predictive control laws and in the proposed infinite gain scheduling generalized predictive control (IGS-GPC). Performance indices concerning the precision, the control signal, and the transient regime are used to assess the efficiency of these control strategies in different functioning regimes, including abrupt changes in the measured disturbances and model mismatch. These simulations serve for validating the proposed control approaches before real-world application.

IV.2. Plant description

The ACUREX field is a PTC based DSCF. It belongs to the solar platform of Almeria. It is located in the desert of Tabernas, in southern of Spain. This field is built for experimental purposes, it has a maximum energy equal to 0.5 MW. The ACUREX field consists of 480 collectors, with a sun tracking system on a single axis. The concentrators are aligned east-west in 10 parallel loops, each loop is formed of two rows whose concentrators are connected in series. The length of the loop is 172 m, of which 30 m are passive zones that do not receive the concentrated rays of the sun. The total area of the mirrors is 2672 m^2.

The HTF used in this installation is Therminol® 55 thermal oil, which can withstand a temperature up to 300°C. The oil is pumped from the bottom of a storage tank (capacity of 115 m^3) through the solar field, where it collects the heat transferred from the walls of the absorber tube, to finally return to the top of the tank. See Figure IV-1 for a schematic of the solar field in the ACUREX plant. The heated fluid is used in boiling water in order to produce steam for a turbine that drives an electricity generator, or to power a heat exchanger of a desalination plant. The operating limits of the oil pump

are between 2.0 and 12.0 l/s (or 0.2 and 1.2 l/s by one loop). The minimum value is indicated for safety, in particular to reduce the risk of decomposition of the oil that occurs when the temperature exceeds 305 ° C (Camacho *et al.*, 2012). More details about this plant can be found in (Camacho, Berenguel and Rubio, 1997; Camacho, Berenguel and Gallego, 2014).

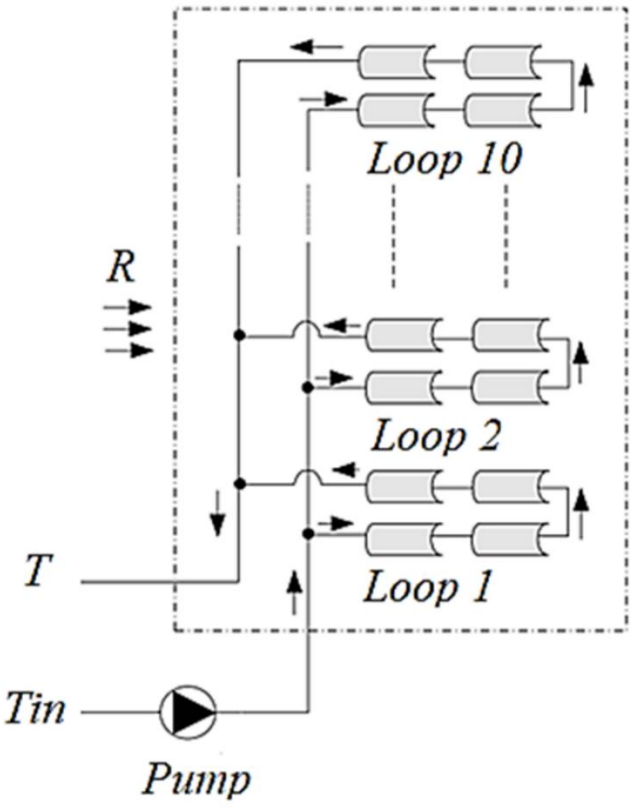

Figure IV-1 PSAs ACUREX Distributed Solar Field Schematics

The outlet temperature behavior in the ACUREX distributed solar field is modelled by the nonlinear model in equation III-10. The parameters of this model are collected from the literature of the field (Carmona, 1985; Camacho, Berenguel and Rubio, 1997; Camacho, F.R. Rubio, *et al.*, 2007; Camacho *et al.*, 2012; Navas, Ollero and Rubio, 2017; Gallego *et al.*, 2022; Masero *et al.*, 2023). Table IV-1 includes the parameters values and expressions of the model in equation III-10.

Table IV-1 Parameters of the ACUREX plant

Symbol	Description	Value	Unit

A_f	Tube cross-sectional area	5.3×10^{-4}	[m^2]
ρ_f	Fluid mass density	$903 - 0.672\,T(i\,\Delta l, t)$	[Kg/m^3]
c_f	Fluid specific heat capacity	$1820 + 3.478\,T(i\,\Delta l, t)$	[J /Kg °C]
L	Length of the active parts of a loop	142	[m]
G	Collector aperture	1.82	[m]
η	Optical efficiency	0.675	Unit-less
n	Number of segments	10	Unit-less
Ts	Sampling time[3]	15	[s]

The parameter $\alpha_i(x(t)$ is,

$$\alpha(x_i(t)) = \frac{0.675 \times\ 1.82}{(\ 1820 + 3.478\ x_i(t))(903 - 0.672\ x_i(t))5.3 \times 10^{-4}} \qquad \text{IV-1}$$

Given the model in III-10 and the parameters in Table IV-1, it's possible now to implement and simulate the model of the ACUREX plant.

IV.3. Neural network identification of the ACUREX plant

IV.3.1 Generating the input-output data

The first step in neural identification of the ACUREX plant is to collect an input-output dataset that expresses its behavior over all the operating regimes. For such a sake, the inputs must be persistent enough, and range inside their real nominal intervals. The model III-10 is used as the real plant to be identified. Three excitation signals generated with the MATLAB® identification toolbox are used, the two measurable disturbances and the input manipulated variable, respectively, the solar irradiance R with values interval from 400 W/m^2 to 1000 W/m^2, the inlet temperature T_{in} with values interval from 25°C to 150°C, and the HTF flow rate with limits between 0.2 and

[3] Many sampling times used in the literature for the ACUREX plant, for example 9s, 15s and 39s. Variable sampling time is also used in some paper researches.

1.2 l /s. These signals are of length of 18000 samples, 16000 samples are used for the training and the rest are used for the validation step. The band width of every signal was carefully chosen so that the output of the process ranges in an acceptable interval, and has enough time to exhibit its dynamics. The irradiation excitation signal is generated in a curved shape to imitate the real irradiance behaviour during a day. And to imitate a real scenario, measurement errors are added to the output given by the simulator of the plant. Figure IV-2 illustrates the first 12 hours of the signals used in the identification task. T_{outlet} is the output of the simulated plant in response of these inputs. The input-output data set is normalized using equation III-26 before being used in the supervised learning process of the neural model.

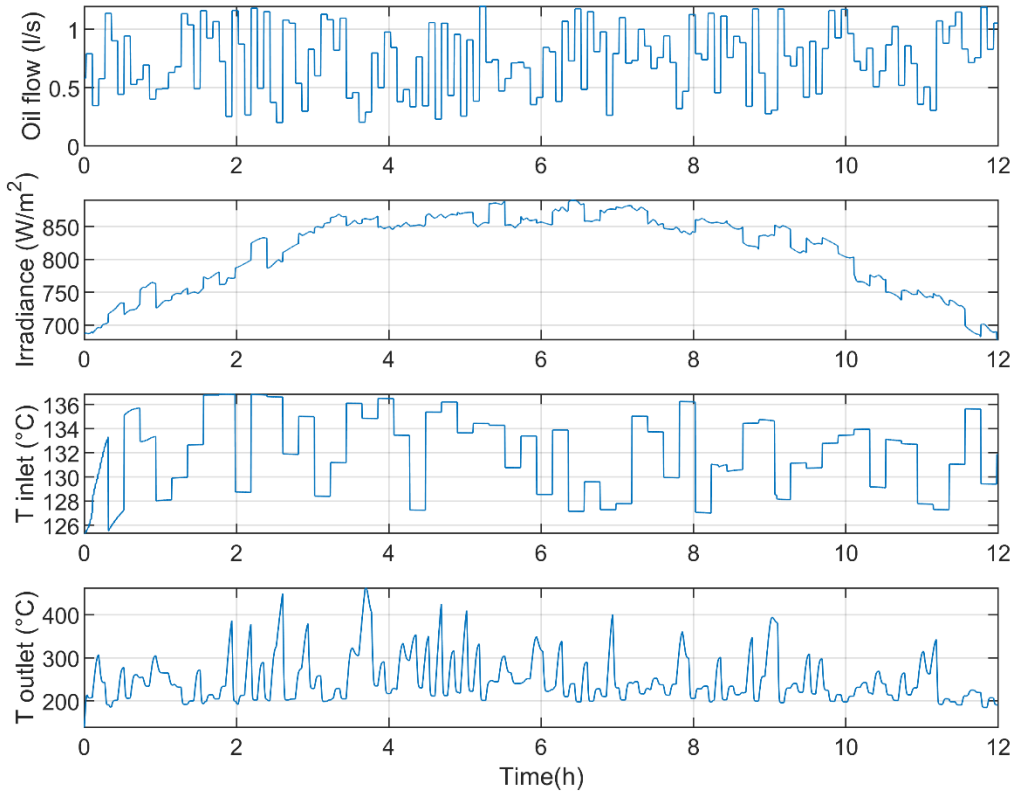

Figure IV-2 Excitation signals and response of the simulated plant

IV.3.2 Selecting the structure and estimation of weights of the neural network

As it was justified and detailed before, see section III.3, an MLP neural network is used, it has one hidden layer with a hyperbolic tangent activation function, and one neuron in the output

layer with no activation function. NARX model structure is adopted and the weights are adjusted with the Levenberg-Marquardt algorithm explained in paragraph III.3.2.

Trial-and-error tests to find convenient parameters of the neural network autoregressive exogenous model (NARX) have been held. Small delay values of past inputs and outputs, and small nodes numbers in the hidden layer were used and increased gradually.

In Table IV-2 are reported the normalized sum squared errors ($NSSE$ is define in equation IV-2, it assesses how well the model is expected to generalize to arbitrary data (Nørgaard, 2000)), given by the validation data, in the case of different parameters used with the NARX one hidden neural network. It's clear that many structures with different parameters can be adopted for use in elaborating the model predictive control law. It's worth to mention that in the training process of the neural network, initial weights are chosen as small random values, this fact makes it possible for a one structure to have slightly different $NSSE$ values for repeated training process. In the rest of this simulation, the structure 12-5433-111 in Table IV-2 will be used.

$$NSSE = \sum_{i=1}^{N} \frac{(y - \hat{y})^2}{N} \qquad \text{IV-2}$$

Table IV-2 Performance of some tested structures of the neural model

$N_h - n_y n_u n_T n_R - d_u d_T d_R$	NSSE
07-3212-111	3.0634
07-5433-111	2.9907
11-3212-111	3.0486
11-5412-111	2.9989
12-3212-111	3.0071
12-5433-111	**2.9344**
20-3212-111	2.9757
20-5433-111	3.0632

The structure notation $N_h - n_y n_u n_T n_R - d_u d_T d_R$ in Table IV-2 stands for:

N_h : Number of neurones in the hidden layer,

$n_y n_u n_T n_R$: Order of delays of the fed back signals, respectively T_{out},u , Tin and R,

$d_u d_T d_R$: Dead time according to inputs, respectively, u, Tin and R,

Results using the MLP with the selected structure 12-5433-111 are illustrated here. The first subplot of Figure IV-3 illustrates the output of the considered system versus the predictions given by the identified neural model. In the second subplot of this figure is illustrated the prediction error. Figure IV-4 depicts the auto-correlation of the prediction error in the first subplot, and the cross-correlation of the prediction error with inputs, namely HTF flow, solar irradiance and inlet HTF temperature. No-correlation with small prediction error means good model.

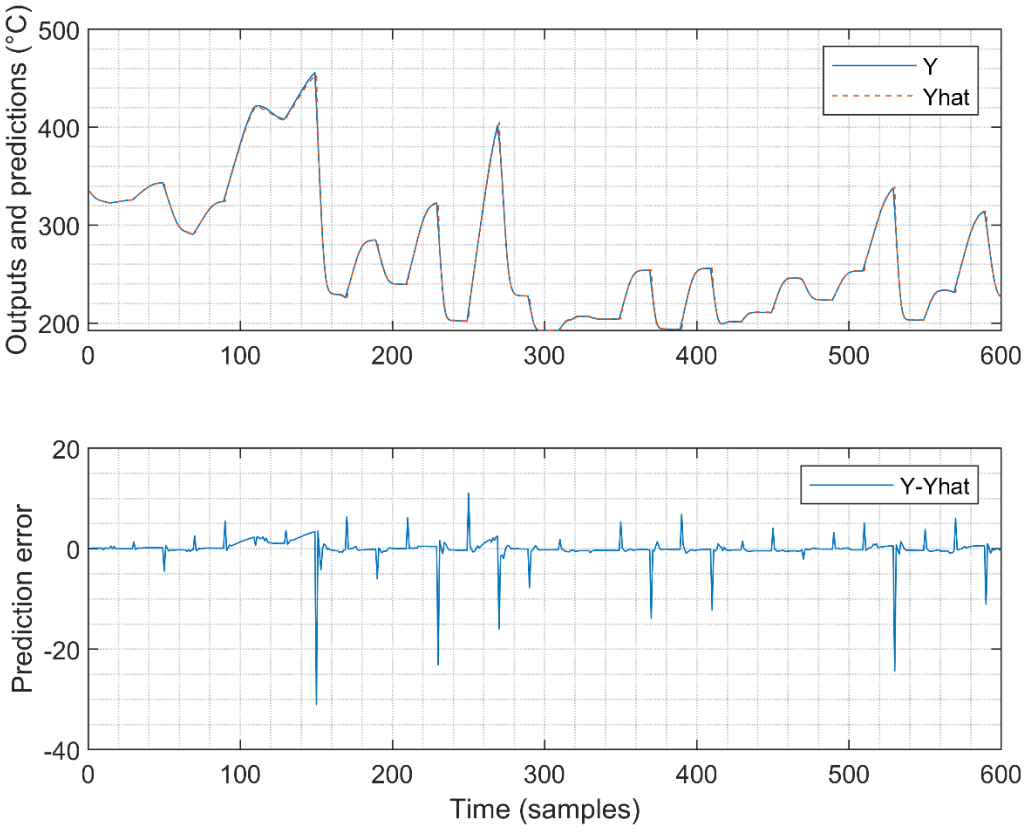

Figure IV-3 Output, one-step ahead prediction and the prediction error of the chosen neural network model

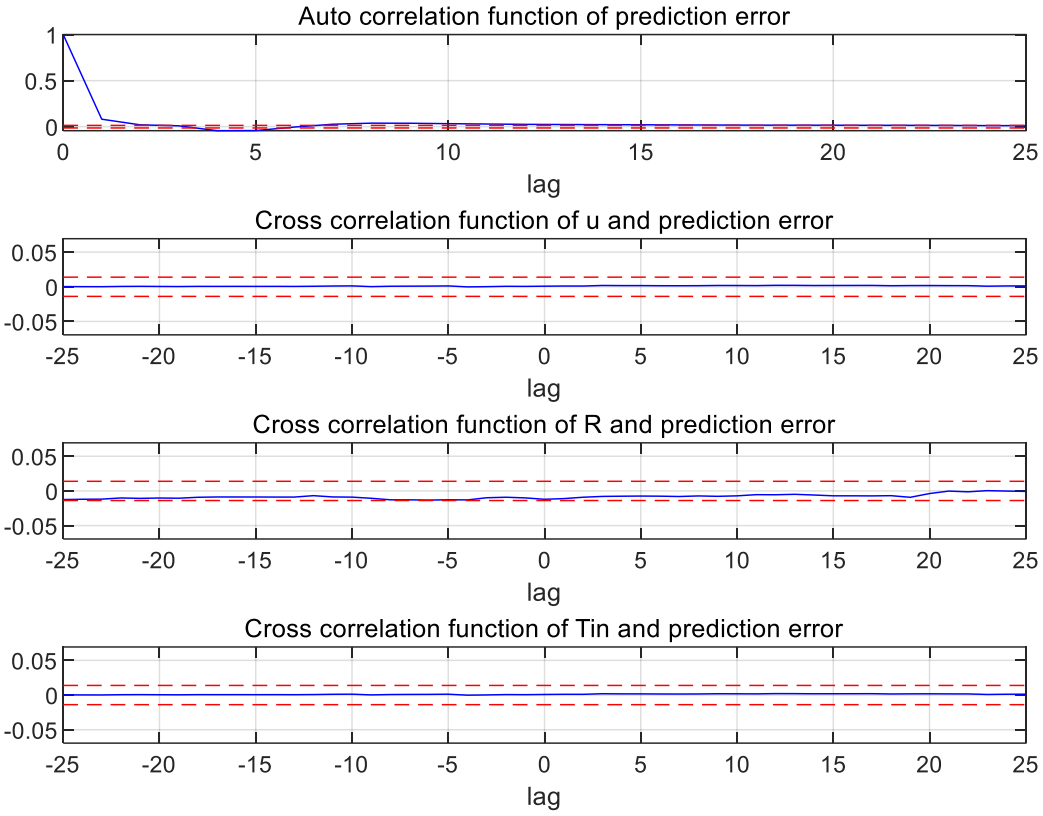

Figure IV-4 Cross correlations of the inputs and the prediction error

IV.3.3 Comments and discussion on the identification results

Making the experiment for input-output data generation on a model rather than the real plant gives more flexibility in the choice of the excitation signals and eliminates the physical and safety limits. However, the need is for a model that reflects the behavior of the real system in its normal functioning conditions, for this reason, the excitation signals are chosen in nominal functioning ranges and convenient bandwidth to keep the output amplitude in the needed range. From Table IV-2 it's clear that increasing only the number of hidden neurons or past inputs and output orders, does not give good results. It turns out that, in order to get better results, when increasing hidden neurons number (thus weights number), at some level it's needed to increase the inputs and the output past signals orders. A good minimization of the criterion in the supervised learning don't always mean good model, it could lead to a model stacked to the behavior pattern in the used data. Thus, when using the model with unseen dataset it gives bad results. This explains the result of the structure in the first row of Table IV-2. However, increasing the number of the

neurons in the hidden layer could lead to an under-training of the neural model even the criterion is well minimized in the training stage. This is the case of the last row in the table. Figure IV-3 and Figure IV-4 confirm the good performance of the adopted structure which corresponds to the smallest NSSE. As it was explained in paragraph III.3.3.3 the absence of correlation between the inputs and the prediction error (see Figure IV-4), when it's an acceptable prediction error, is a good indication of the performance of the identified model. It's clear that the peaks appearing in the prediction error in the second subplot of Figure IV-3 correspond to big and abrupt changes (aggressive variations) in the outlet temperature of the plant, which is not a usual behavior of the temperature in normal functioning conditions. In conclusion, the resulting model is considered as valid to be used in MPC control laws.

IV.4. Nonlinear and infinite gain scheduling MPC control of the ACUREX plant

In this section, five MPC control laws are applied to the ACUREX plant in simulation, where, the first principal model in equation III-10 is used as a simulator of the real model. The control techniques applied are: two unconstrained nonlinear predictive control using two different optimization algorithms, explained previously in sections III.3.2 and III.4.2 : Levenberg-Marquardt method, and Broyden–Fletcher–Goldfarb–Shanno (BFGS) method, two constrained nonlinear predictive control using interior point method: one using a first principal model as an internal model of the control law and the other uses the neural model, and finally, the infinite gain scheduling GPC developed in section III.6. The neural model developed in the previous section is used in these controllers as an internal model, except for the second controller using the interior point method, where the same model used for generating the identification dataset is used for the sake of comparison with the other control laws. A model mismatch is added, to the simulator itself, to test the control strategies' robustness against modelling errors. Performance criteria are used to distinguish which controller does well in respect to what.

IV.4.1 Simulation setup

The herein simulations have been performed in MATLAB®R2021b. The reference signal is chosen to cover a large interval of the operating range of the outlet temperature, with abrupt

ascending and descending changes on 8 levels, this is to test the tracking ability of the controllers. Each stage of the reference is of length of 100 samples (sample time being 15 seconds, this results in 25 minutes for every stage). In the non-constrained predictive control, a threshold is applied on the control signal i.e., the flow rate signal, to respect the limits of security and material constraints:

$$if\ u > 1.2\ l/s\ then\ u = 1.2\ l/s, elseif\ u < 0.2\ l/s\ then\ \ u = 0.2\ l/s$$

These limits are used, naturally, as constraints in the optimization process in the constrained non-linear predictive control methods, resulting in nonlinear non convex optimization problems.

Real data of the inlet temperature and the solar irradiance, extracted from (Camacho *et al.*, 2012), were used in the simulation. In order to demonstrate the robustness of the presented control laws in terms of disturbance rejection, artificial abrupt changes, simulating clouds passage and a fluctuation in the inlet temperature, were added to both of the two disturbance signals. The added aggressive variation on the solar irradiation is of an amplitude of $-100\ \mathrm{W/m^2}$ beginning from the first half hour on a duration of about 12 minutes, and that on the inlet temperature is of an amplitude of -50°C beginning at one hour 20 minutes of simulation time over the same duration (12 minutes). Moreover, the inlet temperature T_{in} and the solar irradiance R are not known over the prediction horizon and must be estimated. Artificial estimated values of the two disturbances are generated by adding artificial estimation errors to the real T_{in} an R, and then used as inputs into the model to predict plant output over the prediction horizon in the predictive control laws. This way the estimation errors are taken into account. In (Arahal, Berenguel and Camacho, 1997) this was done by applying a zero-order hold on the last measured T_{in} and a clear-day solar radiation prediction model to estimate R over the prediction horizon. The profiles of the real measured disturbances and the artificial estimated values are depicted in Figure IV-5. Modelling errors are artificially added on the α_i parameters of the simulator model in equation III-10. The added model mismatches can be interpreted as a variation in the optical efficiency of the concentrators or in one of the oil properties.

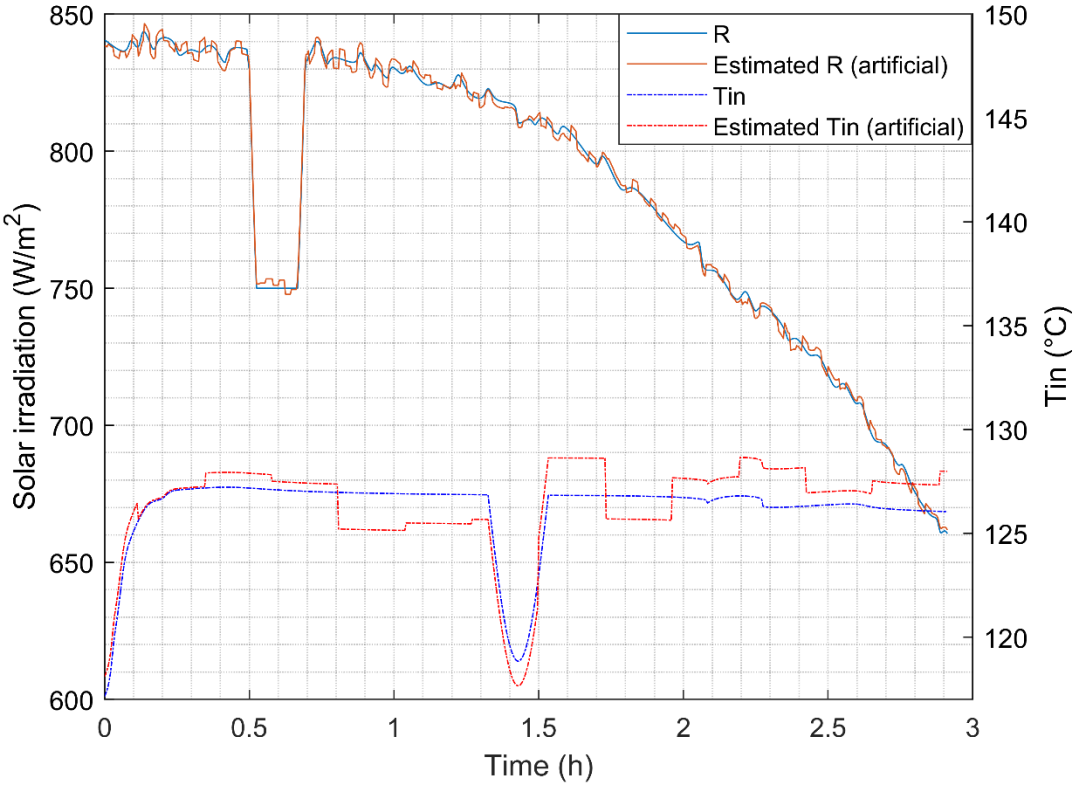

Figure IV-5 Irradiance and inlet temperature profiles

Appropriate tuning parameter values of the MPC control laws are chosen to get the best results as described in (Camacho and Bordons, 2007). In the BFGS, the Levenberg-Marquardt and the interior point schemes, the same values are used, for that the used model to predict the plant output in these techniques is the same model. $N_1 = 1, N_2 = 8,$ and $N_u = 5$. In the case of the infinite scheduled gain predictive control, the prediction horizons are $N_1 = 1$ and $N_2 = 10$, and the control horizon $N_u = 6$.

The following indices are adopted to determine the performance of every control law. Some of theme concern step response, others concern the tracking error and the command signal:

$$IAE = \int_0^\infty |e(t)|dt \qquad \text{IV-3}$$

$$ISE = \int_0^\infty e^2(t)dt \qquad \text{IV-4}$$

$$IAC = \int_0^\infty |u(t)|dt \qquad \text{IV-5}$$

$$CSE = \left|\left|\Delta u(t)\right|\right| \qquad \text{IV-6}$$

Where, IAE is the integrated absolute error, it penalizes small errors. ISE is the integrated squared error, it increases more rapidly with larger errors. IAC is the integral of absolute control, used here to express the effort of the control signal. CSE is the control system effort, its value depends inversely on the smoothness of the control signal.

The step response related performance indices are the first overshoot, the settling time at $\pm 5\%$ and the rise time from 10% to 90%.

The following table shows the notation used for the indices and the predictive control laws.

Table IV-3 Notation of the indices and the used predictive control schemes

IAC	Integral of the absolute control
CSE	Control system effort
IAE	Integrated absolute error
ISE	Integrated squared error
OS	First overshoot
ST	Settling time
RT	Rise time
ET	Mean execution time for one iteration
ISG	Infinite scheduling gain predictive control
BFGS	Predictive control using the BFGS optimization method
LM	Predictive control using the Levenberg-Marquardt optimization method
IP	Constrained neural predictive control using Interior point optimization method
IPIM	Constrained predictive control using an ideal prediction model

IV.4.2 Results

A simulation is conducted to validate the process of filtering the polynomials of the successively linearized models, proposed in section III.6.4. Figure IV-6 shows the results of this simulation where the infinite gain scheduling GPC tunning parameters mentioned above are used. Three values of the parameter $d = 0.2, d = 0.5$ and $d = 0.9$ are tested and compared to the case without filtering, i.e., $d = 0$. Clearly, filtering the polynomials of the linearized models brought best improvement with the value $d = 0.5$. This value will be used for the comparison of the neural infinite gain scheduling GPC control law with the other simulated control strategies.

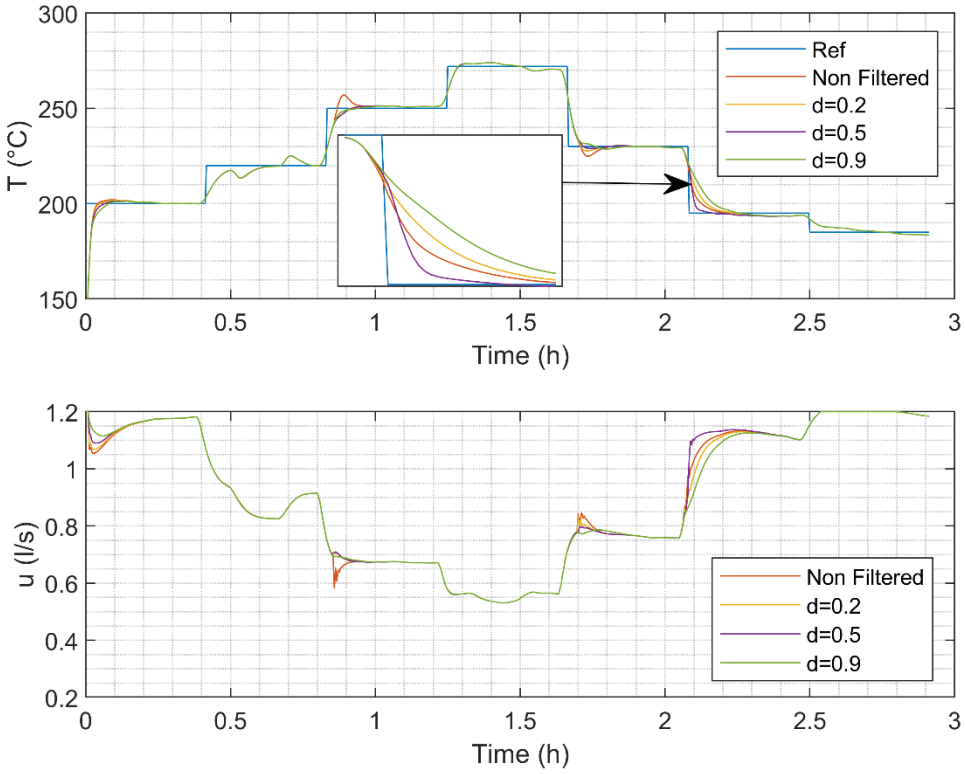

Figure IV-6 Effect of different values of the adaptation smoothing parameter

In the same simulation conditions of the infinite gain scheduling GPC, i.e., model mismatch introduced on the parameter α_i in the equation III-10 of the simulator, the same solar irradiance and HTF temperature inlet with the same injected abrupt changes, same reference and neural model, simulations were held for the other control laws. Figure IV-7 illustrates the results of the infinite scheduling gain predictive control against the unconstrained predictive control schemes i.e., BFGS

and LM. And Figure IV-8 depicts the results of the infinite scheduling gain predictive control against the constrained IP and IPM predictive control.

The results of the performance indices explained above are illustrated in Table IV-4. The run time in the five strategies changes from iteration to another, i.e., every sampling time. The execution time over all the simulation is divided by the number of data samples to find the mean execution time for one iteration in every control scheme. This value is included in the last column of Table IV-4.

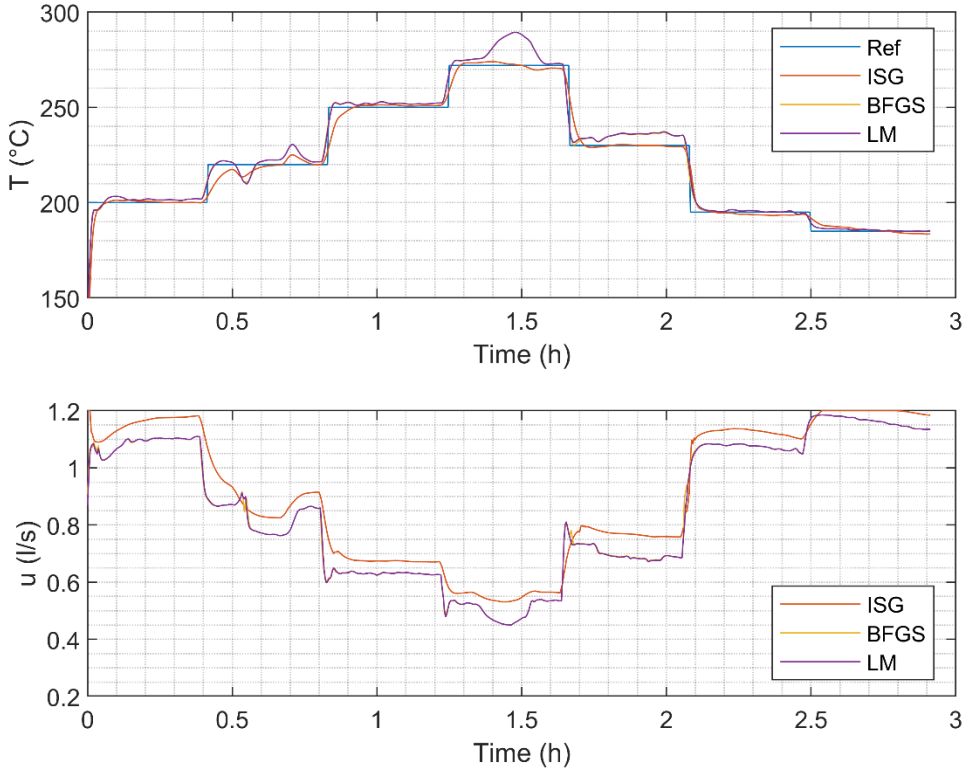

Figure IV-7 Output and control evolution of the BFGS, Levenberg-Marquardt and the improved neural infinite scheduling gain predictive control.

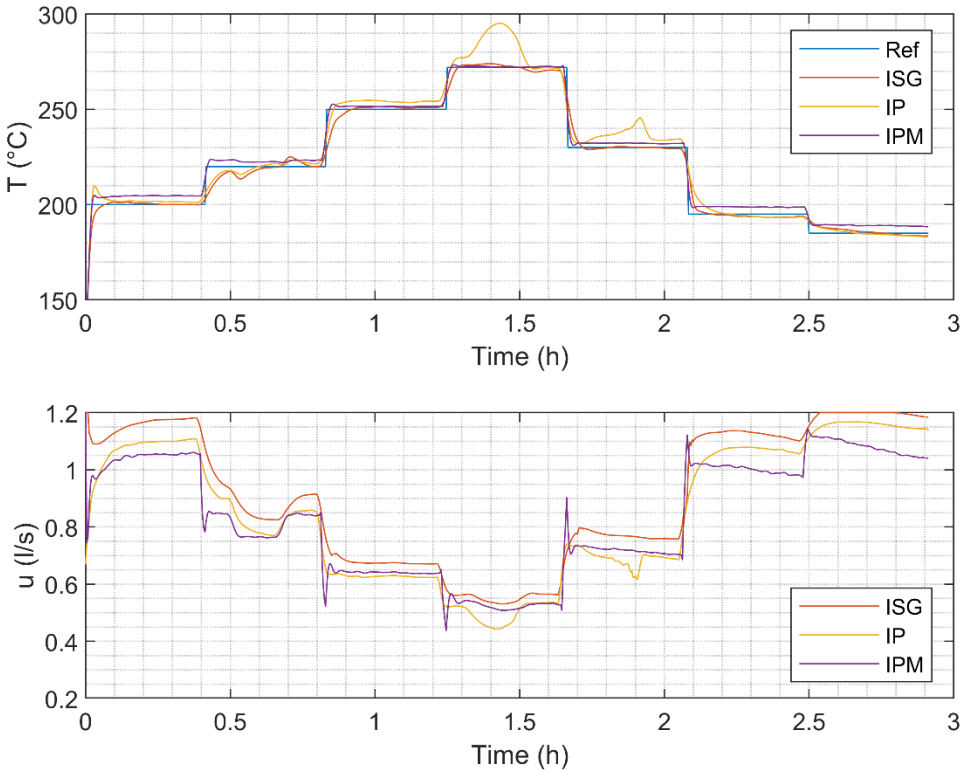

Figure IV-8 Output and control evolution of the IPM, IP and the improved neural infinite gain scheduling predictive control.

Table IV-4 Performance indices of the simulated control strategies

Method	IAC	CSE	IAE	ISE	OS	ST (s)	RT (s)	ET (s)
IPM	1.09e+3	1.60	2.28e+3	2.03e+4	0.0	21.5	47.0	1.6183
IP	1.12e+3	1.08	3.16e+3	4.01e+4	13.31	34.3	58.3	0.2999
BFGS	1.13e+3	1.20	2.45e+3	2.41e+4	4.37	19.6	58.5	0.0181
LM	1.13e+3	1.17	2.46e+3	2.42e+4	4.37	19.6	58.5	0.0047
ISG	1.20e+3	1.07	1.62e+3	2.19e+4	1.71	37.5	80.2	0.0019

IV.4.3 Comments and discussion

As it was expected in paragraph III.6.4, the simulation results in Figure IV-6 confirm the good effect of smoothing the polynomials adaptation of the successively linearized models, on the performance of the infinite gain scheduling GPC, when a good choice of the parameter d is done.

After applying the filtering with $d = 0.5$, the two overshoots appeared in the case without filtering are eliminated. This is without reducing the rapidity performance. In contrary, the rapidity is improved. This can be clearly seen in the zoomed area in the figure. On the control curve, the introduced filtering operation have also eliminated the high frequency variations appearing on instants corresponding to the abrupt changes of the reference, making the control signal smoother and thus increasing the life time of the actuator i.e., the pump. In steady state i.e., in the absence of reference changes and disturbances, the filtering process shows no effect.

A comparison between the results of the infinite gain scheduling GPC (IGS-GPC) and the other nonlinear constrained and unconstrained neural MPC shows that IGS-GPC gives better results in terms of rejecting the abrupt changes of the measured disturbances, see Figure IV-7 for the comparison with unconstrained NMPC and Figure IV-8 for constrained NMPC. This is clearer with the upset injected on the HTF inlet temperature T_{in} corresponding to the fourth stage of the reference where only the IGS-GPC and the NMPC using the first principal model were able to cancel its effect on the outlet temperature, the other schemes have a big deviation of the outlet temperature that reach 20°C. For the abrupt change injected on the solar irradiance, IGS-GPC and the constrained neural NMPC (noted by IP) have almost the same performance which is slightly better than the neural unconstrained NMPC (Levenberg-Marquardt and BFGS based NMPC). However, the IP-NMPC has a bad precision in the regime corresponding to the fifth stage of the reference. The first principal model based NMPC do better with this upset but it also has an amplitude offset with the reference. Violation of the command up-limits appears in IGS-GPC control signal on the part corresponding to the last level of the reference, but does not damage the good behavior of the controlled variable, rather, it gives better precision then the first principal model based-NMPC (IPM) in this stage.

The Table IV-4 gives more insights on the performance of the five control strategies, that can't be noticed visually on the figures. The numbers in this table confirm that the IGS-GPC is the best in terms of precision, and the more robust against the small and large errors. This is obvious throughout the IAE and ISE indices where the IGS-GPC gives the least values, even smaller than those of the first principal model based-NMPC (IPM). The infinite gain scheduling GPC (ISG-GPC) is also the best after the IPM, in terms of overshoots dumping. In spite of being slightly bigger than the other simulated control laws in regards to the integral of absolute control, the more important regarding this is that its control signal is the smoothest (see the *CSE* index in the table). The other advantage of the proposed IGS-GPC scheme over others is its very low execution time.

While the IPM scheme can reach 9 seconds in computing the control signal (not included in the table), with a mean execution time of 1.6183 seconds, the IGS-GPC's mean execution time is 0.0019 seconds, which make it largely secured against the 15 seconds sampling time. Finally, ISG-GPC showed bigger settling time and rise time than others in the first stage of the reference where all the indices related to the transient regime were picked up. The differences are not so large for a process of big inertia as the temperature, one sampling time for the settling time and two for the rise time.

IV.5. Conclusion

In this chapter, nonlinear and gain scheduling neural predictive control of the ACUREX plant have been tested successfully in a simulation framework. In a first stage, an accurate representation of the plant's dynamics was achieved through neural networks identification. The data validation prediction error is very acceptable, and the results showed no autocorrelation of the error prediction or cross-correlation with any of the three inputs. This confirmed the good generalization and performance of the obtained neural model. The precise model enabled effective use of the NMPC and the ISG-GPC control strategies which the performance highly relies on the performance of the used model.

The introduced smoothing operation of the linearized models' polynomials adaptation showed effective improvement in the ISG-GPC performance, in terms of tracking reference with abrupt changes, rejecting aggressive variations of the measured disturbances, and smoothing the control signal. Overshoots that had appeared without filtering were cancelled and the rapidity ameliorated.

All the simulated strategies are tailored to the high nonlinearities and special characteristics of the PTC outlet temperature process. However, the results revealed that the proposed ISG-GPC strategy surpasses the performance of the other simulated control laws, in particular in terms of precision, robustness against abrupt disturbances, and computational efficiency. Despite that the ISG-GPC has slightly bigger IAE index, it demonstrated a smoother control signal with good disturbance rejection even under model mismatches and aggressive variation in operating conditions. It has the absolutely smallest execution time among all other strategies, a fact that makes it safe for real-world implementation. On the basis of these findings, surely the proposed IGS-GPC is a promising approach to cater to the control objectives of the outlet temperature in the ACUREX plant and similar solar PTC fields.

General conclusion

In this thesis, advanced control strategies to enhance the efficiency and reliability of the solar parabolic trough collector (PTC) fields have been developed and validated. The focus was on dealing with high nonlinearities of this type of plants, and the resulting computational problems in the used control technique, i.e., NMPC technique. This led to some contributions in this thesis which are summarized in the following paragraphs.

A thorough state-of-the-art enabled to get deep insights into the context of controlling the outlet temperature in PTC fields, identify existing research gaps, and propose comprehensive modelling and convenient control strategies to address significant challenges, among which, high system nonlinearities, big influence of measured disturbances, and computational efficiency in nonlinear model predictive control (NMPC).

A reduced-complexity dynamic model, has been developed as a trade-off between precision and complexity to capture the essential nonlinear characteristics of PTC fields, enabling efficient control strategy design. This model served as a simulator for the real process, i.e., the outlet temperature, under varying operational conditions. It is implemented in a flexible Simulink® model, where the user can modify the space discretization step by deleting or adding (copying and pasting) volume blocks from/to the set of the in series linked blocks.

A two-layer MLP neural network was employed to identify the complex dynamics of PTC systems, and it was used as an internal model in the NMPC control law. Its performance in approximating high nonlinearities and uncertainties has improved the accuracy and robustness of the control strategies.

Advanced model predictive control strategies, including two unconstrained neural NMPC, a constrained neural NMPC, and a constrained NMPC based on first principal model, were designed. The neural NMPC strategies effectively reduced the computational challenges associated with the nonlinear optimization process in comparison with the NMPC with a first principal model; thus, ensuring real-time feasibility and robust performance.

An infinite neural gain scheduling GPC strategy was proposed. It relies on real time linearization of the internal neural model and using it in a GPC control law. Moreover, a smoothing operation

of the linearized models' polynomials, to mitigate abrupt changes in the reference and in the measured disturbances, was introduced. The results showed improvement in precision, rapidity, and overshoots cancellation.

The designed identification and control strategies were implemented and validated through simulation for the ACUREX plant. The results demonstrated good performance in maintaining the outlet temperature at the desired reference in spite of abrupt changes in the reference and the measured disturbances, and good robustness against the injected model mismatches.

Besides the experimental validation of the proposed techniques in a real-world PTC plant, either on a pilot-scale plant or a commercial plant, future works could involve more research to improve the proposed neural ISG-GPC control scheme. After have being delving to deep details of this work, one can't flee from inspired ideas among which some could be announced as perspectives:

1. Adjust the proposed smoothing parameter value according to future reference and measured disturbances variations.

2. Including the control signal limits in the linear ISG-GPC control law by converting the optimization problem to a constrained quadratic one. By comparison to nonlinear non convex optimization problems, the analytical theory of convex quadratic problems is well established, and the computational difficulties and problems are dramatically reduced.

3. Because the PTC plants have high nonlinearities, the use of some mechanism to adapt the MPC parameters in the neural ISG-GPC to meet the system characteristics in every regime could enhance the performance of the MPC control law, this concerns the first and second prediction horizons, the control horizon, and the control increment's weight in the cost function.

4. Use weighting factors for future prediction errors in the ISG-GPC control law, and adjust them according to the future reference signal, would give control over the importance of the prediction errors in time in the optimization process. For example, if the actual time sample is approaching an abrupt reference change, it's more convenient to give more importance to the error after the reference variation.

Broader perspectives, but always in the sake for dealing with the high nonlinearities of the PTC plants and the computational problems in the NMPC, is to use a local model network (LMN) as an internal model for the MPC control law, this enables, as the ISG-GPC did, to exploit linear MPC techniques and avoid the NMPC optimization process, without failing to handle the high nonlinearities of the plant.

In conclusion, results and findings of this thesis underline the importance of integrating neural networks with nonlinear and gain scheduling model predictive control to overcome difficulties in controlling the outlet temperature in solar PTC fields, and to achieve efficient and reliable thermal solar energy management. By treating critical challenges in the field, this thesis contributes to advancing the state of the art of thermal solar energy technologies.

Published articles in the framework of the thesis:

1- Himour, Y., Tadjine, M. and Boucherit, M.-S. (2023) 'Nonlinear and infinite gain scheduling neural predictive control of the outlet temperature in a parabolic trough solar field: A comparative study', Engineering Applications of Artificial Intelligence, 126, p. 106862. Available at: https://doi.org/10.1016/j.engappai.2023.106862 .
Journal CiteScore 12, Impact Factor 8 (at the date of publication)

2-Himour, Y., Tadjine, M. and Boucherit, M.S. (2025) 'A smooth gain scheduling generalized predictive control', ENP Engineering Science Journal, Vol.5(No.1), pp. 31–36. Available at: https://doi.org/10.53907/enpesj.v5i1.326 .

Bibliography

Alhajeri, M.S. *et al.* (2022) 'Process structure-based recurrent neural network modeling for predictive control: A comparative study', *Chemical Engineering Research and Design*, 179, pp. 77–89. Available at: https://doi.org/10.1016/j.cherd.2021.12.046.

Allgöwer, F. and Zheng, A. (2000) *Nonlinear Model Predictive Control*. Edited by F. Allgöwer and A. Zheng. Basel: Birkhäuser Basel. Available at: https://doi.org/10.1007/978-3-0348-8407-5.

Alsharkawi, A. and Rossiter, J.A. (2017) 'Towards an improved gain scheduling predictive control strategy for a solar thermal power plant', *IET Control Theory & Applications*, 11(12), pp. 1938–1947. Available at: https://doi.org/10.1049/iet-cta.2016.1319.

Arahal, M.R., Berenguel, M. and Camacho, E.F. (1997) 'Nonlinear neural model-based predictive control of a solar plant', *European Control Conference*, (April), pp. 1–4.

Arahal, M.R., Berenguel, M. and Camacho, E.F. (1998) 'Neural identification applied to predictive control of a solar plant', *Control Engineering Practice*, 6(3), pp. 333–344. Available at: https://doi.org/10.1016/S0967-0661(98)00025-2.

Baharoon, D.A. *et al.* (2015) 'Historical development of concentrating solar power technologies to generate clean electricity efficiently – A review', *Renewable and Sustainable Energy Reviews*, 41, pp. 996–1027. Available at: https://doi.org/10.1016/j.rser.2014.09.008.

Barão, M., Lemos, J.M. and Silva, R.N. (2002) 'Reduced complexity adaptive nonlinear control of a distributed collector solar field', *Journal of Process Control*, 12(1), pp. 131–141. Available at: https://doi.org/10.1016/S0959-1524(01)00003-8.

Bayas, A., Škrjanc, I. and Sáez, D. (2018) 'Design of fuzzy robust control strategies for a distributed solar collector field', *Applied Soft Computing*, 71, pp. 1009–1019. Available at: https://doi.org/10.1016/j.asoc.2017.10.003.

Bellman, R.E. (1967) *Dynamic programming*, *Mathematics in Science and Engineering*. Princeton university press. Available at: https://doi.org/10.1016/S0076-5392(08)61063-2.

Bemporad, A. *et al.* (2000) 'The explicit solution of model predictive control via multiparametric quadratic programming', in *Proceedings of the 2000 American Control Conference. ACC (IEEE Cat. No.00CH36334)*. IEEE, pp. 872–876 vol.2. Available at: https://doi.org/10.1109/ACC.2000.876624.

Bemporad, A. (2021) ‘Explicit Model Predictive Control’, in *Encyclopedia of Systems and Control*. Cham: Springer International Publishing, pp. 744–751. Available at: https://doi.org/10.1007/978-3-030-44184-5_10.

Biao, H. and Ramesh, K. (2008) *Dynamic Modeling, Predictive Control and Performance Monitoring*. London: Springer London (Lecture Notes in Control and Information Sciences). Available at: https://doi.org/10.1007/978-1-84800-233-3.

Biswas, D.B. *et al.* (2020) ‘A techno-economic comparison between piston steam engines as dispatchable power generation systems for renewable energy with concentrated solar harvesting and thermal storage against solar photovoltaics with battery storage’, *Energy*, 213, p. 118732. Available at: https://doi.org/10.1016/j.energy.2020.118732.

Broyden, C.G. (1970) ‘The Convergence of a Class of Double-rank Minimization Algorithms: 2. The New Algorithm’, *IMA Journal of Applied Mathematics*, 6(3), pp. 222–231. Available at: https://doi.org/10.1093/IMAMAT/6.3.222.

Brus, L. and Zambrano, D. (2010) ‘Black-box identification of solar collector dynamics with variant time delay’, *Control Engineering Practice*, 18(10), pp. 1133–1146. Available at: https://doi.org/10.1016/j.conengprac.2010.06.006.

Camacho, E.F., Rubio, F. R., *et al.* (2007) ‘A survey on control schemes for distributed solar collector fields. Part I: Modeling and basic control approaches’, *Solar Energy*, 81(10), pp. 1240–1251. Available at: https://doi.org/10.1016/j.solener.2007.01.002.

Camacho, E.F., Rubio, F.R., *et al.* (2007) ‘A survey on control schemes for distributed solar collector fields. Part II: Advanced control approaches’, *Solar Energy*, 81(10), pp. 1252–1272. Available at: https://doi.org/10.1016/J.SOLENER.2007.01.001.

Camacho, E.F. *et al.* (2010) ‘Control of Solar Power Systems: a survey’, *IFAC Proceedings Volumes*, 43(5), pp. 817–822. Available at: https://doi.org/10.3182/20100705-3-BE-2011.00135.

Camacho, E.F. *et al.* (2012) *Control of Solar Energy Systems*, *Solar Energy*. London: Springer London (Advances in Industrial Control). Available at: https://doi.org/10.1007/978-0-85729-916-1.

Camacho, E.F. *et al.* (2024) ‘Control of Solar Energy Systems’, *Annual Review of Control, Robotics, and Autonomous Systems*, 7(1), pp. 175–200. Available at: https://doi.org/10.1146/annurev-control-071023-103936.

Camacho, E.F. and Berenguel, M. (1997) 'Robust adaptive model predictive control of a solar plant with bounded uncertainties', *International Journal of Adaptive Control and Signal Processing*, 11(4), pp. 311–325. Available at: https://doi.org/10.1002/(SICI)1099-1115(199706)11:4<311::AID-ACS410>3.0.CO;2-K.

Camacho, E.F., Berenguel, M. and Bordons, C. (1994) 'Adaptive Generalized Predictive Control of a Distributed Collector Field', *IEEE Transactions on Control Systems Technology*, 2(4), pp. 462–467. Available at: https://doi.org/10.1109/87.338667.

Camacho, E.F., Berenguel, M. and Gallego, A.J. (2014) 'Control of thermal solar energy plants', *Journal of Process Control*, 24(2), pp. 332–340. Available at: https://doi.org/10.1016/j.jprocont.2013.09.026.

Camacho, E.F., Berenguel, M. and Rubio, F.R. (1994) 'Application of a gain scheduling generalized predictive controller to a solar power plant', *Control Engineering Practice*, 2(2), pp. 227–238. Available at: https://doi.org/10.1016/0967-0661(94)90202-X.

Camacho, E.F., Berenguel, M. and Rubio, F.R. (1997) *Advanced Control of Solar Plants*, *Advances in Industrial Control*. Edited by N. Luo, Y. Vidal, and L. Acho. London: Springer London (Advances in Industrial Control). Available at: https://doi.org/10.1007/978-1-4471-0981-5.

Camacho, E.F. and Bordons, C. (2007) *Model Predictive control*, *Advanced Textbooks in Control and Signal Processing*. London: Springer London (Advanced Textbooks in Control and Signal Processing). Available at: https://doi.org/10.1007/978-0-85729-398-5.

Camacho, E.F. and Gallego, A.J. (2015) 'Model Predictive Control in Solar Trough Plants: A Review', *IFAC-PapersOnLine*, 48(23), pp. 278–285. Available at: https://doi.org/10.1016/j.ifacol.2015.11.296.

Camacho, E.F., Rubio, F.R. and Hughes, F.M. (1992) 'Self-Tuning Control of a Solar Power Plant with a Distributed Collector Field', *IEEE Control Systems*, 12(2), pp. 72–78. Available at: https://doi.org/10.1109/37.126858.

Cardoso, A.L., Henriques, J. and Dourado, A. (1999) 'Fuzzy supervisor and feedforward control of a solar power plant using accessible disturbances', in *1999 European Control Conference (ECC)*. IEEE, pp. 1711–1716. Available at: https://doi.org/10.23919/ECC.1999.7099561.

Carmona, R. (1985) *Analysis, Modeling and Control of a Distributed Solar Collector Field with a One-axis Tracking System*. PhD Thesis (in Spanish), University of Seville, Spain. Available at: https://idus.us.es/handle/11441/48222.

Chen, H. and Allgöwer, F. (1997) ‘A quasi-infinite horizon nonlinear model predictive control scheme with guaranteed stability’, *ECC 1997 - European Control Conference*, pp. 1421–1426. Available at: https://doi.org/10.23919/ECC.1997.7082300.

Chitnis, R. *et al.* (2024) ‘IQL-TD-MPC: Implicit Q-Learning for Hierarchical Model Predictive Control’, *Proceedings - IEEE International Conference on Robotics and Automation*, pp. 9154–9160. Available at: https://doi.org/10.1109/ICRA57147.2024.10611711.

Cirre, C.M. *et al.* (2005) ‘Feedback linearization control for a distributed solar collector field’, *IFAC Proceedings Volumes*, 38(1), pp. 356–361. Available at: https://doi.org/10.3182/20050703-6-CZ-1902.01788.

Cirre, C.M. *et al.* (2007) ‘Feedback linearization control for a distributed solar collector field’, *Control Engineering Practice*, 15(12), pp. 1533–1544. Available at: https://doi.org/10.1016/j.conengprac.2007.03.002.

Clarke, D.W. and Gawthrop, P.J. (1979) ‘Self-tuning control’, *Proceedings of the Institution of Electrical Engineers*, 126(6), p. 633. Available at: https://doi.org/10.1049/piee.1979.0145.

Clarke, D. W., Mohtadi, C. and Tuffs, P.S. (1987) ‘Generalized predictive control-Part I. The basic algorithm’, *Automatica*, 23(2), pp. 137–148. Available at: https://doi.org/10.1016/0005-1098(87)90087-2.

Clarke, D.W., Mohtadi, C. and Tuffs, P.S. (1987) ‘Generalized Predictive Control—Part II Extensions and interpretations’, *Automatica*, 23(2), pp. 149–160. Available at: https://doi.org/10.1016/0005-1098(87)90088-4.

Clarke, D.W. and Scattolini, R. (1991) ‘Constrained receding-horizon predictive control’, *IEE Proceedings D Control Theory and Applications*, 138(4), p. 347. Available at: https://doi.org/10.1049/ip-d.1991.0047.

Cutler, C.R. and Ramaker, B.L. (1979) ‘Dynamic matrix control??A computer control algorithm’, in *AIChE National Mtg*. Houston, Texas.

Demircioglu, H. and Clarke, D.W. (1992) ‘CGPC with guaranteed stability properties’, *IEE Proceedings D Control Theory and Applications*, 139(4), p. 371. Available at: https://doi.org/10.1049/ip-d.1992.0049.

Dikin, I.I. (1967) ‘Iterative solution of problems of linear and quadratic programming’, *Soviet Mat. Dokl.*, 8, pp. 674–675.

Elmetennani, S. and Laleg-Kirati, T.M. (2014) ‘Fuzzy universal model approximator for distributed solar collector field control’, in *2014 UKACC International Conference on*

Control, CONTROL 2014 - Proceedings, pp. 203–208. Available at: https://doi.org/10.1109/CONTROL.2014.6915140.

Farkas, I. and Vajk, I. (2002) 'Internal model-based controller for a solar plant', *IFAC Proceedings Volumes*, 35(1), pp. 49–54. Available at: https://doi.org/10.3182/20020721-6-ES-1901.01317.

Fletcher, R. (1970) 'A new approach to variable metric algorithms', *The Computer Journal*, 13(3), pp. 317–322. Available at: https://doi.org/10.1093/COMJNL/13.3.317.

Flores, a *et al.* (2005) 'Fuzzy Predictive Control of a Solar Power Plant', *Trans. Fuz Sys.*, 13(1), pp. 58–68. Available at: https://doi.org/10.1109/TFUZZ.2004.839658.

Gallego, A.J., Merello, G.M., *et al.* (2019) 'Gain-scheduling model predictive control of a Fresnel collector field', *Control Engineering Practice*, 82, pp. 1–13. Available at: https://doi.org/10.1016/j.conengprac.2018.09.022.

Gallego, A.J., MacÍas, M., *et al.* (2019) 'Mathematical Modeling of the Mojave Solar Plants', *Energies 2019, Vol. 12, Page 4197*, 12(21), p. 4197. Available at: https://doi.org/10.3390/EN12214197.

Gallego, A.J. *et al.* (2022) 'Nonlinear model predictive control for thermal balance in solar trough plants', *European Journal of Control*, 67, p. 100717. Available at: https://doi.org/10.1016/J.EJCON.2022.100717.

Gallego, A.J., Yebra, L.J. and Camacho, E.F. (2018) 'Gain Scheduling Model Predictive Control of the New TCP-100 Parabolic Trough Field', in *IFAC-PapersOnLine*, pp. 475–480. Available at: https://doi.org/10.1016/j.ifacol.2018.03.080.

Garcia, C.E. and Morshedi, A.M. (1986) 'Quadratic programming solution of dynamic matrix control (QDMC)', *Chemical Engineering Communications*, 46(1–3), pp. 73–87. Available at: https://doi.org/10.1080/00986448608911397.

Gharat, P. V. *et al.* (2021) 'Chronological development of innovations in reflector systems of parabolic trough solar collector (PTC) - A review', *Renewable and Sustainable Energy Reviews*, 145, p. 111002. Available at: https://doi.org/10.1016/j.rser.2021.111002.

Goldfarb, D. (1970) 'A family of variable-metric methods derived by variational means', *Mathematics of Computation*, 24(109), pp. 23–26. Available at: https://doi.org/10.1090/S0025-5718-1970-0258249-6.

Goodwin, G.C., Carrasco, D.S. and Seron, M.M. (2012) 'Predictive control: a historical perspective', *International Journal of Robust and Nonlinear Control*, 22(12), pp. 1296–1313. Available at: https://doi.org/10.1002/rnc.2824.

Goswami, D.Y. (2022) *Principles of Solar Engineering*, *Principles of Solar Engineering*. Boca Raton: CRC Press. Available at: https://doi.org/10.1201/9781003244387.

Goswami, Y.D. (2007) 'Energy: the burning issue', *Refocus*, 8(1), pp. 22–25. Available at: https://doi.org/10.1016/S1471-0846(07)70024-0.

Hagan, M.T. and Menhaj, M.B. (1994) 'Training Feedforward Networks with the Marquardt Algorithm', *IEEE Transactions on Neural Networks*, 5(6), pp. 989–993. Available at: https://doi.org/10.1109/72.329697.

Henriques, J. *et al.* (2002) 'Scheduling of PID controllers by means of a neural network with application to a solar power plant', in *Proceedings of the 2002 International Joint Conference on Neural Networks. IJCNN'02 (Cat. No.02CH37290)*. IEEE, pp. 311–316. Available at: https://doi.org/10.1109/IJCNN.2002.1005489.

Henriques, J., Gil, P. and Dourado, A. (2002) *Neural output regulation for a solar power plant*, *IFAC Proceedings Volumes (IFAC-PapersOnline)*. IFAC. Available at: https://doi.org/10.3182/20020721-6-ES-1901.01037.

Himour, Y., Tadjine, M. and Boucherit, M.-S. (2023) 'Nonlinear and infinite gain scheduling neural predictive control of the outlet temperature in a parabolic trough solar field: A comparative study', *Engineering Applications of Artificial Intelligence*, 126, p. 106862. Available at: https://doi.org/10.1016/j.engappai.2023.106862.

Hornik, K., Stinchcombe, M. and White, H. (1989) 'Multilayer feedforward networks are universal approximators', *Neural Networks*, 2(5), pp. 359–366. Available at: https://doi.org/10.1016/0893-6080(89)90020-8.

Jebasingh, V.K. and Herbert, G.M.J. (2016) 'A review of solar parabolic trough collector', *Renewable and Sustainable Energy Reviews*, 54, pp. 1085–1091. Available at: https://doi.org/10.1016/j.rser.2015.10.043.

Johansen, T.A., Hunt, K.J. and Petersen, I. (2000) 'Gain-scheduled control of a solar power plant', *Control Engineering Practice*, 8(9), pp. 1011–1022. Available at: https://doi.org/10.1016/S0967-0661(00)00043-5.

Kalman, R.E. (1960) 'Contributions to the Theory of Optimal Control', *Boletin Sociedad Matematica Mexicana*, pp. 102–119. Available at: https://api.semanticscholar.org/CorpusID:845554.

Kalogirou, S.A. (2023) *Solar Energy Engineering: Processes and Systems, Solar Energy Engineering: Processes and Systems*. Elsevier. Available at: https://doi.org/10.1016/C2021-0-02041-1.

Karmarkar, N. (1984) 'A new polynomial-time algorithm for linear programming', *Proceedings of the Annual ACM Symposium on Theory of Computing*, pp. 302–311. Available at: https://doi.org/10.1145/800057.808695.

Keerthi, S.S. and Gilbert, E.G. (1988) 'Optimal infinite-horizon feedback laws for a general class of constrained discrete-time systems: Stability and moving-horizon approximations', *Journal of Optimization Theory and Applications*, 57(2), pp. 265–293. Available at: https://doi.org/10.1007/BF00938540.

Kothare, M. V., Balakrishnan, V. and Morari, M. (1996) 'Robust constrained model predictive control using linear matrix inequalities', *Automatica*, 32(10), pp. 1361–1379. Available at: https://doi.org/10.1016/0005-1098(96)00063-5.

Kouvaritakis, B. and Cannon, M. (2016) *Model Predictive Control*. Cham: Springer International Publishing (Advanced Textbooks in Control and Signal Processing). Available at: https://doi.org/10.1007/978-3-319-24853-0.

Lee, E.B. and Markus, L. (1967) *Foundations of optimal control theory*. New York: John Wiley and Sons.

Leineweber, D.B. (1996) *Analyse und Restrukturierung Eines Verfahrens Zur Direkten Lösung Von Optimal-Steuerungsproblemen:(the Theory of MUSCOD in a Nutshell)*. Doctoral dissertation, IWR.

Lemos, J.M. (2006) 'Adaptive control of distributed collector solar fields', *International Journal of Systems Science*, 37(8), pp. 523–533. Available at: https://doi.org/10.1080/00207720600783686.

Lemos, J.M., Neves-Silva, R. and Igreja, J.M. (2014) *Adaptive Control of Solar Energy Collector Systems*. Cham: Springer International Publishing (Advances in Industrial Control). Available at: https://doi.org/10.1007/978-3-319-06853-4.

Li, L., Li, Y. and He, Y.-L. (2020) 'Flexible and efficient feedforward control of concentrating solar collectors', *Applied Thermal Engineering*, 171, p. 115053. Available at: https://doi.org/10.1016/j.applthermaleng.2020.115053.

Limon, D. *et al.* (2008) 'Robust control of the distributed solar collector field ACUREX using MPC for tracking.', *IFAC Proceedings Volumes*, 41(2), pp. 958–963. Available at: https://doi.org/10.3182/20080706-5-KR-1001.00164.

Luk, P.C.K. *et al.* (1997) 'Incremental fuzzy PI control of a solar power plant', *IEE Proceedings - Control Theory and Applications*, 144(6), pp. 596–604. Available at: https://doi.org/abs/10.1049/ip-cta:19971461.

Manjunath, R. and Raman, S. (2011) 'Fuzzy Adaptive PID for Flow Control System based on OPC', *IJCA Special Issue on "Computational Science–New ...*, pp. 5–8. Available at: https://www.ijcaonline.org/specialissues/nccse/number1/1850-152/.

Marquardt, D.W. (1963) 'An Algorithm for Least-Squares Estimation of Nonlinear Parameters', *Journal of the Society for Industrial and Applied Mathematics*, 11(2). Available at: https://doi.org/10.1137/0111030.

Masero, E. *et al.* (2021) 'A light clustering model predictive control approach to maximize thermal power in solar parabolic-trough plants', *Solar Energy*, 214, pp. 531–541. Available at: https://doi.org/10.1016/j.solener.2020.11.056.

Masero, E. *et al.* (2023) 'A fast implementation of coalitional model predictive controllers based on machine learning: Application to solar power plants', *Engineering Applications of Artificial Intelligence*, 118. Available at: https://doi.org/10.1016/j.engappai.2022.105666.

Masero, E., Maestre, J.M. and Camacho, E.F. (2022) 'Market-based clustering of model predictive controllers for maximizing collected energy by parabolic-trough solar collector fields', *Applied Energy*, 306, p. 117936. Available at: https://doi.org/10.1016/j.apenergy.2021.117936.

Mayne, D.Q. *et al.* (2000) 'Constrained model predictive control: Stability and optimality', *Automatica*, 36(6), pp. 789–814. Available at: https://doi.org/10.1016/S0005-1098(99)00214-9.

Mayne, D.Q. and Michalska, H. (1990) 'Receding horizon control of nonlinear systems', *IEEE Transactions on Automatic Control*, 35(7), pp. 814–824. Available at: https://doi.org/10.1109/9.57020.

Meaburn, A. and Hughes, F.M. (1993) 'Resonance characteristics of distributed solar collector fields', *Solar Energy*, 51(3), pp. 215–221. Available at: https://doi.org/10.1016/0038-092X(93)90099-A.

Meaburn, A. and Hughes, F.M. (1994) 'Prescheduled adaptive control scheme for resonance cancellation of a distributed solar collector field', *Solar Energy*, 52(2), pp. 155–166. Available at: https://doi.org/10.1016/0038-092X(94)90065-5.

Meaburn, A. and Hughes, F.M. (1996) 'A simple predictive controller for use on large scale arrays of parabolic trough collectors', *Solar Energy*, 56(6), pp. 583–595. Available at: https://doi.org/10.1016/0038-092X(96)00003-5.

Michalska, H. and Mayne, D.Q. (1993) 'Robust receding horizon control of constrained nonlinear systems', *IEEE Transactions on Automatic Control*, 38(11), pp. 1623–1633. Available at: https://doi.org/10.1109/9.262032.

Navas, S.J., Ollero, P. and Rubio, F.R. (2017) 'Optimum operating temperature of parabolic trough solar fields', *Solar Energy*, 158(February), pp. 295–302. Available at: https://doi.org/10.1016/j.solener.2017.09.022.

Nørgaard, M. *et al.* (2000) *Neural networks for modelling and control of dynamic systems : a practionner's handbook*. 1st edn. London: Springer London. Available at: https://link.springer.com/book/9781852332273 (Accessed: 5 November 2021).

Normey-Rico, J.E. and Camacho, E.F. (2008) 'Control of Dead-Time Processes', *IEEE Control Systems*, pp. 136–137. Available at: https://doi.org/10.1109/MCS.2008.927324.

Pataro, I.M.L. *et al.* (2024) 'A Stochastic Nonlinear Predictive Controller for Solar Collector Fields Under Solar Irradiance Forecast Uncertainties', *IEEE Transactions on Control Systems Technology*, 32(1), pp. 99–111. Available at: https://doi.org/10.1109/TCST.2023.3298230.

Pérez de la Parte, M. *et al.* (2008) 'Application of predictive sliding mode controllers to a solar plant', *IEEE Transactions on Control Systems Technology*, 16(4), pp. 819–825. Available at: https://doi.org/10.1109/TCST.2007.916298.

Pipino, H.A. *et al.* (2020) 'Nonlinear temperature regulation of solar collectors with a fast adaptive polytopic LPV MPC formulation', *Solar Energy*, 209, pp. 214–225. Available at: https://doi.org/10.1016/j.solener.2020.09.005.

Ponce, C., Sáez, D. and Núñez, A. (2014) 'Fuzzy predictive control strategy for a distributed solar collector plant', *IEEE Latin America Transactions*, 12(4), pp. 626–633. Available at: https://doi.org/10.1109/TLA.2014.6868864.

Propoi, A.I. (1963) 'Application of linear programming methods for the synthesis of automatic sampled-data systems', *Avtomat. i Telemekh.*, 24(7), pp. 912–920. Available at: https://www.mathnet.ru/eng/at11905.

Qin, S.J. and Badgwell, T.A. (2003) 'A survey of industrial model predictive control technology', *Control Engineering Practice*, 11(7), pp. 733–764. Available at: https://doi.org/10.1016/S0967-0661(02)00186-7.

Ramón D. Frejo, J. and F. Camacho, E. (2020) 'Centralized and distributed Model Predictive Control for the maximization of the thermal power of solar parabolic-trough plants', *Solar Energy*, 204, pp. 190–199. Available at: https://doi.org/10.1016/J.SOLENER.2020.04.033.

Rato, L. *et al.* (1997) 'Multirate MUSMAR cascade control of a distributed collector solar field', in *1997 European Control Conference (ECC)*. IEEE, pp. 1009–1013. Available at: https://doi.org/10.23919/ECC.1997.7082230.

Ren, Y.M. *et al.* (2022) 'A tutorial review of neural network modeling approaches for model predictive control', *Computers and Chemical Engineering*. Pergamon, p. 107956. Available at: https://doi.org/10.1016/j.compchemeng.2022.107956.

Richalet, J. *et al.* (1977) 'Model algorithmic control of industrial processes', *IFAC Proceedings Volumes*, 10(16), pp. 103–120. Available at: https://doi.org/10.1016/S1474-6670(17)69513-2.

Richalet, J. *et al.* (1978) 'Model predictive heuristic control', *Automatica*, 14(5), pp. 413–428. Available at: https://doi.org/10.1016/0005-1098(78)90001-8.

Rubio, F.R., Berenguel, M. and Camacho, E.F. (1995) 'Fuzzy logic control of a solar power plant', *IEEE Transactions on Fuzzy Systems*, 3(4), pp. 459–468. Available at: https://doi.org/10.1109/91.481955.

Rubio, F.R., Camacho, E.F. and Carmona, R. (1986) 'Adaptive Control of the One-Axis Tracking Collector Field', in *The IEA/SSPS Solar Thermal Power Plants — Facts and Figures—Final Report of the International Test and Evaluation Team (ITET)*. Berlin, Heidelberg: Springer Berlin Heidelberg, pp. 105–105. Available at: https://doi.org/10.1007/978-3-642-82684-9_45.

Ruiz-Moreno, S., Frejo, J.R.D. and Camacho, E.F. (2021) 'Model predictive control based on deep learning for solar parabolic-trough plants', *Renewable Energy*, 180, pp. 193–202. Available at: https://doi.org/10.1016/j.renene.2021.08.058.

Rumelhart, D.E., Hinton, G.E. and Williams, R.J. (1986) 'Learning representations by back-propagating errors', *Nature*, 323(6088), pp. 533–536. Available at: https://doi.org/10.1038/323533a0.

De Ryck, T., Lanthaler, S. and Mishra, S. (2021) 'On the approximation of functions by tanh neural networks', *Neural Networks*, 143, pp. 732–750. Available at: https://doi.org/10.1016/J.NEUNET.2021.08.015.

Saki, S. and Fatehi, A. (2020) 'Neural network identification in nonlinear model predictive control for frequent and infrequent operating points using nonlinearity measure', *ISA Transactions*, 97, pp. 216–229. Available at: https://doi.org/10.1016/j.isatra.2019.08.001.

Sánchez-Amores, A. *et al.* (2023) 'Coalitional model predictive control of parabolic-trough solar collector fields with population-dynamics assistance', *Applied Energy*, 334, p. 120740. Available at: https://doi.org/10.1016/j.apenergy.2023.120740.

Sathyamurthy, R. *et al.* (2017) 'A Review of integrating solar collectors to solar still', *Renewable and Sustainable Energy Reviews*, 77(October 2015), pp. 1069–1097. Available at: https://doi.org/10.1016/j.rser.2016.11.223.

Schwenzer, M. *et al.* (2021) 'Review on model predictive control: an engineering perspective', *International Journal of Advanced Manufacturing Technology*. Springer, pp. 1327–1349. Available at: https://doi.org/10.1007/s00170-021-07682-3.

Shanno, D.F. (1970) 'Conditioning of quasi-Newton methods for function minimization', *Mathematics of Computation*, 24(111), pp. 647–656. Available at: https://doi.org/10.1090/S0025-5718-1970-0274029-X.

Siegelmann, H.T., Horne, B.G. and Giles, C.L. (1997) 'Computational capabilities of recurrent NARX neural networks', *IEEE Transactions on Systems, Man, and Cybernetics, Part B (Cybernetics)*, 27(2), pp. 208–215. Available at: https://doi.org/10.1109/3477.558801.

Silva, R.N. *et al.* (1997) 'Cascade control of a distributed collector solar field', *Journal of Process Control*, 7(2), pp. 111–117. Available at: https://doi.org/10.1016/S0959-1524(96)00019-4.

Silva, R.N., Lemos, J.M. and Rato, L.M. (2003) 'Variable Sampling Adaptive Control of a Distributed Collector Solar Field', *IEEE Transactions on Control Systems Technology*, 11(5), pp. 765–772. Available at: https://doi.org/10.1109/TCST.2003.816407.

Simpson, L. *et al.* (2024) 'A Learning-based Model Predictive Control Scheme with Application to Temperature Control Units *', *2024 IEEE Conference on Control Technology and Applications, CCTA 2024*, pp. 675–680. Available at: https://doi.org/10.1109/CCTA60707.2024.10666571.

Song, Y. *et al.* (2023) 'Temperature homogenization control of parabolic trough solar collector field', *IFAC-PapersOnLine*, 56(2), pp. 5413–5418. Available at: https://doi.org/10.1016/J.IFACOL.2023.10.190.

Tagle-Salazar, P.D., Nigam, K.D.P. and Rivera-Solorio, C.I. (2020) 'Parabolic trough solar collectors: A general overview of technology, industrial applications, energy market,

modeling, and standards', *Green Processing and Synthesis*, 9(1), pp. 595–649. Available at: https://doi.org/10.1515/gps-2020-0059.

Ungar, L. *et al.* (1996) 'Process Modeling and control using neural networks', in Aic.& CACHE (ed.) *Intelligent Systems in Process Engineering.*, pp. 57–67.

Velarde, P. *et al.* (2023) 'Scenario-based model predictive control for energy scheduling in a parabolic trough concentrating solar plant with thermal storage', *Renewable Energy*, 206, pp. 1228–1238. Available at: https://doi.org/10.1016/j.renene.2023.02.114.

Wächter, A. and Biegler, L.T. (2006) 'On the implementation of an interior-point filter line-search algorithm for large-scale nonlinear programming', *Mathematical Programming*, 106(1), pp. 25–57. Available at: https://doi.org/10.1007/s10107-004-0559-y.

Wilkinson, D.J., Morris, A.J. and Tham, M.T. (1994) 'Multivariable constrained predictive control (with application to high performance distillation)', *International Journal of Control*, 59(3), pp. 841–862. Available at: https://doi.org/10.1080/00207179408923107.

Appendix A. Industrial applications of low and medium temperature heat

The following table shows industrial applications of low and medium temperature heat where PTC fields are already applied or appropriate to be applied. The data herein is extracted from the two works (Tagle-Salazar, Nigam and Rivera-Solorio, 2020; Gharat *et al.*, 2021)

Table A.1 Industrial application of low and medium temperature heat

Industry	**Operation/Application**	**Temperature Range (^{o}C)**
Food Industry, Beverage Industry, and milk processing	Drying	30-90
	Washing	60-90
	Boiling	95-105
	Pasteurization	60-150
	Sterilization	400-140
	Pressurization	60-80
	Cooking`	60-90
	Bleaching	60-90
Chemical Industry	Distillation	100-200
	Drying	12-170
	Evaporation	110-170
	Soaps	200–260
	Processing heat	120–180
	Preheating water	60–90
Textile industry	Bleaching – dying	60-90
	Printing	40-130
Automobile Industry	Paint pre-treatment	40-50
	Paint Drying	150-175
Rubber Industry	Drying	70-100
	Distillation	140-150
Bricks and blocks	Curing	60–140

Plastics	Preparation	120–140
	Distillation	140–150
	Separation	200–220
	Extension	140–160
	Drying	180–200
	Blending	120-140
Paper	Cooking, drying	60–80
	Boiler feed water	60–90
	Bleaching	130–150
Heating of buildings	–	25–75
Desalination	–	100–250
Power cycles (Rankine)	Vapor generation	300–450
	Phase change	300–375
Others	General steam generation	130–210

Appendix B. Details of calculating the Jacobian matrix in the Levenberg-Marquardt algorithm for FFANN learning

The Jacobian matrix in equation III.17, $J(t,\theta_k) = \frac{\partial \hat{y}(t,\theta)}{\partial \theta}|_{\theta=\theta_k}$, is the partial derivatives of the neural network outputs $\hat{y}(t)$ with respect to all elements of θ, where θ contains the biases and weights of the network.

To calculate this matrix, let's consider the general case of a feedforward neural network, i.e., with L the number of layers, $x(t)$ inputs to the input layer, and $\hat{y}(t,\theta)$ the outputs of the neural network, i.e., of the layer L. Then the computation at layer l is:

1- Linear combination of the layer inputs,

$$Z^{(l)} = W^{(l)} h^{(l-1)} + b^{(l)}$$

2- The output of the layer,

$$h^{(l)} = f^{(l)}\left(Z^{(l)}\right)$$

Where,

$f^{(l)}(\cdot)$: the activation function of layer l.

$W^{(l)}$: Matrix of weights between layer l and layer $(l-1)$.

$b^{(l)}$: vector of biases between layer l and layer $(l-1)$.

$h^{(l)}$: vector of outputs of layer l.

The network outputs are $\hat{y}(t,\theta) = h^{(L)}$, and $h^{(0)} = x(t)$ are the input of the network.

The partial derivatives can be propagated backwards by using the chain rule:

$$\frac{\partial \hat{y}(t,\theta)}{\partial \theta} = \frac{\partial \hat{y}(t,\theta)}{\partial Z^{(L)}} \cdot \frac{\partial Z^{(L)}}{\partial \theta} \qquad \text{IV-7}$$

The partial derivatives of the linear combination of the inputs of the layer l ,i.e., $Z^{(l)}$ w.r.t θ equals to partial derivatives w.r.t weights $W^{(l)}$ and biases $b^{(l)}$:

$$\frac{\partial Z^{(l)}}{\partial W^{(l)}} = h^{(l-1)}$$

and,

$$\frac{\partial Z^{(l)}}{\partial b^{(l)}} = 1$$

Let's define,

$$\delta^{(L)} = \frac{\partial \hat{y}(t,\theta)}{\partial Z^{(L)}} = f'^{(L)}\left(Z^{(L)}\right)$$

Propagate backwards through layers gives,

$$\delta^{(l)} = \left(W^{(l+1)}\right)^T \delta^{(l+1)} \odot f'^{(l)}\left(Z^{(l)}\right), l = 1,2,\dots,L-1$$

where, $\odot$ is the element-wise multiplication operator, and $f'^{(l)}\left(Z^{(l)}\right)$ is the derivative of the activation function.

The gradients of the outputs of the neural network w.r.t any of its weights and biases are then,

- For the weights:

$$\frac{\partial \hat{y}(t,\theta)}{\partial W^{(l)}} = \delta^{(l)}\left(h^{(l-1)}\right)^T.$$

- And for biases:

$$\frac{\partial \hat{y}(t,\theta)}{\partial b^{(l)}} = \delta^{(l)}$$

Appendix C. Partial derivatives of the MLP outputs $\widehat{\boldsymbol{y}}(\boldsymbol{t})$ w.r.t inputs $\boldsymbol{z_i(t)}$

The details of developing a general expression for the calculation of the partial derivatives of the overall function $F(z(t))$ (or $y(t)$) of an MLP with respect to any input $z_i(t)$ i.e., $\frac{\partial F(z(t))}{\partial z_i(t)}$ is given here. The used MLP in this work is an FFNN with one hidden layer where a hyperbolic tangent function is used as the activation function, and no activation function in the output layer. A such MLP's mathematical expression is given in equation III-46,

$$y(t) = F\big(z(t)\big) = V \tanh(W\, z(t) + W_0) + V_0$$

Where $z(t)$, for an NARX model, is:

$$z(t) = [y(t-1)\ldots y(t-n)\, u(t-\ d_u - 1)\ldots u(t - d_u - 1 - m)]$$

The derivative of the function $\tanh(\cdot)$ (the hyperbolic tangent function) is:

$$\frac{d\ tanh\ (x)}{dx} = 1 - tanh^2(x)$$

Then the partial derivatives of $F\big(z(t)\big)$ in respect to $z_i(t)$.

$$\begin{aligned}\frac{\partial F\big(z(t)\big)}{\partial z_i(t)} = \frac{\partial y(t)}{\partial z_i(t)} &= V \cdot \frac{\partial}{\partial z_i(t)} \cdot \big(tanh(W\, z(t) + W_0)\big) \\ &= V \cdot (1 - \tanh^2(W\, z(t) + W_0)) \cdot \frac{\partial}{\partial z_i(t)}(W\, z(t) + W_0) \\ &= V \cdot (1 - \tanh^2(W\, z(t) + W_0)) \cdot W_{:,i}\end{aligned}$$

The partial derivatives of $y(t)$are:

$$\frac{\partial y(t)}{\partial z_i(t)} = V \cdot (1 - \tanh^2(W\, z(t) + W_0)) \cdot W_{:,i}$$

Where $z_i(t)$ is the i^{th} element of the input vector $z(t)$, and $W_{:,i}$ is the i^{th} column of the weights' matrix W.

Appendix D. Armijo rule for computing optimal step size in the BFGS algorithm

Consider the problem of finding the optimum step α in the optimization BFGS algorithm in Table III-2 where we are brought to minimize a one variable function $\varphi(\alpha) \equiv J(U_k - \alpha H_k^{-1}\nabla J_k),\ \alpha \in [0, \infty[$.

The idea is to make the cost function J decreases sufficiently and proportionally to the step α from J_k until it reaches a value J_{k+1} (here k is the actual algorithm iteration but not time sample):

$$J(U_k) - J(U_k - \alpha_k H_k^{-1}\nabla J_k) \geq \alpha_k \gamma$$

$$\Rightarrow\ J(U_k) - \alpha_k \gamma \geq J(U_k - \alpha_k H_k^{-1}\nabla J_k)\ \ldots.(*)$$

The value γ cannot be chosen arbitrarily. Especially, it must vary from one iteration to another. It is more appropriate to define it in terms of the slope of the function at the point x_k :

$$\gamma = -\beta\ \nabla J(U_k)^T\ H_k^{-1}\nabla J_k, \quad \beta \in]0,1[$$

The condition (*) becomes then (Armijo rule) :

$$J(U_k) + \alpha_k\ \beta\ \nabla f(x_k)^T\ H_k^{-1}\nabla J_k, \geq J(U_k - \alpha_k\ H_k^{-1}\nabla J_k),\ \beta \in]0,1[$$

In practice we take $\beta = 10^{-4}$,

And at each iteration point $i + 1$,

$$\alpha_k^{i+1} \in [\tau\ \alpha_k^i\ ,\ (1-\tau)\alpha_k^i]$$

Or directly,

$$\alpha_k^{i+1} = \tau\ \alpha_k^i$$

with $\tau \in [0, \frac{1}{2}]$

Table Appendix D. 1. Backtracking algorithm (Armijo rule)

1. Initialization
   - Chose $\alpha_k^1 > 0,\ \tau \in]0, \frac{1}{2}]$ and put $i = 1$
2. Main loop
   - While $J(U_k) + \alpha_k^i\ \beta\ \nabla J(x_k)^T\ H_k^{-1} \nabla J_k < J\left(U_k - \alpha_k^i\ H_k^{-1} \nabla J_k\right)$ is not satisfied
     - Chose $\alpha_k^{i+1} \in [\tau\ \alpha_k^i\ ,\ (1-\tau)\alpha_k^i]$, (or directly: $\alpha_k^{i+1} = \tau\ \alpha_k^i$,)
     - Put $i = i + 1$;